TÜRKİYE CUMHURİYETİ'NİN YÜZÜNCÜ YILI

Yer Bilimleri ve Mühendisliği 1

Editör
Esin Ünal

BİDGE

BIDGE Publications

Yer Bilimleri ve Mühendisliği 1

Editor: Dr. Öğr. Üyesi Esin Ünal

ISBN: 978-625-372-493-1

Page Layout: Gözde YÜCEL

1st Edition:

Publication Date: 25.12.2024

BIDGE Publications,

Certificate No: 71374

www.bidgeyayinlari.com.tr - bidgeyayinlari@gmail.com

Krc Bilişim Ticaret ve Organizasyon Ltd. Şti.

Güzeltepe Mahallesi Abidin Daver Sokak Sefer Apartmanı No: 7/9 Çankaya / Ankara

Content

An Assessment of the Physical and Major Chemical Parameters of Drinking Water in Relation to Human Health. 5
Fatih ERBAŞ 5
Ayla BOZDAĞ 5
Natural Graphite: Industrial Applications, Global Distribution, and Türkiye's Potential 24
Hatice KANBUR ÇAVUŞ 24
Berna YAVUZ PEHLİVANLI 24
Origin, Formation and Characteristics of Cenozoic Evaporite Deposits in Eastern Anatolia (Türkiye) 49
Pelin GÜNGÖR YEŞİLOVA 49
Natural Monument and Geological Key; Adilcevaz (Eastern Anatolia) Tufas 89
Çetin YEŞİLOVA 89
Esin ÜNAL 89
Relationship Between Physical and Abrasion Properties and Cutting Performance of Igneous Rocks 107
İsmail İNCE 107
Hayri ARABACI 107
Mustafa FENER 107
Estimation of Uniaxial Compressive Strength (UCS) Values of Igneous Rocks Using Gene Expression Programming (GEP) 119
Mehmet Can BALCI 119
İsmail İNCE 119

Dünit Bloklarının Önemi, Oluşumları Ve Özellikleri: Guleman Ofiyoliti Örneği 133
Ayşe Didem KILIÇ 133

CHAPTER I

An Assessment of the Physical and Major Chemical Parameters of Drinking Water in Relation to Human Health.

Fatih ERBAŞ[1]
Ayla BOZDAĞ[2]

Introduction

People demand that the water they consume daily for a healthy life is fresh, clear and drinkable. Ensuring that the water to be used for drinking purposes has certain characteristics is one way of meeting this requirement. The water that will come from the source to the treatment plant, from there to the distribution network and to the end user must have important physical, chemical and microbiological parameters and the ions, minerals, gases and

[1] Lecturer Fatih ERBAŞ; Selcuk University Kulu Vocational School Occupational Health and Safety Department. fatih.erbas@selcuk.edu.tr ORCİD ID: 0000-0002-2914-8362
[2] Prof. Dr. Ayla BOZDAĞ; Konya Technical University Faculty of Engineering & Natural Sciences Department of Geological Engineering. aylabozdag@ktun.edu.tr ORCID ID: 0000-0002-6114-0678

bacteria, if any, must be within the permissible limit values for human health. The physico-chemical parameters relevant to drinking water are determined as a result of these assessments.

Recently, the increasing use of water due to population growth and industrial development as well as global warming causes both the reduction of existing water resources and pollution due to unconscious use and imprudence. Water chemistry is naturally affected by water-rock interaction and anthropogenic processes. Whether geological or anthropogenic, water may contain ions at levels that may adversely affect human health. For this reason, most countries, especially the World Health Organisation (WHO), have set limit values for physicochemical parameters in drinking water to indicate suitability as safe drinking water. However, the most important parameter for drinking water in these standarts is the effect of water on human health.

Drinking Water Quality Parameters

Especially until the beginning of the 20th century, drinking water was analysed only for disease-causing agents in terms of the diseases it caused. After the mid-20th century, it has become important to monitor chemicals due to the increased use of metals and other organic chemicals. The fact that disease-causing agents cause disease in a very short time and the effects of other pollutant chemicals in the medium and long term have revealed the view that the examination of water not only biologically but also physically and chemically will be more comprehensive (Oğuz, 2015).

Physically, when people evaluate water, they first evaluate it according to its appearance. This appearance is the general evaluation of physical parameters such as color, odor, taste, which are the aesthetic features of water. Although these parameters do not

have direct effects on the usability and health of water, they hesitate to consume and do not use water that is too colorful and has too much smell (WHO, 2011). Therefore, it is important to determine the chemical properties of water along with these aesthetic appearances and to determine the elements that cause this aesthetic appearance.

Drinking water standards set by the World Health Organisation (WHO) and the US Environmental Protection Agency (USEPA) are widely used worldwide. In addition, the Turkish Standards Institute (TSE) regulation (TS 266) is also used in Turkey for water intended for human consumption (Table 1).

Table 1. Physicochemical parameters and limit values used in drinking water

Parameter	Turkish Standards (TS 266, 2005)	World Health Organization (WHO, 2011)	US Environmental Protection Agency (US-EPA, 2018)
pH	6.5 - 9.5	6.5 – 8.5	6.5 – 8.5
Colour	20	15	15
Taste	sensorial	sensorial	sensorial
Smell	sensorial	sensorial	sensorial
Turbidity (NTU)	5	5	5
Conductivity (µS/cm)	2500		
Total dissolved substance (TDS) (mg/l)	-	1000	500
Calcium (mg/l)	200	100	-
Magnesium (mg/l)	50	-	-
Sodium (mg/l)	200	200	-
Potassium (mg/l)	-	-	-
Chloride (mg/l)	250	250	250
Sulfate (mg/l)	250	250	250
Fluoride (mg/l)	1.5	1.5	2
Nitrite (mg/l)	0.50	0.20	-
Nitrate (mg/l)	50	50	45
Ammonium (mg/l)	0.50	1.50	-

1. Physical Parameters

pH: pH is used to evaluate water for acidity and alkalinity as a logarithmic measure of the concentration of hydrogen ions in solution. At 25 ºC, pH= 7 is neutral, pH<7 is acidic and pH >7 is alkaline (Freeze & Cherry, 1979; Poeter et al., 2020). If the pH is below 7, the water has a bitter metallic taste and is corrosive, and if the pH is above 7, the water feels slippery and tastes like soda (Oğuz, 2015). According to the WHO (2011), the pH of drinking water should be in the range of 6.5 to 8.5 (Table 1).

Color: Drinking water should not have a colour that is noticeable to humans. In general, a colour above 15 TCU (true colour unit) is perceived by humans (WHO, 2011).

Change in the colour of drinking water; it can be caused by the interaction of the water with the lithological unit in which it circulates, by pollutants, organic substances, industrial waste and metals.

Taste: Water has a unique taste. Substances found in water can change its unique taste, and changing the taste of water makes it necessary to investigate the substances causing the change.

Smell: From an aesthetic point of view it is undesirable for water to have an odour. It is very important to identify the source of odour in drinking water if it is noticeable. Odours in water can be caused by organic and inorganic chemicals, plastics and biological agents (Gray, 2005). The parameters identified by Gray (2005) that can cause noticeable odours in drinking water are as follows;

Decomposition of plants: When organisms such as algae decompose, they give off odours such as grass and mould, and fish, while their living forms can cause serious health problems.

Mould and actinomycetes: These cause mould and foul odours. They can be seen when water is hot and left in the pipes for too long.

Iron and Sulphur bacteria: These bacteria form a sediment in the water and give off a bad odour.

Wastes generated by industrial processes: Wastes that are produced industrially in any sector and the by-products that result from this production can give rise to different odours in the water.

Chlorine: Although chlorine does not cause an odour in the water on its own, it can cause an odour when it reacts with compounds that are present in drinking water.

Turbidity: The turbidity of water is an indication of the presence of suspended solids or other organic matter in the water. The turbidity level of water is therefore important for the quality of drinking water in terms of the detection of these undesirable substances. According to the TSE, the WHO and the USEPA limit values for drinking water, the turbidity value must be a maximum of 5 NTU (Nephelometric Turbidity Unit) (Table 1).

Conductivity: Electrical conductivity (EC) is defined as the conductivity of 1 cm^3 of water at 25 ^oC and its unit is microsiemens/cm (µS/cm). The EC value increases with increasing ion concentrations in the water. In particular, the electrical conductivity of groundwater varies depending on the rocks with which these waters interact until they reach the surface, the

dissolution properties and types of rocks, the prevailing climate type and precipitation, etc. (Day & Nightingale, 1984; Hem, 1985).

There is no data to suggest that conductivity has a health effect on drinking water consumption (WHO, 2011). The conductivity of water is a measure of the ability of water to conduct electricity and is a measure of water pollution.

Temperature: Water resources can have different temperatures depending on a number of factors such as the region in which they are located, the climatic conditions, the geological structure, etc. Water temperature affects the density and solubility of substances in water, as well as the acceleration and deceleration of chemical and biological activities (Crittenden et al., 2012). High water temperatures can increase problems such as the development of micro-organisms, colour, taste, odour and corrosion in the water (WHO, 2011).

Water temperature does not have an immediate impact on human health, but water temperatures below 16°C are preferable to ensure potability (Nemerow et al., 2009).

Hardness: Water hardness is the sum of bicarbonate, chloride, sulphate and nitrate concentrations formed by dissolved calcium or magnesium ions and metal cations (Sr^{2+}, Mn^{2+}, Fe^{2+}, Fe^{3+}, Al^{2+} etc.) with an ionic charge of "+2" or higher (Hounslow, 1995). Although it has no direct effect on human health as drinking water, high hardness water may indirectly affect health if it is high in the specified ions.

Total Dissolved Substance (TDS): TDS is defined as the total dissolved solids in water, representing the sum of inorganic and

organic constituents. In natural water bodies, the inorganic ions present are predominantly potassium, sodium, calcium, magnesium, bicarbonate, sulfate, and chlorine, with the presence of heavy metals such as copper, bromide, iron, or manganese as well (Hem, 1985). The consumption of water with a high TDS is frequently associated with a poor taste (salty or metallic) and an unsatisfactory mouthfeel.

The majority of drinking water treatment plants that process fresh water sources do not include desalination operations with the specific objective of removing total dissolved solids (USEPA, 1999). Accordingly, in the event of elevated TDS concentrations in the source water, the drinking water that emerges from the treatment plant and traverses the distribution network will also exhibit elevated TDS levels upon arrival at the consumers. Drinking water treatment plants are of particular interest with respect to the chloride, sulfate, and bromide compounds of the TDS. The reason for this is that elevated chloride and sulfate levels can result in increased pipe corrosion or decreased efficiency of boilers and heat exchangers, and increased scaling or scaling problems that may lead to alterations in the taste and odor of drinking water (USEPA, 2012). Moreover, even minimal bromide concentrations in water can facilitate the formation of disinfection by-products (DBPs) in drinking water plants, resulting in an increase of brominated DBPs. These DBPs are recognised as carcinogenic and teratogenic (USEPA, 1998), and it is evident that the risk posed to human health by brominated DBPs is greater than that of chlorinated DBPs (Richardson et al., 2007; Richardson, 2008; Wilson et al., 2014).

Total Suspended Solids (TSS): Suspended solids that are higher than normal are an undesirable parameter for drinking water

quality because they provide a habitat for micro-organisms that may be present in the water. Suspended solids can also adversely affect human health by absorbing heavy metals, hydrophobic chemicals, pesticides, etc. (AWWA, 2011).

2. Major Ions

Calcium and Magnesium: Water generally contains between 10 and 100 mg of calcium per litre and similar quantities of magnesium. Calcium is important for the health of teeth and bones and for plant development (Hounslow, 1995), but an excess of these ions will cause the taste of the water to deteriorate, and an excess of magnesium will cause the water to taste bitter and undrinkable (Hounslow, 1995). If these ions are above the limits set by the WHO and USEPA (Table 1), they can cause calcification.

Sodium (Na^+): Sodium chloride, which is quite abundant in the earth's crust, can easily dissolve as a result of contact with water. In addition, the Na+ ratio in drinking water increases as a result of the weathering of Na-plagioclases in rocks in contact with water and/or chemical replacement of Ca and Na ions in clay minerals (Foster, 1950; Feth vd., 1964; Back, 1966; Garrels, 1967; Akgiray, 2003; Soyaslan, 2004).

The rate of Na^+ in water also increases as a result of salt water intrusion from the sea, mineral deposits, sewage wastes and road salting for de-icing on highways (WHO, 2011). In terms of human health, high concentrations of sodium chloride can cause high blood pressure (WHO, 2003).

Potassium (K^+): Potassium, an important and essential ion for human life, is present in minor amounts in drinking water but can pose a potential health risk if it exceeds the limit value (WHO, 2011).

Chloride (Cl^-): It comes to groundwater as a result of seawater intrusion, contact of evaporitic rocks with groundwater and atmospheric precipitation (Hounslow, 1995). In addition to these, it can also be added to drinking water sources from sewage, industrial wastes, and salting works on highways (NHMRC, 2014).

In terms of human health, chloride is a very important element for maintaining fluid balance in the body (NHMRC, 2014). People can tolerate high levels of chloride from freshwater sources over time, but higher concentrations can lead to sodium chloride-induced hypertension (WHO, 2003).

Sulfate ($SO4^{2-}$): Sulfate, which is found in sedimentary rocks of evaporitic origin such as gypsum and anhydrite and metamorphic rocks such as shale, as well as igneous and other organic materials, is transferred to natural water resources through interaction with these rocks and materials. In addition, domestic wastes from human habitats, sulfate fertilizers used in agricultural activities, industrial activities and acid drainage of sulphurous mining sites can also enter groundwater (Eisen & Anderson, 1979; Hem, 1985; Ford & Tellam 1994; Hounslow, 1995).

High sulfate content in water consumed as drinking water has been observed to cause diarrhea in people who use the water, and the competent authorities should be informed about sulfate contents above 500 mg/l (WHO, 2011).

Fluoride (F^-): Fluorine, which is widespread and widely distributed in the Earth's crust, is present in all waters, even in trace amounts. It can enter groundwater as a result of fertilizer use in agriculture, discharges from aluminum factories and erosion from natural fluorine sources (WHO, 2011).

From a human health perspective, low fluoride levels (minimum 0.5 mg/l) provide protection against tooth decay. However, as the concentration value increases (0.9-1.2 mg/l), it causes dentalfluorosis and even higher values (3-6 mg/l) cause skeletal fluorosis (WHO, 2004) Figure 1).

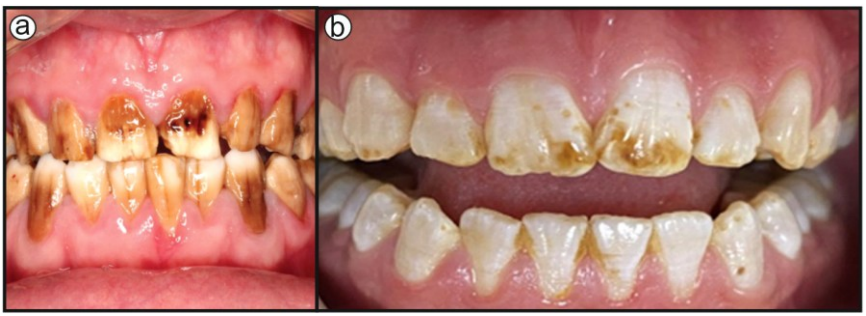

Figure 1. *Dental fluorosis (a) (https://momentumsaglik.com/dental-florozis/ - Retrieved on: 07/09/2024), (b) Dental fluorosis, (Kaya, 2021).*

3. Nitrogen Derivatives and Phosphate

Nitrite (NO^{2-}): Nitrite, which is a derivative of nitrogen, indicates that there is a biological contamination in water. Compared to the amount of nitrate, nitrite is found at a very low rate, and nitrite is added to the groundwater with the wastes of decomposed plants and animals, the use of fertilizers in agriculture, wastewater discharged from industrial plants, and the washing of nitrogen in the

earth as a result of precipitation (McNeely et al., 1979, Erguvanlı & Yüzer, 1987; Yalçın et al., 2004).

Nitrate (NO^{3-}): Nitrate, which is an important nutrient source for living life and plants, is found in natural resources and can be mixed into groundwater from fertilizers and pesticides used in agricultural activities, industrial wastewater, human and animal fertilizers and domestic wastes (Gray, 2008).

In the human body, nitrate turns into nitrite and becomes harmful to health. If there is more than 5-10 mg/l of nitrate in drinking water, it indicates that the water is contaminated with an external pollutant. If there is more than 45 mg/l nitrate in drinking water, methemoglobinemia disease called blue baby syndrome can be seen (Freeze & Cherry, 1979; Hem, 1985; Uslu & Türkman, 1987; Bouchard et al., 1992; Aiuppa et al., 2003) (Figure 2).

Figure 2. *Blue baby syndrome (https://www.americanscientist.org/article/the-blue-baby-syndromes - Retrived on: 07/09/2024)*

Phosphate (PO_4^{3-}): Phosphate, which has a widespread use in chemical fertilizers, cleaning and food industry, is found more intensively in groundwater sources than in surface water sources (Oğuz, 2015).

Phosphate, which is an inorganic structural element for bone and dental health, is an important component for human health. The maximum intake of phosphate, which has a need close to the same dose as the daily calcium need, has been determined as 800 mg/l (De Zuane, 1990). WHO and US-EPA do not specify a limit value for phosphate.

Ammonium (NH^{4+}): Ammonium, which is a derivative of nitrogen and mixes into groundwater from pollutants and sources of organic, inorganic and anthropogenic origin, is found intensively especially in wastewater produced domestically. The limit value determined as 1.5 mg/l in drinking water according to WHO (2011) is 0.5 mg/l according to TS-266.

Conclusion

The determination of the purposes for which water resources can be used is revealed by determining the physico-chemical parameters of water. This provides numerous concrete benefits to human life by revealing the major and minor elements contained in the water, which can be used for a variety of purposes, including agricultural activities, industrial activities and, most importantly, as a source of drinking water. This is achieved through detailed analyses and the provision of easily accessible water of good quality.

The contamination of water, which is a necessity for human existence, can have significant adverse effects on human health. The

World Health Organization (WHO) has established standard guidelines that determine the parameters and limit values to be monitored in water intended for human consumption. The necessity for monitoring elements that exceed the specified limit values is often determined through the implementation of accurate analytical procedures. It is of great importance to monitor the quality of drinking water, which is one of the most fundamental food sources, particularly for infants, the elderly and individuals with weakened immune systems who are susceptible to waterborne pathogens. After the mid-20th century, it has become important to monitor chemicals due to the increased use of metals and other organic chemicals. The fact that disease-causing agents cause disease in a very short time and the effects of other pollutant chemicals in the medium and long term have revealed the view that the examination of water not only biologically but also physically and chemically will be more comprehensive. It is of particular importance to conduct regular monitoring of specific parameters, including nitrate and its derivatives, fluorine, and total dissolved substances, for individuals belonging to vulnerable groups. In order to determine the accumulation that may occur in cells at daily doses and long-term use and the damages that this accumulation may cause, it is necessary to establish a monitoring network in the natural conditions of drinking water sources and in distribution network.

REFERENCES

Aiuppa, A., Belomo, S., Brusca, L., D'Alessandro, W. & Federico, C. (2003). Natural and anthropogenic factors affecting groundwater quality of an active volcano (Mt. Etna, Italy). *Applied Geochemistry*, 18, 863-882.

Akgiray, Ö. (2003). İçme Suyu ve Su Arıtımı, Suyumuzun Geleceği ve Türkiye Su Politikaları, *22 Mart Dünya Su Günü Paneli, Zekai Şen, Sevinç Sırdaş (Editör)*, Bildiriler, İstanbul. 62-75.

Australian Government- National Health and Medical Research Council (NHMRC), (2014). *Australian Drinking Water Guidelines*, Canberra, 6-2011.

AWWA, (1999), Water Quality and Treatment – *A Handbook of Community Water Supplies. (5th edition)* ABD: Mc Graw Hill.

AWWA, (2011). Water Quality and Treatment – *A Handbook on Drinking Water. (6th edition)* ABD: Mc Graw Hill.

Back, W. (1966). Hydrochemical facies and ground-water flow patterns in northern part of Atlantic coastel plain. *U.S. Geol. Surv. Profess. Papers* 488-A, 1-42.

Bouchard, D.C.,Williams, M.K. & Surampalli, R.Y., (1992). Nitrate contamination of groundwater: sources and potential health effects. J. Am. *Water Work Assoc*. *84*, 85-90.

Crittenden, J.C., Trussell, R.R., Hand, D.W., Howe, K.J., & Tchobanoglous, G. (2012). *MWH's water treatment: principles and design*. John Wiley & Sons.

Day, B.A. & Nightingale, H.I. (1984). Relationships between groud- water silica, total dissolved solids, and specific electrical conductivity: *Ground Water, 22*, 1, 80- 85.

De Zuane, J. (1990). *Handbook of Drinking Water Quality*. *(2nd edition)*. ABD: John Wiley & Sons Inc.

Eisen, C. & Anderson, M. P. (1979). The effects of urbanization on ground water quality –A case study: *Ground Water, 17*, 5, 456- 462

Erguvanlı, K. & Yüzer, E. (1987). *Yeraltısuları Jeolojisi*, İTÜ yayın no: 23, İstanbul, 339s.

Feth, J. H., Roberson, E. & Polzer, W. L. (1964). Sources of mineral constituents in water from granitic rocks Sierra Nevada, California and Nevada. *U. S. Geol. S. Survey Water Supply Paper*, 1535-I, 1-70.

Ford, M. & Tellam, J.H. (1994). Source type and extent of inorganic contamination within the Birmingham urban system, *UK. J. Hydrol.,* 156:101-135.

Foster, M.D. (1950). The origin of high sodium bicarbonate waters in the Atlantic and Gulf Coastal Plains. *Geochim. Cosmochim. Acta 1*, 33 -48.

Freeze, R.A. & Cherry, J.A. (1979). *Groundwater*: Prentice Hall, Inc., New Jersey 07632.

Garrels, R.M. (1967). Genesisof graund waters from igneous rocks. In: *Researches in geochemistry, vol. II (P. H. Abelson, ed.)*. New York, John Wiley.

Gray, N.F. (2005). *Water Technology - An Introduction for Environmental Scientists and Engineers. (2nd edition)*. Elsevier Science & Technology Books.

Gray, N.F. (2008). *Drinking Water Quality – Problems and Solutions. (2nd edition)*. New York: Cambridge University Press.

Hem, J.D. (1985). Study and interpretation of the chemical characteristics of natural water: U.S. Geological Survey Water-Supply Paper 2254, U.S. Geological Survey, Alexandria, VA 22304, USA, 263 p.

Hounslow, A.W. (1995). *Water Quality Data: Analysis and Interpretation*. Lewis Publishers, 54.

https://momentumsaglik.com/dental-florozis/ (Retrieved on: 07/09/2024)

https://www.americanscientist.org/article/the-blue-baby-syndrome. (Retrieved on: 07 / 09 / 2024)

Kaya, İ. (2021). Dental Florozise Bağlı Oluşan Renklenmenin Mikroabrazyon, Beyazlatma ve Rezin İnfiltrasyon ile Kombine Tedavisi: Olgu Sunumu, *Selçuk Dent Journal, RDD Kış Sempozyumu ve 21. Anabilim Dalları Toplantısı Özel Sayı.*

McNeely, R.N., Neimanis, V.P. & Dwyer, L. (1979). *Water Quality Sourcebook- A guide to water quality parameters: Inland Waters Directorate, Water Quality Branch*, Ottowa, Canada, 88 p.

National Health & Medical Research Council. All grants 2000–2015. Canberra: NHMRC, 2016. [Cited 12 May 2016]. Available from URL: https://www.nhmrc.gov.au/grants-funding/research-funding-statistics-and-data

Nemerow, N. L., Agardy, F. J., Sullivan, P. J., & Salvato, J. A. (2009). *Environmental engineering: water, wastewater, soil and groundwater treatment and remediation*. John Wiley & Sons.

Oğuz, T.C. (2015). İçme Suyu Arıtımında Yaygın Olarak Karşılaşılan Su Kalite Problemleri ve Arıtımı İçin Çözüm Önerileri. *Orman ve Su İşleri Bakanlığı*, 92p. Ankara,

Poeter, E., Fan, Y., Cherry J., Wood, W. & Mackay, D. (2020). *Groundwater in Our Water Cylcle,* Groundwater Project, Guelph, Ontario, Canada, ISBN:978-1-7770541-1-3, 136p.

Richardson, S.D., Plewa, M.J., Wagner, E.D., Schoeny, R. & DeMarini, D.M. (2007). Occurrence, genotoxicity, and carcinogenicity of regulated and emerging disinfection by-products in drinking water: A review and roadmap for research. *Mutation Res. Rev. Mutation Res., 636:*, 178-242.

Richardson, S.D., Fasano, F., Ellington, J.J., Crumley, F.G., Buettner, K.M., Evans, J.J., ... & Plewa, M.J. (2008). Occurrence and mammalian cell toxicity of iodinated disinfection byproducts in drinking water. *Environmental science & technology*, 42(22), 8330-8338.

Soyaslan, İ.İ. (2004). Eğirdir Gölü Doğusunun Hidrojeoloji İncelemesi ve Yeraltısuyu Modellemesi, *SDÜ, Fen Bilimleri Enstitüsü, Doktora Tezi*, 260syf., Isparta.

TS 266 (2005). ICS 13.060.20, Sular-İnsani Tüketim Amaçlı Sular. Türk Standartlar Enstitüsü, Ankara, Türkiye

US EPA (1998). *Guidelines for Ecological Risk Assessment*. Enviromental Protection Agency.

US EPA (1999). "Drinking water and health: What you need to know." *EPA 816-K-99-001*, Enviromental Protection Agency. Washington, DC.

US EPA (1999). *National Air Quality and Emissions Trends Report.* Enviromental Protection Agency

US EPA, (2012). *Guidelines for Water Reuse*. Enviromental Protection Agency

US EPA (2014). *Drinking Water Treatability Database (DWTD*). Enviromental Protection Agency. http://iaspub.epa.gov/tdb/pages/general/home.do

US EPA (2018*). Drinking Water Standards and Health Advisories Tables.* Enviromental Protection Agency.

Uslu, O. & Türkman, A., (1987). Su Kirliliği ve Konrtolü, *Çevre Genel Md. Yay. Eğitim Dizisi*, 1, 364 s

Yalçın, A., Davraz, A. & Özçelik, M., (2004). Yeraltısularının Kirlenmesinde Litoloji ve Yerleşim Alanlarının Etkisi: Ulupınar Kaynağı, Sorkuncak-Eğirdir-Isparta. *Jeoloji Mühendisliği Dergisi, 28 (2)*, 21-29.

Wilson, J. M., Wang, Y. & VanBriesen, J.M. (2014). Sources of high total dissolved solids to drinking water supply in southwestern Pennsylvania. *Journal of Environmental Engineering, 140(5)*, B4014003.

WHO (2003). *Chloride in Drinking-water Background document for development of WHO Guidelines for Drinking-water Quality*. Geneva: World Health Organization.

WHO (2004). *Copper in Drinking-water Background document for development of WHO Guidelines for Drinking-water Quality*. Geneva: World Health Organization.

WHO (2011) *Guidelines for Drinking Water Quality. 4th edn*. Geneva: World Health Organization.

CHAPTER II

Natural Graphite: Industrial Applications, Global Distribution, and Türkiye's Potential

Hatice KANBUR ÇAVUŞ
Berna YAVUZ PEHLİVANLI

1. Introduction

The world is entering a transformative era of industrial development, driven by innovation and the rapid growth of strategic emerging industries [1-3]. Amid this global shift, the graphite industry has gained unprecedented attention as a critical raw material for both traditional applications and emerging technologies. Despite its significance, natural graphite extracted through mining often contains high levels of impurities, necessitating beneficiation and purification to meet the demands of advanced applications. Once refined, natural graphite serves as a vital material for thermal management, lithium-ion battery anodes, nuclear reactors, and more [1-5].

Türkiye, with its rich mineral reserves and strategic geographic location, holds untapped potential for contributing to the

global graphite supply chain. Although less developed compared to major global producers, Türkiye’s graphite resources present promising opportunities for utilization in traditional industries and cutting-edge technologies. This review explores the comprehensive utilization of natural graphite, including its classification and distribution with a specific focus on Türkiye's graphite reserves. Finally, this work highlights future opportunities and strategies for enhancing the development and sustainable use of graphite resources, with an emphasis on Türkiye's role in the global market [4,5].

2. Classification and Distribution Natural Graphite

The basic compounds that make up the living structure are examined in two groups as inorganic and organic. Water, acid, base, salt and minerals are inorganic; carbohydrates, lipids, proteins, enzymes, hormones, vitamins, nucleic acids and ATP are organic components (Figure 1).The process from organic matter to graphite formation involves a series of stages that occur over long geological time periods. Organic matter (plant and animal remains) accumulates in aquatic environments or swamps. During this accumulation, decomposition begins in oxygen-free environments (anaerobic conditions). The accumulated organic matter turns into peat, called bog coal. Peat is a type of sediment in which low-degree decomposed organic matter is concentrated.Over time, peat turns into low-quality coal, called lignite, under the influence of increasing pressure and temperature. As the coalification process continues, lignite turns into denser and carbon-rich coal types (bituminous coal, anthracite). Following the coalification process, under higher temperature and pressure conditions (metamorphic conditions), coal

can turn into graphite. This process is called metamorphism and can last for millions of years. During metamorphism, the crystal structure of organic carbon is rearranged and carbon atoms form graphite crystals. During this process, the crystals are arranged in layers and acquire the graphite structure. As a result, the initial organic matter is transformed into carbon minerals called graphite. Graphite has high thermal and electrical conductivity due to the layered crystal arrangement in its structure. These processes occur in nature as a result of complex and long-term geological events that last millions of years [6,7].

The chemical content of graphite formation is determined by various geological and environmental factors. During metamorphism, organic carbon is transformed into graphite under high temperature and pressure. These conditions determine the purity and crystal structure. Low-grade coals or organic materials in the initial stage produce graphite with lower purity and more impurities. Different organic materials, such as plant or animal residues, have different chemical compositions. This directly affects the chemical content of the graphite that will be formed. The rocks that contribute to graphite formation (e.g. limestone or shale) affect the level of impurities and mineral composition. The pH and redox potential of the medium during graphite formation determine the purity and mineral phases. Acidic or alkaline conditions can cause the formation of different impurities (e.g. silicates, oxides). The water and other components in the solution (e.g. ionic compounds) present during the graphite formation process affect the chemical composition of graphite. Metamorphism over long periods of time helps carbon crystallize into a purer form. Higher grade metamorphic processes tend to produce higher purity graphite.

Mineral impurities in graphite (e.g. sulfur, iron) affect the quality and economic value of graphite. For example, graphite with lower sulfur and iron content is considered more valuable.

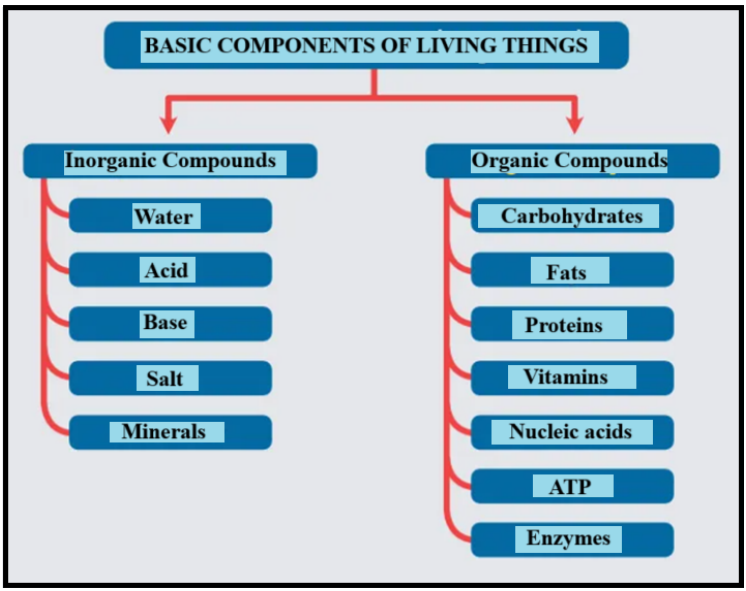

Figure 1. Main components of living things [6]

The minerals frequently encountered in graphite generally depend on the environmental and chemical conditions present during the formation of graphite. Quartz (SiO_2); It is usually found alongside graphite deposits and is known for its hardness. Quartz can be separated with graphite due to its lack of magnetic properties. Feldspar ($KAlSi_3O_8$ - $NaAlSi_3O_8$ - $CaAl_2Si_2O_8$); It is usually found in igneous and metamorphic rocks and can be part of graphite deposits. Mica ($KAl_2(AlSi_3O_{10})(F, OH)_2$); Especially biotite and muscovite mica species are common in graphite deposits. Mica minerals can be an important source of impurities in the process of enrichment of graphite. Pyrite (FeS_2); Pyrite, known as a sulphide

mineral, is usually found in graphite deposits. It is recognized by its bright golden yellow color. Calcite ($CaCO_3$); It is usually associated with carbonate rocks and can be found as a calcium carbonate mineral in graphite deposits. Dolomite ($CaMg(CO_3)_2$); Dolomite, a carbonate mineral similar to calcite, is commonly found in graphite deposits. Magnetite (Fe_3O_4); Magnetite, an iron oxide mineral, can be distinguished in graphite deposits due to its magnetic properties [7].

The conditions of graphite formation determine the physical properties as well as the chemical content and purity. These factors directly affect the potential for use in industrial applications of graphite [7].Naturally occurring graphite is composed almost entirely of carbon, with a typical carbon content ranging from 70% to 98%, depending on the type of graphite. There are three main types of natural graphite; Amorphous Graphite: Contains about 70-90% carbon. It is the most common type and is formed by the metamorphism of coal or shale, Flake Graphite: Contains about 85-98% carbon. [7].Natural graphite is composed primarily of the element carbon, which is the most stable allotropic form of carbon. However, other minerals are often found in natural graphite deposits. Carbon (C); the main component of graphite and is usually found in high purity.

Natural graphite is a mineral resource with abundant reserves, particularly concentrated [8,9]] in Türkiye, Brazil, and China (Table 1). Natural graphite, particularly in its high-purity crystalline forms, is critical for industries requiring advanced materials like batteries, refractories, and lubricants. Based on its mineralization conditions and crystal size, natural graphite is

classified into three main types [8-10]. Amorphous (microcrystalline) graphite: Also referred to as cryptocrystalline graphite, this type forms through the metamorphism of coal beds under high pressure and temperature. It appears as fine, earthy particles within metamorphic rocks and is primarily produced in Mexico, China, and South Korea. Flake graphite: Flake graphite forms through the metamorphism of organic material deposited in sedimentary layers. These deposits are later altered under high temperature and pressure, often in association with gangue minerals such as schist and gneiss. Crystalline graphite (vein or lump graphite): This variety represents the highest quality of natural graphite, with the highest purity and crystalline form. Vein graphite typically forms in the fissures and cavities of metamorphic rocks through the accumulation of organic materials, often accompanied by minerals like feldspar, quartz, mica, pyroxene, zircon, and apatite (Table 2).

The most important component in natural graphite is carbon. There are also elements such as oxygen, sulphur, aluminium, iron, silicon [8, 14, 15] in graphite (Table 3). This graphite can be made suitable for industrial use with purification processes (flotation, chemical washing, and thermal treatment). Purified graphite provides high performance especially in applications such as lithium-ion batteries, graphene production, electronics and energy storage systems. Graphite is a critical component in the anode section of lithium-ion batteries and the high electrical conductivity, chemical stability and capacity providing properties of these batteries increase the efficiency of energy storage systems.

Graphite mining in Türkiye began in 1941, and to date, over 22 regions with economically valuable graphite deposits have been identified. Although Turkiye has the largest natural graphite resources in the world actively operated graphite deposits are quite limited. These deposits are located in the provinces of Kastamonu, Yozgat, Balıkesir, Kütahya, Muğla, Adıyaman, İzmir, İstanbul, Aydın and Artvin. Almost all of the graphite in Turkey is disseminated in the form of microcrystalline structures within rocks that fall under the “amorphous” graphite classification found in most deposits worldwide. The graphite formations in Balıkesir (Susurluk), Kastamonu, Yozgat, and Adıyaman are identified as Türkiye's most highly graphitized carbon-bearing regions. On the other hand, the formations in Kütahya, Bandırma, Konya, Kastamonu, and Muğla exhibit characteristics that occasionally contain graphite but are mostly transitional formations between "semi-graphite" and "meta-anthracite" [4].Other graphite-like formations found in almost every region of Türkiye are typically "meta-anthracite" deposits, representing organic matter that has undergone relatively less metamorphism, with a degree of coalification closer to the "meta-anthracite" stage (Table 4) (Figure 2) [16].

The first graphite mine in Türkiye was operated in Çatalca, Istanbul [17-18]. It is reported that the mine was worked in a very rudimentary manner in two nearby open pits, with manual sorting carried out to enrich the material. After enrichment, samples taken from the mine were reported to contain 40.33% graphite [4]. The graphite occurs as a thin layer with a thickness of 30-35 cm, embedded within crystalline strata, with shale at the base and quartzite at the top. However, the graphite mineralization in the Kütahya Oysu deposit, the only operational mine in Türkiye, is

found in the Emirgazi Formation of Upper Palaeozoic age, which consists of amphibolite gneiss, schist, quartzite, and marble, representing high temperature and high pressure conditions. The amorphous graphite mineralization is distributed along the metamorphic layers. Due to strong tectonic deformation, the ore zones are often discontinuous, and the ore thickness ranges from 5 to 10 meters.

Table 1:World production of nature graphite by country or locality (unit is ton)[8-11]

Country or Locality	Graphite Category	2017	2018	2019	2020	2021
China	Flake	350000	416000	392000	762000	820000
China	Amorphous	275000	277000	308000	636000	680000
Brazil	Flake	90000	95000	96000	63600	68000
Canada	Flake	40000	40000	110000	8000	8600
India	Flake	31500	31500	31500	6000	6500
India	Amorphous	3500	3500	3500	3500	3500
Mozambique	Flake	1042	104000	107000	28000	30000
Russia	Flake	13200	13200	13100	25000	27000
Russia	Amorphous	12000	12000	12000	25000	27000
Madagascar	Flake	14529	46900	48000	20900	22000
Ukraine	Flake	20000	20000	20000	16000	17000
Norway	Flake	11000	16000	16000	12000	13000
North Korea	Flake	4500	4920	4920	8100	8700
Vietnam	Flake	5000	5000	5000	5000	5400
Sri Lanka	Vein	3900	4000	4000	4000	4300
Mexico	Amorphous	9000	9000	9000	3300	3500
Turkey	Amorphous	1300	1300	1000	500	600
Australia	Amorphous	1000	1000	1000	250	270
World Total		**880000**	**1110000**	**1100000**	**966000**	**1000000**

Table 2: Classifications and Features of Different Natural Graphite [8-12].

Graphite Type	Morphology	Ore Grade	Crystallinity	Grain Size
Vein (Lump)	Interlocking aggregates of coarse graphite crystals	40%–90%	Crystalline	Up to 10 cm
Flake	Well-developed crystal platelets of graphite	5%–50%	Crystalline	1 μm–4 cm
Microcrystalline	Earthy to compact fine-grained graphite	50%–90%	Microcrystalline	<1 μm

Table 3: Chemical composition and major mineral impurities of nature graphite [8, 13, 14].

Graphite Type	Chemical Composition	Major Mineral Impurities
Flake	C, O, Si, Al, Mg, Ca, Fe	Quartz, feldspar, biotite, pyrite, pyrrhotite, rutile, monticellite, etc.
Microcrystalline	C, O, Si, Al, Mg, Fe, Ca	Quartz, chlorite, serpentine, montmorillonite, calcite, illite, mica, chalcopyrite, pyrite, kaolin, limonite, petalite, etc.
Vein	C, O, Fe, Ca, Mg, Si, Al	Quartz, pyroxene, pyrrhotite, pyrite, chalcopyrite, sphalerite, marcasite, chlorite, calcite, siderite, dolomite, copper, etc.

Figure 2.Türkiye graphite deposits map [16].

Table 4: Türkiye Graphite Mines, Reserves and Resources [4].

Province	District	Location	Type	Source, Reserve	Carbon Content	Host Rock	Status
Kütahya	Altıntaş	Oysu	Amorphous	7.2 Mt	20%	Metamorphic	Active Mine
Muğla	Milas		Amorphous	500 Kt	10%	Metamorphic	Old Mine
Istanbul	Çatalca	Domuzderesi	Crystalline	Unknown	-	Metamorphic	Old Mine
Balıkesir	Susurluk		Crystalline	Unknown	-	Metamorphic	
İzmir	Tire		Amorphous	350 Kt	<10%	Metamorphic	
Adıyaman	Sincik		Amorphous	30 Kt	45%	Metamorphic	
Yozgat	Akdağmadeni		Crystalline	100 Kt	45%	Metamorphic	
Kastamonu	İnebolu	Anday	Amorphous	Unknown	60%	Metamorphic	
Konya	Selçuklu	Derbent	Amorphous	3.42 Kt	-	Metamorphic	
Kastamonu	Doğanyurt		Amorphous	4.5 Mt	6.06%	Metamorphic	Source
Kahramanmaraş	Göksu	Fındıklıkoyak	Amorphous	2.3 Mt	5.6%	Metamorphic	Research
Kastamonu	Merkez	İmam	Amorphous	74.5 Kt	3.05-4.67%	Metamorphic	
Kastamonu	Tosya	Özboyu	Amorphous	33 Kt	5.25-6.07%	Metamorphic	
Kastamonu	Merkez	Miskinler Dere	Amorphous	137.7 Kt	10.5%	Hydrothermal Alteration	
Kastamonu	İnebolu	Gölmet	Amorphous	23.7 Kt	5.6-7.19%		
Kırklareli	Demirköy						
Kütahya	Altıntaş	Saraycık Şıbılık Dere		31.42 Kt	30.2%		
Artvin	Değirmentaşı (Lusuncur)	village					
Balıkesir	Bandırma	Çığmış					

3.Purification and Applications of Natural Graphite

There are some important differences between pure graphite and graphite in nature. Pure graphite consists of high purity carbon atoms and is usually produced in a laboratory environment. It can be 99% or higher purity. Since it has high electrical conductivity, it is used in electronic devices, nuclear reactors and high temperature applications. High thermal and electrical conductivity, chemical resistance, low coefficient of friction. Natural graphite is usually

found in crystal, flake or amorphous form. The purity rate varies and can usually be between 70-90%. It is used in pencils, foundries, lubricants, battery rods and refractory materials. Natural graphite has electrical and thermal conductivity, chemical resistance and mechanical properties that vary depending on its purity.

Pure graphite is much more purity and homogeneous than natural graphite.While pure graphite is preferred in applications requiring high technology, natural graphite is preferred in more common and general-purpose uses. Pure graphite has more consistent and predictable properties, while natural graphite can exhibit variable properties depending on its purity and form.In order for natural graphite to be economically evaluated, its chemical content is very important. The economic value of graphite depends on its fixed carbon content. Generally, high-quality graphite deposits have a fixed carbon content of 90% and above. However, economically exploitable graphite deposits can usually have a fixed carbon content between 30% and 90%.The economic value of graphite is determined not only by the fixed carbon content, but also by the amount and type of impurities. For example, graphite with low sulfur and iron content is more valuable. In order for graphite deposits to be economically exploited, factors such as the size, depth and extraction costs of the deposits should be taken into account in addition to the fixed carbon content [19].

Graphite, owing to its exceptional physical and chemical properties, finds applications in a broad range of industries. These properties include excellent thermal and electrical conductivity, high resistance to heat and acids, lubricity, and structural stability. High-purity graphite is a critical component in lithium-ion batteries, dry

cells, and other energy storage devices due to its superior electrical conductivity and stability. Graphite's excellent electrical conductivity and ability to withstand high temperatures make it ideal for electrodes in arc furnaces and electrical motors, as well as for brushes used in electric motors. Used in the manufacture of components for electronics, such as conductive parts and thermal interface materials.

3.1. Methods to Remove Inorganic Substances from Organic Compounds

Removing inorganic substances from organic compounds typically depends on the specific nature of the substances involved. Here are common methods used in laboratory and industrial settings

3.1.1.Filtration

Filtration is a fundamental physical method used to separate solid inorganic substances from liquid organic compounds. If the inorganic substance is insoluble, such as a salt or metal oxide, it can be separated using filter paper and a funnel.Vacuum filtration is often employed to speed up the process. In this technique, a Buchner funnel and a flask connected to a vacuum source are used to pull the liquid through the filter, leaving the solid residue behind. This method is commonly used in laboratory settings for small-scale samples.Extraction: Utilizes the differences in solubility of organic and inorganic compounds in different solvents. Organic compounds are generally soluble in organic solvents, while inorganic compounds are soluble in polar solvents like water.

3.1.2. Extraction

Extraction involves the use of two immiscible solvents to separate organic compounds from inorganic substances. Inorganic

impurities typically dissolve in a polar solvent like water, while organic compounds dissolve in a non-polar solvent like ether.Using a separatory funnel, the mixture is shaken, allowing the two layers to separate based on density and solubility. The inorganic impurities partition into the aqueous phase, while the organic compound remains in the organic phase. This method is highly effective for purification.These methods increase the purity of organic compounds by removing inorganic contaminants, and the choice of method depends on the properties of the mixture and the desired level of purity.

3.1.3. Washing

Washing is used to remove inorganic impurities adhering to or mixed with organic compounds. For instance, washing an organic solution with water can remove water-soluble salts. Similarly, acidic impurities can be neutralized with a basic aqueous solution (e.g., sodium bicarbonate), and basic impurities can be neutralized with a dilute acidic solution (e.g., hydrochloric acid). This process is often combined with extraction and is effective for removing surface impurities. Care must be taken to select a solvenPrecipitation

3.1.4. Precipitation

Precipitation is used to selectively remove inorganic substances by converting them into insoluble solids. For example, metal ions can be precipitated as insoluble salts using a suitable reagent. Calcium ions, for instance, can form calcium oxalate precipitate when treated with oxalate ions.The resulting precipitate can be separated using filtration or centrifugation. This method is particularly useful for removing trace inorganic impurities.t that does not react with the organic compound.

3.1.5. Decantation

Decantation relies on differences in density to separate substances. When the inorganic substance is a heavy precipitate, it settles at the bottom of the container over time. The liquid organic phase can then be carefully poured off, leaving the inorganic precipitate behind. This method is simple and quick but does not achieve complete separation. It is often followed by filtration for better results.

3.1.6. Distillation

Distillation separates components based on differences in boiling points. If the inorganic impurities are non-volatile and the organic compound is volatile, distillation can purify the organic compound. For example, distillation can remove water from an alcohol-water mixture. For mixtures with close boiling points, fractional distillation may be required. It is important that the organic compound is thermally stable to prevent decomposition during heating.

3.1.7. Crystallization

Crystallization is a method for purifying organic solids contaminated with inorganic impurities. The mixture is dissolved in a solvent that dissolves the organic compound but not the inorganic impurities. Upon cooling, the organic compound crystallizes, leaving the impurities in the solvent. This method is widely used in industries like pharmaceuticals, where high-purity organic compounds are essential. The choice of solvent and cooling rate greatly influence the quality of the crystals.

3.1.8. Sublimation

Sublimation is used for organic compounds that can transition directly from solid to gas without passing through a liquid phase. If inorganic impurities do not sublime, the organic compound can be purified by heating under reduced pressure. This method is suitable for volatile organic solids, such as naphthalene, and is often used in small-scale laboratory settings.

3.1.9. Ion exchange

Ion exchange removes ionic inorganic impurities by passing the solution through an ion exchange resin. Cation exchange resins remove positively charged ions (e.g., metal cations), while anion exchange resins remove negatively charged ions (e.g., chloride or sulfate). This technique is frequently employed in water treatment and in the purification of solutions containing sensitive organic compounds.

3.1.10. Dialysis

Dialysis separates small inorganic ions from larger organic molecules using a semipermeable membrane. The membrane allows inorganic ions to diffuse out while retaining larger organic molecules. This method is particularly useful in biochemistry for purifying proteins or removing salts from biological samples. A dialysis bag is typically used for this purpose.

3.1.11. Drying agents

When water is the inorganic impurity, drying agents such as anhydrous magnesium sulfate ($MgSO_4$) or calcium chloride ($CaCl_2$) can be added to the organic solution. These agents absorb water, forming hydrates, which are then removed by filtration. This method

is widely used to dry organic solvents or remove residual water from organic reactions.

3.1.12. Electrodialysis

Electrodialysis is a technique that removes inorganic ions by applying an electric field. The ions migrate through selective ion-exchange membranes, leaving the organic compound behind. This method is commonly used for desalination and in processes requiring the removal of ionic impurities from complex mixtures.

Each of these methods is chosen based on the specific properties of the organic compound and the nature of the inorganic impurities. Combining multiple techniques is often necessary to achieve optimal purification.

3.2. Purification Methods of Natural Graphite

Purification of graphite is essential to enhance its quality and expand its range of applications. Below is an overview of each method and its key features.

3.2.1.Flotation

Flotation is a separation process that utilizes the unique hydrophobic (water-repelling) properties of certain materials, such as graphite. In this method, the material to be separated (e.g., graphite) is mixed with water, along with specially selected chemicals, to enhance its natural hydrophobicity. These chemicals often include surfactants or frothers that help create stable bubbles in the liquid.Graphite, mixed with water and chemicals, rises to the surface and is collected. However, it is generally suitable for achieving moderate purity levels.

Flotation is a cost-effective and widely used technique. Flotation is widely used in the mining industry for graphite ore beneficiation. It is an essential step in producing graphite suitable for applications such as lubricants, refractories, and pencil manufacturing. For higher-purity requirements, such as in lithium-ion batteries or fuel cells, flotation is often combined with chemical leaching or thermal purification.In summary, flotation leverages graphite's natural hydrophobicity to separate it from impurities in a cost-effective and scalable manner, making it a cornerstone of graphite processing techniques.Magnetic Separation: This method is used to remove magnetic minerals from graphite ore by applying a magnetic field. It is particularly preferred for graphite ores containing magnetic impurities and is easy to implement.

3.2.2. Electrostatic separation

Electrostatic separation is a purification method that utilizes differences in the electrical conductivity of materials to separate them. Graphite, being a good conductor of electricity, can be effectively separated from non-conductive impurities using this technique. This method is especially effective when a high level of graphite purity is required, such as for use in advanced industrial applications like batteries or electronics. Leaching Method: Through chemical dissolution, impurities in the graphite ore are removed. Using suitable solvents based on the chemical structure of graphite, high-purity levels can be achieved. However, environmental impacts and chemical costs should be considered.

3.2.3. Gravity separation

Gravity separation is a physical process used to separate materials based on differences in their specific gravities or densities.

This method is commonly applied to mixtures where the components have significant density differences. For graphite purification, gravity separation can be used to remove heavier impurities like silicates, metal oxides, and other minerals that are denser than graphite. While it may not achieve the ultra-high purity required for specialized applications, it is an excellent first step in the beneficiation process, particularly for large-scale mining operations.

The choice of purification method depends on the physical and chemical properties of the graphite ore, the desired purity level, and cost/environmental considerations. Purified graphite offers high performance, especially in applications such as energy storage, electronics, composite materials, and lubricants[19].

These methods are widely applied to increase the purity of graphite and make it suitable for industrial applications.Graphite is extensively used in the production of steel and in electrometallurgical processes, where it serves as a high-temperature electrode material. Lower-grade graphite is used in making refractory coatings, furnace linings, and crucibles due its resistance to high temperatures and chemical stability.It is an essential material for foundry applications, especially as a mold release agent and additive in casting processes. Graphite's versatility ensures its relevance across traditional industries like metallurgy and advanced technologies such as energy storage, electronics, and nuclear power. Its properties, particularly its resistance to heat, acids, and wear, along with its high conductivity and lubricating capabilities, make it a vital material in both modern and conventional applications.

3.3 Applications of Natural Graphite

The application areas of graphite are quite wide due to its properties. It is used in the casting and refractory industry, crucibles and laboratory materials due to its resistance to heat and acids. It is used in the production of electrodes, motor brushes, battery bars and electronic devices due to its good electrical conductivity [20-22].

Graphite is an excellent refractory material due to its high temperature stability and chemical inertness. The use of graphite in this industry has a large place in the world market. Initially, very large flake graphite was preferred in refractory products [20].Grafit kayganlığı, yumuşaklığı ve makina parçaları üzerine uzun müddet yapışabilmesi özelliği nedeniyle makina yataklarında yağlama maddesi olarak uygulanabilir. Bu sahada kullanılabilecek grafitin çok saf olması (en az %95 grafitleşmiş karbon) ve kuvars gibi sert mineralleri içermemesi gerekmektedir. Dola-yısıyla en uygun grafit türü, pulsu şekilde olanlardır.Graphite can be used as a lubricant in machine bearings due to its slipperiness, softness and ability to adhere to machine parts for a long time. The graphite to be used in this field must be very pure (at least 95% graphitized carbon) and must not contain hard minerals such as quartz. Therefore, the most suitable type of graphite is the flake type [21].Since graphite has a very high melting point, it is heat resistant. Its expansion constant is very low; its resistance to mechanical loading, chemical effects and temperature changes is very good. Its properties such as conducting heat very well and its outer surfaces being slippery so that a liquid cannot grip and hold the metal are among the preferred qualities for casting crucibles [20,21].

Efficient and stable anodes based on graphite are being made for batteries manufactured with both synthetic and natural graphite. The increasing demand for graphite in this market is due to the growth in the production of lithium-ion batteries. In order to increase the existing high electrical storage and good charge cycle properties of natural graphite to be used in this sector; after impact milling, acid or thermal purification (>99.5% Graphitic carbon 'Cg') is applied to turn graphite flakes into round shapes and then coated with a thin amorphous carbon film [20]. The graphite and its derivatives have applications in the aviation industry due to their extremely high thermal stability properties. Substances with small amounts of graphite added are applied in rockets due to their resistance to very high thermal shocks [22].In addition, Pebble-bed nuclear energy generators, which are gaining importance today, are small modular reactors that are gaining importance in the energy sector. Pebble-bed reactors use uranium fuel embedded in golf ball-sized graphite-coated pebbles that act as a moderator, instead of uranium-enriched rods [22].The consumption of graphite, which replaces asbestos in the automotive industry, has increased significantly since the 1980s when the dangers of asbestos were recognized. Graphite is more useful in brake pads of heavy vehicles as opposed to passenger cars.

4. Conclusion

Natural graphite is a fascinating material with several unique properties. Graphite is composed of carbon atoms arranged in a hexagonal lattice, forming layers. These layers are held together by weak van der Waals forces, allowing them to slide over each other easily. Due to the delocalized electrons within its layers, graphite is an excellent conductor of electricity. Graphite remains stable at high

temperatures and sublimates at around 3,000°C, making it useful in high-temperature applications. The weak bonding between layers gives graphite a slippery feel, making it an effective dry lubricant. Graphite is very soft and can cleave with light pressure, which is why it is used in pencils. It has a low specific gravity and density, which contributes to its lightweight nature. Graphite is relatively non-reactive, making it stable in. It has a metallic luster and is typically black or dark gray in color. These properties make natural graphite valuable in many applications, including as a lubricant, in batteries, and as a moderator in nuclear reactors.

Graphite is becoming an increasingly vital strategic and critical raw material due to its diverse and expanding range of applications in high-tech industries such as energy storage, electronics, metallurgy, and nuclear technologies. The global demand for graphite continues to rise, driven by its role in advanced technologies like lithium-ion batteries for electric vehicles, renewable energy systems, and emerging industrial applications.

Given these factors, it is imperative to focus on enhancing the beneficiation and enrichment of domestic graphite resources to reduce reliance on imports and support the growth of national industries. Producing high-quality graphite concentrates with elevated carbon content is essential for meeting the stringent requirements of industries such as battery manufacturing and high-temperature applications.Traditional beneficiation techniques such as flotation, magnetic separation, and leaching may need to be supplemented or replaced with innovative methods, such as bioleaching, advanced chemical treatments, or environmentally friendly processes, to improve recovery rates and reduce

environmental impact.The creation of specialized graphite grades tailored for specific applications (e.g., spherical graphite for batteries, nuclear-grade graphite, or expanded graphite for thermal management) will enable the country to meet the needs of high-value markets.Promoting research into novel graphite processing technologies and fostering collaborations between industry, academia, and government institutions can accelerate the development of competitive technologies and sustainable processes.While pursuing technological advancements, it is essential to prioritize eco-friendly processing methods and cost-efficient practices to ensure the long-term viability of graphite production.

Acknowledgments

This research did not receive any specific grant from funding agencies in the public, commercial, or not-for-profit sectors.

References

[1]. H. A.Taylor Graphite in Industrial Minerals and Rocks. SME Society for Mining,Metallurgy, and Exploration, Inc. Colorado, USA, 7th Editionp: 507-518, (2006).

[2]. L. Sun, C.Xu,K.Xiao, Y.Zhu and L. Yan Geological characteristics, metallogenicRegularities and the exploration of graphite deposits in China. China Geology 3: 425-434(2018).

[3]. P. Sanyal, B. C.Acharya, S. K.Bhattacharya, A. Sarkar, S. Agrawal and M. K.Bera. Origin Of graphite, and temperature of metamorphism in Precambrian Eastern Ghats Mobile Belt, Orissa, India: A carbon isotope approach. Journal of Asian Earth Sciences 36:2-3, (2009).

[4]. O. Kaya and M.Canbazoglu. Chemical demineralization of three different graphiteoresfrom Turkey. Minerals & Metallurgical Processing26(3): 158-162, (2009).

[5]. O. Kaya and M. Canbazoglu. A study on the floatability of graphite ore from YozgatAkdagmadeni. Journal of Ore Dressing 9(17): 40-44, (2007).

[6]. https://bikifi.com/biki/canlilarin-temel-bilesenleri/

[7]. http://www.mta.gov.tr/v3.0/bilgi-merkezi/maden-rezervleri

[8]. S. Duan, X. Wu, Y. Wang , J. Feng , S. Hou , Z. Huang , K. Shen , Y. Chen , H. Lıu and F. Kang. Recent progress in there search and development of natural Graphite foruse in thermal management, battery electrode sand the nuclear industry. New Carbon Materials 38(1): 73-95 (2023).

[9]. X. Wang, H. Li, H.Yao, Z. Chen, and Q. Guan. Network feature and influence factors of global nature graphite trade competition. Resources Policy 60: 153-161, (2019).

[10]. C. L.Mantell Natural Graphite. Carbon and Graphite Handbook. John Wiley&Sons. P: 61-71,(1968).

[11]. https://www.usgs.gov/centers/national-minerals-information-center/graphite-statistics-and-information 1996-2024.

[12]. H .A., Rakoto, R.Rajaomahefasoa,R Razafiarisera, et al. Evaluation of flake graphite ore using self-potential (SP), electrical resistivity tomography (ERT) and induced polarization (IP) methods in east coast of Madagascar. Journal of Applied merhaba Geophysics 169: 134-141,(2019).

[13]. S. Z.Duan, X W Wu, X Min, et al. Effect of purity and proportion of microcrystalline graphite ore on the electrical,mechanical and tribologicalperformance of copper-carbon composites. Materials Research Express6(12): 125604, (2019).

[14].Hewathilake H P T S, Balasooriya N W B, Nakamura Y, et al. Geochemical, structural and morphological characterization of vein graphite deposits of Sri Lanka: Witness to carbon rich fluid activity. Journal of Mineralogical Petrological Sciences, 113(2): 96-105, (2018).

[15].Gamaralalage R A K, Herath M G T A P, Buddika K, et al. Development of a chemical-free floatation technology for the purification of vein graphite and characterization of the products. Scientific Reports 11(1): 22713, (2021).

[16]. A., İlhan, R. Sarı, ve Y. Y. Çörtenlioğlu. “Avrupa İçin Yeni Bir Kaynak: Türkiye Grafit Oluşumları”, *Madencilik Türkiye*, 2020.

[17].https://yermam.org.tr/uploads/kutuphane/259761_avrupa_icin_yeni_bir_kaynak_turkiye_grafit_olusumlari_01_06_2020.pdf, Erişim tarihi: 24.01.2023.

[18]. M. Aykulu. Türkiye Grafit Envanteri, MTA Genel Müdürlüğü, Derleme Rapor, 3642: 30-31, (1966).

[19].Ö. Kaya. Grafit Zenginleştirme Yöntemleri Ve Zenginleştirmeye Etki Eden Parametrelerin Araştırılması, Cumhuriyet Üniversitesi / Fen Bilimleri Enstitüsü / Maden Mühendisliği Ana Bilim Dalı, Doktora Tezi, 248 s, (2006)..

[20] Keeling, J. "Graphite–South Australian potential". MESA Journal 84, pages 28–41. Goverment of South Australia Department for Energy and Mining, 2017.

[21]Toprak, S. “Sekizinci Beş Yıllık Kalkınma Planı Madencilik Özel İhtisas Komisyonu Endüstriyel Hammaddeler Alt Komisyonu Genel Endüstri Mineralleri 1. (Asbest-Gra-fit-Kalsit-Fluorit-Titanyum) Çalışma Grubu Raporu”. Devlet Planlama Teşkilatı, 2001. s. 21-51. https://www.maden.org.tr/meslegimiz/oik629.pdf, Erişim tarihi: 24.01.2023.

[22] Fetherston, J. M. “Graphite in Western Australia”. Geological Survey of Western Aust-ralia, Mineral Resources Bulletin 26, 84,2015, p. 11, 12, 37, 41. https:/dmpbookshop.eruditetechnologies.com.au//product/graphite-in-western-australia.do, Erişim tarihi: 03.02.2023.

CHAPTER III

Origin, Formation and Characteristics of Cenozoic Evaporite Deposits in Eastern Anatolia (Türkiye)

Pelin GÜNGÖR YEŞİLOVA

1.Introduction

Numerous marine and non-marine evaporites that were deposited at different times throughout the Cenozoic can be found in Anatolia. These deposits are significant because they provide insight into the tectonic events and climatic shifts of those eras, as well as the paleogeographic development of the Tethys Ocean (such as opening-closing-shallowing-deepening). Both large and small continental blocks make up Anatolia, which is encircled by the branches of Paleotethys and Neotethys (Şengör & Yılmaz, 1983; Gürer & Gürer, 1999). During the Early Mesozoic Era, the northern region of Gondwana began to rift, opening the Neotethys Ocean (Platzman & et al., 1994). The Neotethys Ocean was divided into two branches, the northern and southern Neotethys, in an area located on the Anatolian plateau today (Yılmaz, 1993) (Figure 1). Yılmaz & Yılmaz (2019) stated that the closure of the northern and

southern branches of Neotethys may have occurred in different periods. The branches of this ocean started to close from the Late Cretaceous. The closure of the northern branch between the Pontide arc and the Anatolide-Tauride platform continued until the Middle Eocene (Yılmaz, Boztuğ & Öztürk, 1993; Platzman & et al., 1994). The southern branch of Neotethys, south of the Bitlis and Pütürge continental units, closed in the Middle Miocene (Yılmaz, 1993; Robertson & et al., 2006, 2007; Okay, Zatin & Cavazza, 2010).

The northern branches of Neotethys are divided into İzmir-Ankara-Erzincan ocean and Inner Taurus ocean, while the southern branches are divided into Maden (=Berit) ocean and Çüngüs ocean (Karadenizli & et al., 2016). Erzincan basin located on Inner Taurus and Malatya basin located on Maden (=Berit) ocean are forearc basins and accumulated marine origin rocks between Late Eocene and Early Miocene. The closure of Inner Tauride ocean is at the end of Late Early Miocene (Gökten, 1983). When Inner Tauride ocean shrank, evaporites accumulated during Chattian (Upper Oligocene) period due to arid climate. In Early Miocene period, carbonate sedimentation became dominant due to tropical-humid climate (Karadenizli & et al., 2016).

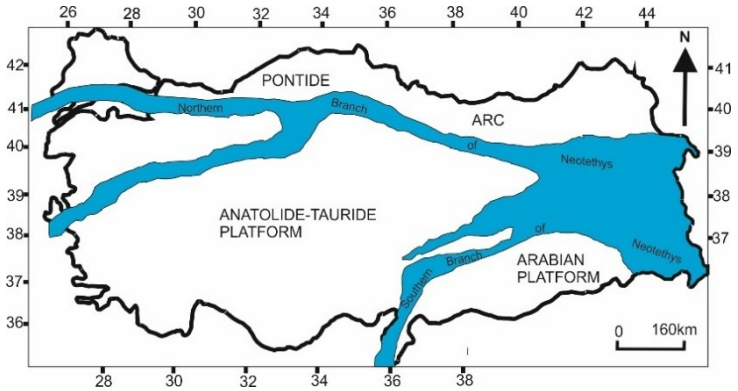

Figure 1. Paleogeographic distribution of the northern and southern branches of Neotethys in Turkey (modified Şengör & Yılmaz, 1983)

Gürer & Gürer (1999) attributed the origin of evaporites in Western and Central and Eastern Anatolia to changes in latitude and altitude. For example, during the Oligocene, Western Anatolia was higher and located at northern latitudes than at present. On the other hand, at this time, Central and Eastern Anatolia was located at southern latitudes and partly at almost sea level, and evaporitic conditions were dominant (Luttig & Steffens, 1976). During the Early Oligocene, continental basins such as Sivas and Erzincan developed in Eastern-Central Anatolia. Approximately in these basins, reddish conglomerates, sandstones and mudstones extending in the E-W direction were deposited. Considerable amounts of gypsum were observed in these deposits (Kurtman, 1971). During the Late Oligocene, under arid climate conditions, these basins expanded and underwent short-term marine transgression (from Iran) leading to widespread evaporite deposits (such as gypsum and halite) (Cater & et al., 1991; Steininger, 1985). In Southern, Central, and Eastern Anatolia, marine transgression and the development of local rift systems took place during the Early Miocene (Fairbridge &

et al., 1997). The majority of Eastern Anatolia was still underwater. During this time, the Mediterranean Sea transgressively covered Malatya, Erzincan, and their environs, depositing carbonates and clastics (Luttig & Steffens, 1976). The Middle Miocene saw the beginning of the neotectonic regime in Anatolia due to the collision of continents (Şengör & Yılmaz, 1981), which resulted in a change in the region's climate (Fairbridge & et al., 1997). In Eastern Anatolia, this tectonic regime led to uplift and N-S compression. Consequently, the sea between Eastern Anatolia and Central Anatolia retreated entirely (Şengör & Yılmaz, 1981). The collision of the Anatolian and Arabian plates during the Late Miocene caused East-Central Anatolia to be uplifted and displaced to northern latitudes. This led to the end of evaporative conditions and evaporative accumulation and the local development of glacial environments (Gürer & Gürer, 1999).

2.Eastern Anatolian evaporite deposits

Part of the Alpine-Himalayan orogeny, the Eastern Anatolian High Plateau is a 200 km wide belt that runs roughly east-west between the Bitlis-Zagros suture mountains in the south and the Pontide Mountains in the north. The geological evolution of Eastern Anatolia has been greatly impacted by the neotectonic regime that began in the Middle Miocene (Şengör & Yılmaz, 1981). Folds, thrust and strike-slip faults, and extensive extensional fractures have all been created as a result of the region's compressional tectonic regime during the neotectonic era. Both intermountain and pull-apart basins have developed as a result of the influence of all these structural components. (Şengör & Yılmaz, 1981). Among these, the Muş, Ahlat-Adilcevaz, Erzurum-Pasinler-Horasan and Karayazı-Tekman

basins are intermountain basins affected by strike-slip faults. The Kağızman-Tuzluca basin developed in the pull-apart type (Hüsing & et al., 2009) (Figure 2).

The Eastern Anatolia Region contains many marine and continental evaporite basins of Paleocene-Pliocene age. At the same time, there are many marine and terrestrial evaporite deposits of the same age range in the Siirt, Bismil-Diyarbakır, Batman, Şırnak basins of the Southeastern Anatolia Region within the southern branch of the Neotethys (Stöcklin, 1968; Özkaya, 1974; Dağıstan & Şimşek, 2005; Doğan, 2005; Özdoğan & et al., 2011; Yeşilova, Güngör-Yeşilova & Helvacı, 2011; Yeşilova & Helvacı, 2012, Güngör-Yeşilova & Helvacı, 2012; Yeşilova & Helvacı, 2013; Güngör-Yeşilova & Helvacı, 2013; Hoşgörmez & et al., 2014; Güngör-Yeşilova & Helvacı, 2017, Yeşilova, Helvacı & Carillo, 2018). The basins in Eastern Anatolia that contain evaporite are Malatya-Darende-Balaban, Erzincan-İliç-Kemah-Refahiye, Erzincan-Tercan-Çayırlı, Erzurum-Aşkale, Erzurum-Tekman-Karayazı, Erzurum-Hınıs, Iğdır-Tuzluca, Elâzığ-Baskil, Elâzığ-merkez, Muş-Bulanık-Malazgirt, Ağrı-Doğubeyazıt, Van-Başkale, and Van-Timar (Figure 3).

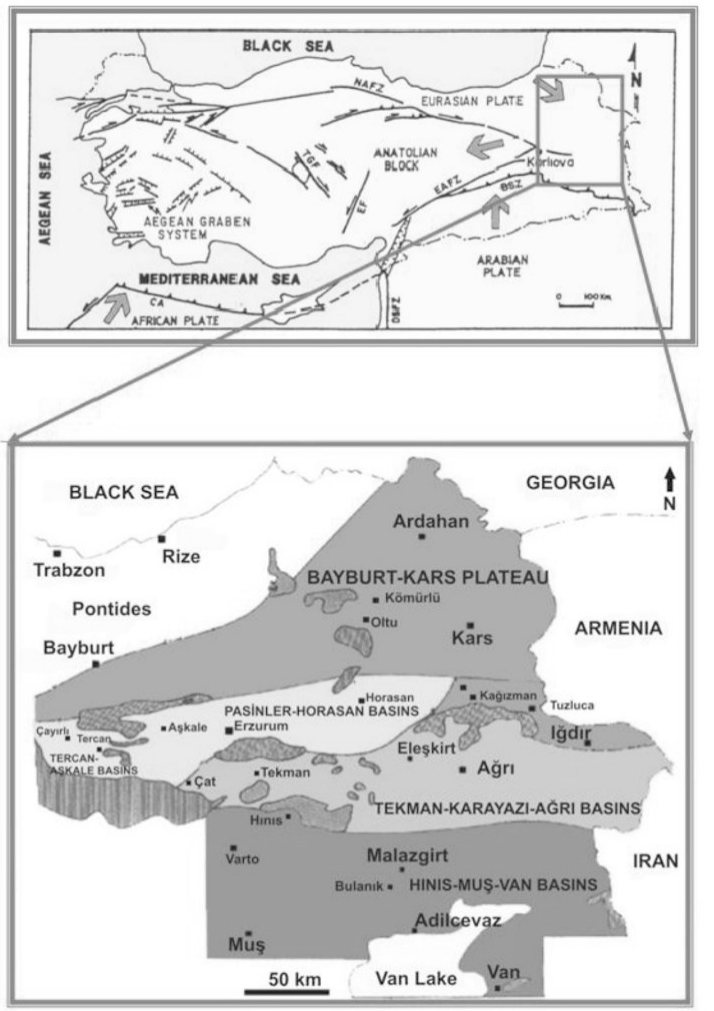

Figure 2. Location map of the subbasins in Eastern Anatolia (NAFZ: North Anatolian Fault Zone, EAFZ: East Anatolian Fault Zone, TGF: Tuz Gölü Fault, EF: Ecemiş Fault, DSFZ: Death Sea Fault Zone, BSZ: Bitlis Suture Zone (modified from Şahintürk, Şaroğlu & Çaptuğ, 1988b; Koçyiğit, 1991, and Sancay, 2005).

The Southeastern Anatolian suture zone and the Karlıova triple junction of the South Anatolian and North Anatolian faults (Allen, 1969; Arpat & Şaroğlu, 1972; Şengör, 1979) border the Pontides. The eastern Anatolian basins are located at the northwest end of the Turkey-Iran plateau (e.g. Tekman-Karayazı, Tercan-Aşkale, Pasinler-Horasan, and Hınıs-Muş-Van) (Figure 2). The origin and age of evaporite deposits belonging to all these basins in Eastern Anatolia have been revealed by some researchers so far with isotopes such as Sr, S, O, elemental analyses, sedimentological-petrographic and mineralogical studies, stratigraphic, palynological and paleontological data. (Şenalp,1969; Kurtman, 1973; Tatar, 1978; Özgül & et al., 1981; Şengör & Canıtez, 1982; Hempton & Dunne, 1984; Şaroğlu & Yılmaz 1984; Sümengen &et al. 1987; Yazgan, 1987; Barka & Gülen, 1989; Koçyiğit, 1991b; Şahintürk, 1992; Karaman & et al., 1993; Poisson & et al., 1996; Palmer, Helvacı & Fallick, 2004; Sancay, 2005; Batı & Sancay, 2007; Bilgiç, 2008; Hüsing & et al., 2009; Gedik, 2010; Sirel & Gedik, 2011; Şen & et al., 2011; Aydınçakır, 2013; Abdioğlu et al., 2015; Varol et al., 2015; Karadenizli & et al., 2016; Güngör-Yeşilova, 2020; Güngör-Yeşilova & et al., 2020; Güngör Yeşilova & Gökmen, 2020; Abdioğlu-Yazar & et al., 2021, Güngör-Yeşilova & Yeşilova, 2021; Güngör-Yeşilova & Yavuz, 2021; Güngör-Yeşilova & Baran, 2023, etc.).

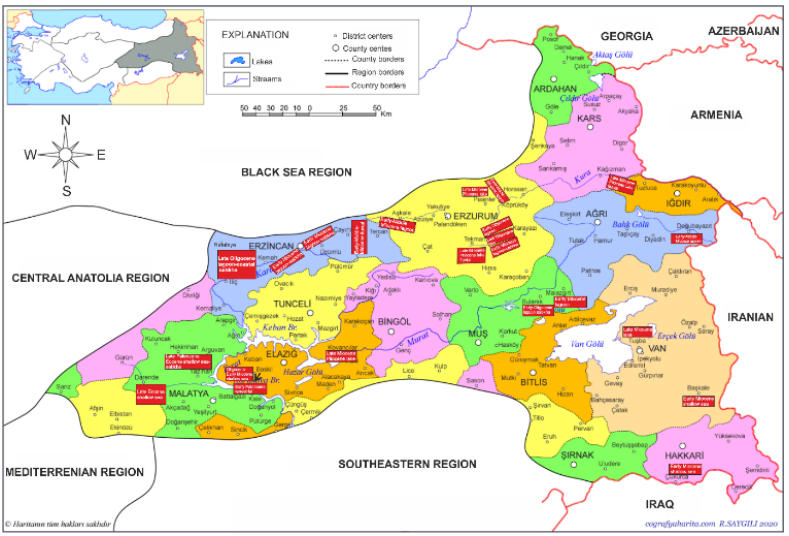

Figure 3. Distribution of Cenozoic evaporite deposits in Eastern Anatolia (modified from Saygılı, 2020).

2.1.Characteristics of evaporites in the basins located in the northern branch of Neotethys

2.1.1.Kemah-İliç-Refahiye basin (SW Erzincan)

Munzur limestones form the base of this basin, followed by the Bozbel formation and Güneş ophiolites. These units are unconformably covered by the evaporites in this basin (Figure 4). These marine-derived, Late Oligocene (Shattian) evaporites are situated southwest of Erzincan and are composed of primary, secondary, and anhydrite gypsum (Altunsay, 1993; Kavak, 1998; Güngör-Yeşilova & Yavuz 2021). Rocks like limestone, dolomite, mudstone, sandstone, claystone, tuff, and basalt are interbedded with them. Primary gypsum changes into secondary gypsum and primary anhydrite grows in the host sediment during early-late diagenetic processes. Sedimentary structures (chicken-wire, enterolithic, and cross-bedding) resulting from tectonism and diagenesis are

frequently observed in lithofacies (Figure 5a). There are several types of secondary sulphate lithofacies, including satin spar gypsum, anhydrite, massive, massive-bedded, intraclastic, nodular brecciated, nodular, nodular banded, and nodular laminated (Karadenizli & et al. 2009, 2016; Güngör-Yeşilova & Yavuz 2021). These exhibit secondary gypsum textures of the alabastrin or porphyroblastic types, where primary gypsum is anhydritized and then transformed into secondary gypsum. Gypsarenite, gypsum rose, radial-fibrous gypsum, free-growing twinning selenitic gypsum, and prismatic-lenticular gypsum are the main types of gypsum lithofacies found in this basin. Based on these lithofacies in the basin, Güngör-Yeşilova & Yavuz (2021) separated the depositional environment of evaporites into coastal sabkha, lagoon, and seaside areas.

2.1.2.Erzincan-Kemah basin

Evaporites belonging to this basin are distinguished within the Lower Miocene Kemah formation coal member. It overlies the Eocene Gulandere formation (Figure 4). These evaporites crop out in the south of the North Anatolian Fault between Kemah district and Erzincan and in the north and south of the Erzincan-Kemah road. The unit generally consists of sandstone, claystone, mudstone, clayey limestone, siltstone alternation. In addition, this unit contains red, yellow, white and green colored, thin-medium-thick bedded, folded and overturned thin carbonates, coal and gypsum. The gypsiferous units here are primary and secondary (alabastrine textured) (Figure 5b) and may have carbonate intercalations. These evaporites were deposited in environments ranging from shallow

marine to lagoonal and terrestrial environments (Aktimur & et al., 1995).

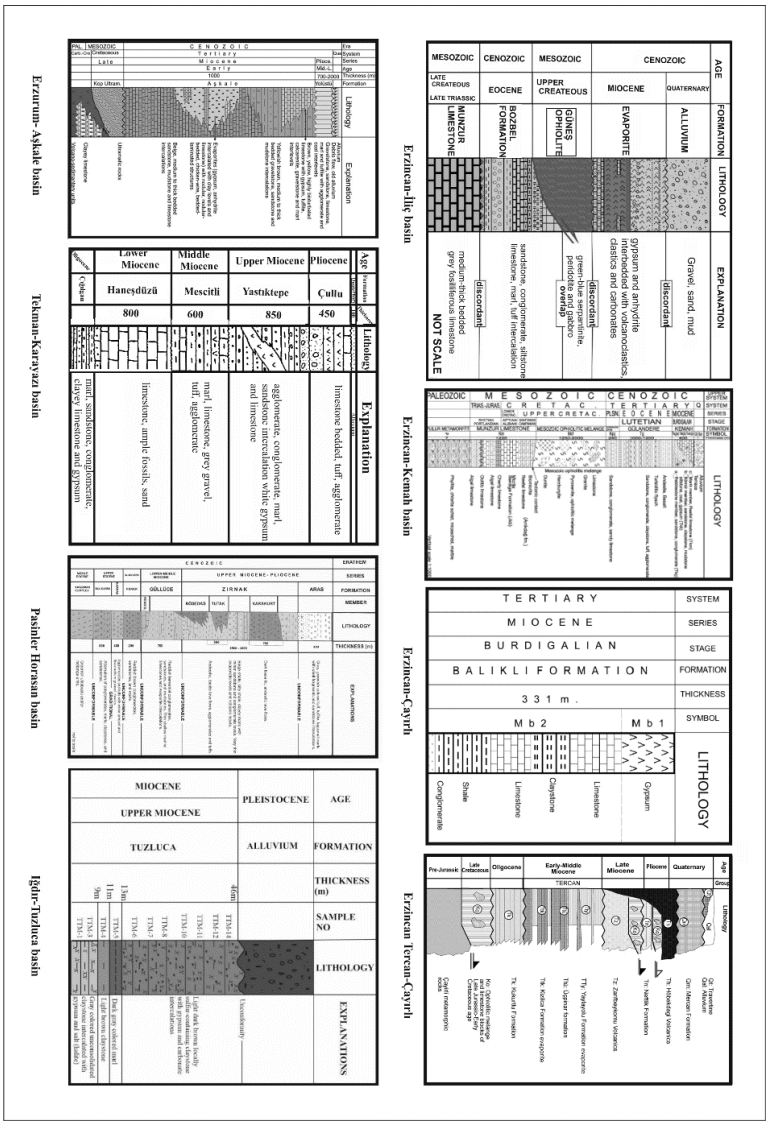

Figure 4. Generalized stratigraphic sections of the basins in the northern branch of Neotethys.

2.1.3.Erzincan-Çayırlı basin

The Lower Miocene Balıklı formation, which appears in the Çayırlı region, contains evaporites that are part of this basin. Bituminous marl, claystone, shale, bituminous limestone, and gypsum alternations make up the formation, which begins with conglomerate (Arpat, 1964) (Figure 4). These gypsums have lost water and transformed into anhydrite in some areas, and are typically seen as primary selenitic gypsum (Figure 5c). Lagoon and coastal sabkha environments are where they originated.

2.1.4.Tercan-Çayırlı basin

Tercan group evaporites can be found in this basin in both the Yaylayolu and Kızılca formations (Figure 4). The evaporites of the Kızılca formation are terrestrial-fluvial in origin and date to the Early-Middle Miocene (Temiz & et al., 2002). In the southeast of the Tercan-Çayırlı region, the Kızılca formation, which contains evaporite units, appears. This formation is composed of siltstone, yellow mudstone, cross-bedded red conglomerates, and a lot of gypsum. Thin-bedded mudstones, siltstones, small sandstones, and limestones make up the Yaylayolu formation, which is situated in this basin and above the Kızılca formation. Gypsum is found in the upper layers of the formation. Microfossils indicate that this formation is Early-Middle Miocene in age (Temiz & et al., 2002).

2.1.5.Erzurum-Aşkale basin

The Aşkale formation contains the evaporites in this basin (Figure 4). Sandstone, mudstone, limestone, and evaporites make up the formation (Abdioğlu & et al., 2015). Anhydrite and gypsum make up evaporites, and the formation contains massive, nodular, nodular banded, laminated, and laminated-banded gypsum

lithofacies in addition to chicken-wire and uncommon enterolithic structures (Figure 5d). These are Early-Middle Miocene in age and suggest a sabkha, lagoon, or shallow marine environment (Sungurlu, 1971; Abdioğlu-Yazar & et al., 2021).

2.1.6.Tekman-Karayazı basin

The northern branch of Neotethys started to spread in the eastern part of the Anatolian plate in this basin during the Jurassic period, and its subduction and closure occurred between the Late Cretaceous and Middle Eocene (Yılmaz & Yılmaz, 2013). The evaporites in this basin are located in the north of Tekman-Karayazı, southeast of Erzurum. It consists of Oligocene evaporite shallow marine-lagoon units (Çığılgan Formation) (İlker, 1966, Aziz, 1971; Erdoğan, 1972; Havur, 1972; Tanrıverdi, 1971; Gedik, 1985) (Figure 4). The formation is mostly composed of shale, claystone and marl, occasionally gravelly sandstone levels and clayey-sandy limestone beds. The uppermost parts of the formation contain occasional gypsum-bearing interlayers. The formation is generally greenish-bluish in color and thin to medium-thick layered. Base structures, gradation, parallel and folded laminations and sand-concretions are common in this unit (Figure 5e). Andesitic basalt interlayers are rarely observed. This basin consists of limestone and marl lake sediments starting from the Late Oligocene (Ağcakoca Formation) (Gedik, 1985; Yılmaz, Terlemez & Uysal, 1988; Ayyıldız & et al., 2018). In the Early Miocene, it is again composed of conglomerate, variegated sandstones and marl alternations belonging to the lagoonal Yastıktepe formation, and sometimes there are white gypsum and limestone layers (Figure 4). The upper part of the

Yastıktepe formation is intercalated with volcaniclastic rocks (Şaroğlu & Yılmaz, 1986).

2.1.7.Pasinler-Horasan basin

This basin's evaporites are situated northeast of Erzurum. The Early-Middle Miocene Güllüce Formation is represented in this basin by reddish conglomerates, sandstones, and claystones with some gypsum layers. (Figure 4) (Sungurlu, 1972). According to Şahintürk & Kasar (1979), the Güllüce Formation is typically 700 meters thick and reflects shallow marine depositional conditions (Figure 4). Beige silty shale, clayey marl, and trace amounts of sandstone and conglomerate levels from the Zırnak formation are found in this basin during the Upper Miocene-Pliocene period. Furthermore, there are very thin evaporitic layers with carbonate rocks (dolomite and dolomitic limestone) and volcanic rocks (basalt andesite, tuff). According to Şahintürk & Kasar (1979), this formation is representive of transitional and continental-lacustrine environments.

2.1.8.Hınıs-Tekman basin

Evaporites belonging to this basin are in the Alibonca formation between Hınıs and Tekman (Erdoğan & Soytürk, 1974). The Upper Miocene Alibonca formation consists of conglomerate, sandstone, mudstone, marl, clayey limestone, gypsum, and pyroclastic rocks (İlker, 1966b; Sungurlu, 1967, Şaroğlu & Yılmaz, 1986). This formation corresponds to the lowest levels of the Zırnak formation (Soytürk, 1973). The Alibonca formation accumulated in a terrestrial environment between a stream and a lake where volcanic activity took place. In addition, there is a unit consisting of the alternation of conglomerate, sandstone, claystone, mudstone,

carbonate, marl and gypsum belonging to the Upper Miocene-Pliocene Hacıömer formation in this basin. The gypsum here was formed in a fluvial environment (Erdoğan & Soytürk, 1974; Gedik, 1985).

2.1.9.Kağızman-Iğdır-Tuzluca basin

East of the point where the main North and East Anatolian Fault systems converge (near Karlıova), this basin is situated in northeastern Anatolia (Allen, 1969; Şengör, 1979). There are lake and fluvial environments in this intermountain basin (Varol & et al., 2015). The Tuzluca formation contains evaporites here (Figure 4). Claystone, siltstone, sandstone, mudstone, limestone levels, their intermediate bands, clay-rich evaporite units, primary gypsums, halite, recrystallized salts, and gypsum pseudomorphs make up the Tuzluca Formation (Figure 5f, g, h). Evaporites consist of selenite (Figure 4g), gypsum arenite, halite and small anhydrite nodules. This sequence is approximately 170 m thick. Grooves, folds, ripples and parallel laminations are frequently observed in gypsum. Varol & et al. (2015) and Güngör-Yeşilova & Yeşilova (2021) stated the existence of these formations as playa lakes and salt-mud flats. The evaporites here are Upper Miocene in age (Varol & et al., 2015; Güngör-Yeşilova & Yeşilova, 2021).

2.1.10.Ağrı-Doğubeyazıt basin

This basin's Lower-Miocene evaporites have a marine origin. Marl, limestone, gypsum, and fine-grained detrital rocks alternate with green marl and limestones at the beginning of this basin's sequence (Altınlı, 1953).

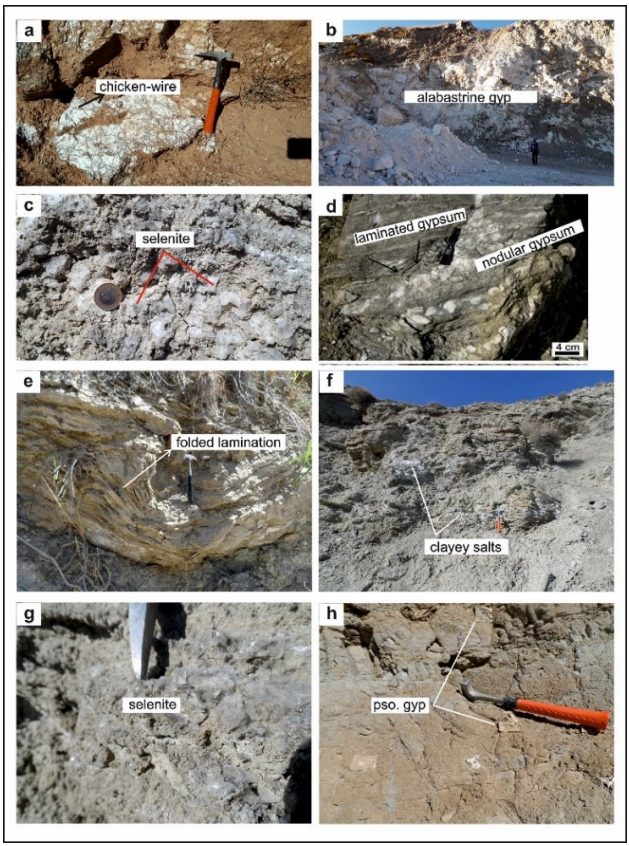

Figure 5. Evaporites belonging to the basins in the northern branch of Neotethys. (a) Clustered structures of the İliç-Kemah Basin, (b) gypsums with alabastrin texture (gyp) of the Erzincan-Kemah Basin, (c) selenites with carbonate intercalations of the Erzincan-Çayırlı Basin, (d) laminated and nodular gypsums of the Erzurum Aşkale Basin (modified Abdioğlu et al. 2015), (e) laminated-folded gypsums of the Tekman-Karayazı Basin, (f, g) recrystallized salts intercalated with clays and selenitic gypsum with carbonate intercalations of the Iğdır-Tuzluca Basin, (h) pseudomorphic gypsums in mudstone cracks of the Kağızman Basin (pso gyp).

2.2.Characteristics of evaporites in the basins located in the southern branch of Neotethys

2.2.1.Malatya-Darende basin

The Darende formation contains evaporites that are associated with this basin. The Late Eocene-aged units in this formation were formed in shallow waters. Light gray-brown gypsum alternations, marl, sandstone, claystone, conglomerate, and limestone make up the formation (Akkuş, 1971; Karaman & et al., 1993; Gedik, 2010). According to Karaman & et al. (1993) and Nazik, Gürbüz & Erdoğan (2016), the foraminiferal assemblage in this basin indicates that these evaporite units are Middle-Late Eocene in age. The layers of siltstone and sandstone contain load and flute cast traces from sedimentary structures. The sediments of the Eocene (Lutetian) sea began to fold with the Pyrenean orogenic phase. During this time, the sea lost its character and became an inland sea, and in this inland sea, gypsum formations that filled the center of the basin were deposited. The thickness of the gypsum increases from 3 meters to 12 meters at the base (Akkuş, 1970). The gypsum is observed as layered and laminated.

2.2.2.Malatya-Hekimhan basin

The Late Paleocene-Early Eocene Darende formation contains these evaporites, which were formed in a variety of environments, including continental, coastal, and shallow marine sabkha (Gürer, 1994; Yalçın & Bozkaya, 1996). Light gray gypsum makes up the evaporites in this basin, which are intercalated with red sandstone, siltstone, and marl (Figure 6). The gypsum exhibits chicken-wire, laminated, folded, and folded structures. Nonetheless, some gypsums exhibit chaotic folding, which could be the

consequence of syn-tectonic deformation or partial dissolution and collapse. Because of diagenetic processes, the gypsums have secondary textures like some alabastrine and porphyroblastic, and they are laterally discontinuous.

2.2.3.Elâzığ-Baskil-Kuşçular basin

The Elâzığ basin developed during the closure of the southern branch of Neotethys during the Tertiary period. Aktaş & Robertson (1984) define the boundary line of an active plate margin of southern Neotethys south of Elâzığ. The Tethyan sea became shallower during the Oligocene and retreated northward. Shallow marine carbonates and clasts accumulated in the basin from Oligocene to Early Miocene time (Aksoy, Türkmen & Turan, 2005). The evaporites here are in the Kuşçular formation in the southwest of Elâzığ, in the Baskil district (Figure 6). This formation contains terrestrial red beds including massive conglomerate, layered conglomerate, sandstone, mudstone and secondary gypsum (Türkmen, 2004). The gypsum is layered and intercalated with mudstone and sandstone. Secondary gypsum is observed as nodular and is observed between red-green mudstones or mudstone cracks. In addition, nodular, nodular banded gypsum and alabastrine satin-spar gypsum and chicken-wire structures are present (Türkmen, 2004) (Figure 7a). Gypsum crystals are common in the sandstone and most of the grains are cemented with gypsum. Anhydrite is found as very fine microcrystalline inclusions in the gypsum. These secondary gypsums are derived from anhydrite. This formation is Lower Paleocene in age and is of terrestrial origin (Figure 6). These evaporites are of terrestrial origin and were formed in the playa salt mud flats environment (Turan & Türkmen, 1996).

2.2.4.Elâzığ-Kovancılar basin

The evaporites in this basin are found in the Çaybağı formation in the vicinity of Kovancılar in the east of Elâzığ. They are Upper Miocene-Pliocene in age and have a lacustrine character. Elâzığ Çaybağı formation consists of conglomerate, sandstone, mudstone, claystones with coal intercalations, marl, tuffite and limestone (Türkmen, 1991). Conglomerates are generally red in color and are composed of andesite, basalt, sandstone and limestone pebbles. Mudstones are red in color and contain coal seams. Claystones are seen intercalated with coal. Very well preserved leaf traces are found in these. Claystones are gray, yellow in color, have many cracks and the cracks are filled with secondary gypsum with alabastrin texture (Türkmen, 1991).

2.2.5.Muş-Bulanık basin

This basin is located in the northeast of Muş. Evaporites in this basin consist of gypsum and anhydrite. Gypsum consists of primary and secondary gypsum. Primary and secondary gypsum are intercalated or alternated with beige-white colored marl, yellowish-gray claystone, siltstone and sandstone, yellowish-gray and red colored mudstone and limestone units (Güngör-Yeşilova, 2019) (Figure 6). Due to regional compressional tectonism, the layers in these places are very close to right angles and are generally observed as post-sedimentary folds (Şaroğlu & Yılmaz 1986). Primary and secondary gypsums are divided into lithofacies. They are distinguished as massive nodular, nodular banded and laminated banded secondary gypsum, discoidal (Figure 7b), selenitic and gypsum arenite primary gypsums (Güngör-Yeşilova & et al., 2020).

In addition, sedimentary structures such as chicken-wire, enterolithic structures, ripple marks and folds are observed (Figure 7c).

When evaluated with all these elements, it was determined that the evaporites in this basin were deposited in an environment ranging from shallow marine to lagoon and coastal sabkha (Güngör Yeşilova & et al., 2020). Isotope evidence indicated that this basin is of marine origin and Lower Oligocene age (Figure 6) (Güngör-Yeşilova & et al., 2020).

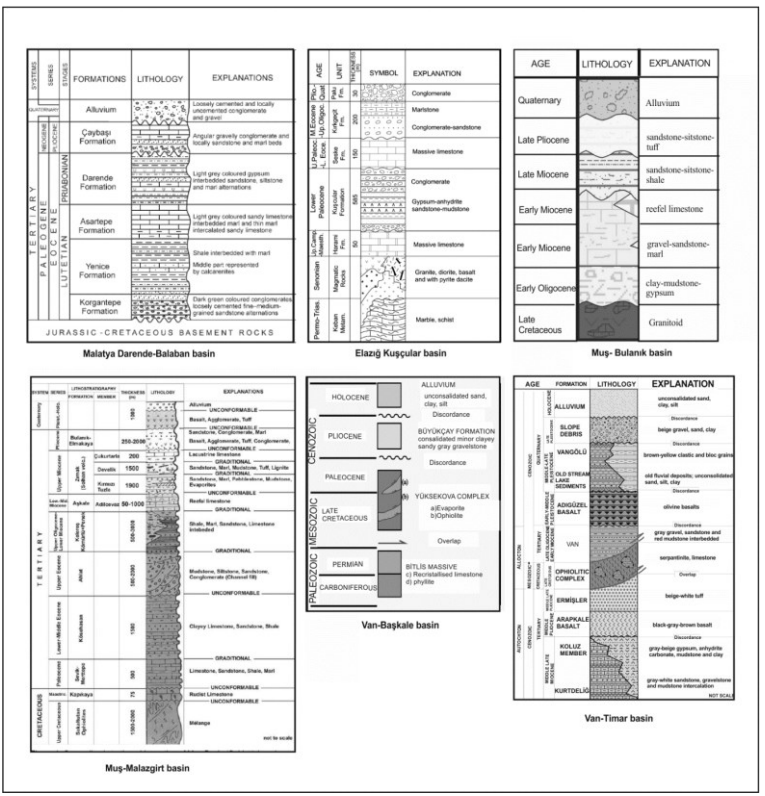

Figure 6. Generalized stratigraphic sections of the basins in the southern branch of Neotethys.

2.2.6.Muş-Malazgirt basin

This basin's evaporites are found in the Zırnak region's Aktuzla Formation (Figure 6). Conglomerate, sandstone, marl, mudstone, clay bands, carbonate, and gypsum make up the formation. In certain locations, these evaporites are intercalated with clasts and carbonate (Figure 7d). Arenite and selenitic gypsum make up the majority of these gypsums (Figure 7d). In certain locations, temperature, sedimentation, and diagenetic processes have converted these gypsums into anhydrite. These evaporites are marine in origin and date to the Lower Miocene (Aquitenian) based on stratigraphic and palynological data. The basin resembles a shallow platform lagoon (Sancay, 2005; İlker, 1966; Şenalp, 1966; Birgili, 1968).

2.2.7.Van-Timar basin

This basin is located in the Tuşba district in the northwest of Van. The evaporites here are within the Koluz gypsum member of the Middle-Late Miocene Kurtdeliği formation (Figure 6). These evaporites are Upper Miocene in age and are of terrestrial origin (Acarlar & et al., 1991; Ateş & et al., 2007; (Güngör-Yeşilova & Gökmen, 2020). These evaporites are composed of gypsum and anhydrite and are intercalated with limestone, dolomite, travertine, sandstone, claystone, mudstone, marl and clay interbands (Gökmen & Güngör-Yeşilova, 2017; Güngör-Yeşilova & Gökmen, 2020). The gypsums here are primary and secondary formations. Primary gypsums are separated as selenite, discoidal and radial. Some selenites are observed as carbonate or gypsum cemented (Figure 7e). Secondary gypsums are formed as massive, laminated, nodular and satin spar. Secondary gypsums are formed after the hydration of

anhydrite and anhydritized primary gypsums (Güngör-Yeşilova & Gökmen, 2020). Nodular anhydrites are encountered at some levels (Figure 7f). Tectonics, climate, salinity change, biological activity and diagenetic and hydrothermal fluids have played a major role in the formation and transformation of these sediments. According to all these data, Güngör-Yeşilova & Gökmen (2020) indicated that these evaporites were deposited in an environment ranging from mud flat to playa lake.

2.2.8.Van-Başkale basin

This basin is located southeast of Lake Van. Evaporites in this basin are overlain by the Yüksekova complex (Figure 6). Evaporites in this basin mainly consist of primary (selenite and gypsum arenite) and secondary (massive, laminated and satin-spar) gypsum lithofacies and also minor amounts of anhydrites and are intercalated and alternated with clastic and carbonate units. Primary gypsums are transformed into massive alabastrine textured gypsums with diagenesis (Figure 7g). Sedimentological-mineralogical and geochemical findings reveal that the depositional basin extended from a lagoon to the inner regions. These evaporites were subjected to diagenesis and alteration under the influence of hot-dry and slightly humid climate, tectonism and pressure. Isotope values indicate that these evaporites are of Lower Miocene marine origin (Güngör-Yeşilova & Baran, 2023).

2.2.9.Hakkâri basin

The evaporites are distributed in Narlı village of Çukurca district in the south of Hakkâri. These evaporites in the Kapıkaya formation are Early Miocene in age. Evaporites are interlayered and intercalated with red sandstone, mudstone, shale and limestone

(Duran & et al., 1988; Perinçek, 1990; Tetiker, Baran & Dinç, 2015). It consists of red-brown and gray mudstone, siltstone and sandstone intercalations with gypsum, tuffite and limestone. White gypsum minerals are found in sulfate rocks, and it has been determined that these minerals are accompanied by calcite and quartz minerals.

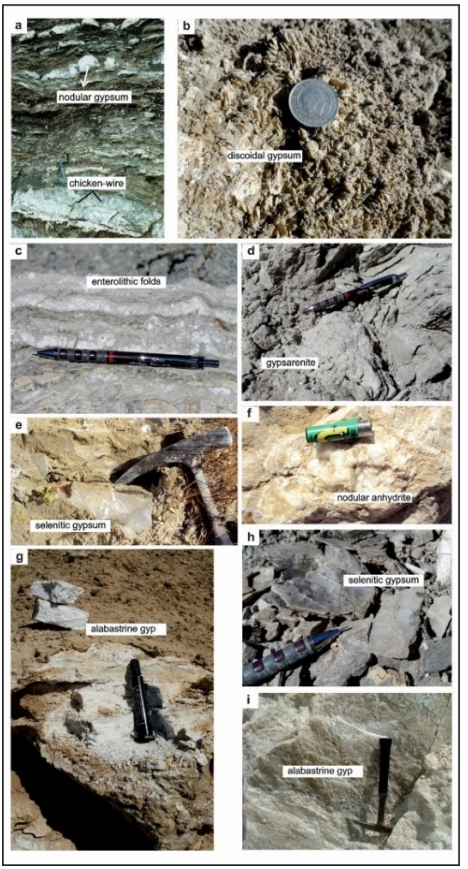

Figure 7. Evaporites belonging to the basins in the southern branch of Neotethys. (a) Nodular gypsums and clustered structures of the Elazığ-Kuşçular Formation (modified Türkmen, 2004), (b, c) Discoidal gypsum and enterolithic folds of the Muş Bulanık Basin,

(d) Gypsarenites with carbonate intercalations of the Muş-Malazgirt Basin, (e, f) Carbonate-cemented selenitic gypsum and nodular anhydrite of the Van-Timar Basin, (g) Alabastrin-textured massive gypsum (gyp) of the Van Başkale Basin, (h, i) Carbonate-intercalated selenitic gypsum (gyp) and alabastrin-textured gypsum of the Hakkari Basin.

Volcaniclastic levels accompanying rocks representing shallow marine sediments were fed by the Miocene volcanism active in the region and caused the formation of analcime and smectite minerals. Lower Miocene Kapıkaya formation unconformably overlies these units. The upper levels of Kapıkaya formation are represented by Zokayıt limestone member. The gypsum-bearing parts of the unit are defined as Derge Evaporite member (Perinçek, 1978). Red-brown and gray colored conglomerate-sandstone, siltstone and mudstone alternations are dominant in Kapıkaya Formation. However, evaporites (gypsum) are observed especially in the base levels and carbonate rocks (limestone) in the upper levels. The gypsums observed as intercalations in the lower part of the unit are white, 50-70 cm thick and have a layered appearance. The gypsums consist of transparent selenite and white colored alabastrine gypsum and satin-spar gypsum (Figure 7h, i).

These contain clay intercalations in the lower levels and have transformed into anhydrite. Considering the sedimentological features of these evaporites, it was determined that they were deposited in the shoreline-shallow marine environment (Duran & et al., 1988, 1989).

3.Conclusion

While the evaporites in the Upper Eocene-Oligocene Malatya Darende-Balaban basin located in the southern branch of

the Neotethys in Eastern Anatolia are of marine origin, the evaporites in the Elâzığ-Baskil basin (Kuşçular Formation) are of Early Paleocene lacustrine origin. Again, the evaporites in the Lower Oligocene (Rupelian) Muş-Bulanık-Malazgirt, Lower Miocene Muş-Zırnak Aktuzla Formation and Lower Miocene Van-Başkale basins located along the southern line of the Neotethys are of shallow marine-lagoon character, while the Van-Timar Basin is of Upper Miocene lacustrine character. The Upper Oligocene Erzincan-Kemah-Refahiye Basin evaporites located in the northwestern parts of the Eastern Anatolia Region and within the northern branch of Neotethys are of marine origin and contain shallow marine-lagoon-coastal sabkha environments, while the Tercan-Çayırlı basin evaporites located in the eastern parts of Erzincan are of Lower-Middle Miocene continental origin. Moving northeast, the Early-Middle Miocene Erzurum-Aşkale, Oligocene Erzurum-Hınıs and Upper-Eocene-Oligocene Erzurum-Karayazı basins evaporites were formed in shallow marine lagoonal environments, while the Erzurum-Tekman and Erzurum-Pasinler-Horasan evaporites were deposited in the Upper Miocene lacustrine environment. Further north, the evaporites in the Ağrı-Doğubeyazıt basin are of Lower-Middle Miocene age and of marine origin, while the evaporites in the Kars-Kağızman and Iğdır-Tuzluca basins are of Middle-Upper Miocene age and accumulated in a lacustrine environment. Accordingly, Erzincan and Erzurum basins contained shallow marine lagoonal environments in the Lower Oligocene, while Erzincan was still shallow marine and Erzurum was terrestrial-fluvial in the Upper Oligocene. While Erzurum and Ağrı basins were shallow marine in the Lower-Middle Miocene, the sea in the Erzincan basin completely regressed in the Middle Miocene and the

basin became terrestrial. Starting from the Upper Miocene, all basins located in the northern branch of Neotethys turned into terrestrial lacustrine and fluvial basins until the Pliocene.

Malatya and Elâzığ Basins contained shallow marine environments from the Late Eocene to the Middle Miocene, and Muş, Van and Hakkâri basins contained shallow marine lagoonal environments from the Lower Oligocene to the Middle Miocene. Later, all these basins transitioned to a terrestrial environment until the Middle-Late Miocene and Pliocene.

In other words, the northern and southern branches of Neotethys in Eastern Anatolia became shallower from the west towards the mountains from the Lower Oligocene to the Pliocene and were completely closed. While all these evaporitic basins were forming, the paleogeographic conditions of that period such as climate, tectonism and volcanism also came to the fore in their formation.

References

Abdioğlu, E., Arslan, M., Aydınçakır, D., Gündoğan, İ. & Helvacı, C. (2015). Stratigraphy, mineralogy and depositional environment of the evaporite unit in the Aşkale (Erzurum) sub - basin, Eastern Anatolia (Turkey). *Journal of African Earth Sciences*, 111, 100-112.

Abdioğlu Yazar, E., Arslan, M., Helvacı, C., Gündoğan, İ., Temizel, İ. & Aydınçakır, D. (2021). Geochemistry of Miocene evaporites from the Aşkale region (Erzurum, Eastern Turkey): constraints for Paleo-environment. *Bulletin of Mineral Research and Exploration*, 165, 113-140

Acarlar, M., Bilgin, Z. A., Erkalın, T., Güner, E., Şen, A. M., Umut, M., Elibol, E., Gedik, İ., Hakyemez, Y. & Uğuz, M. F. (1991). *Van Gölü doğu ve kuzeyinin jeolojisi*. Ankara: MTA

Akkuş, M. F. (1970). Darende-Balaban havzasındaki (Malatya, ESE Anadolu) litostratigrafik birimler ve jipsli formasyonların yaşı hakkında yeni bilgiler. *M.T.A. Dergisi*, 75.

Akkuş, M. F. (1971). The geologic and stratigraphical research of Darende-Balaban Basin (Malatya ESE Anatolia). *Miner. Res. Explor. Inst., Bull*., 76, 1-60.

Aksoy, E., Türkmen İ & Turan, M. (2005). Tectonics and sedimentation in convergent margin basins: an example from the Tertiary Elâzığ basin, Eastern Turkey. *Journal of Asian Earth Sciences,* 25 (3), 459-472.

Aktaş, G., Robertson, A. H. F. (1984). The Maden Complex, SE Turkey: evolution of a Neotethyan continental margin. In: Dixon, J.E. & Robertson, A. H. F (Eds.), *The geological evolution of the*

Eastern Mediterranean. (pp. 375-402). London: Geol. Soc., Spec. Publ.

Aktimur, H. T., Sarıaslan, M., Kecer, M., Tursucu, A., Olcer, S., Yurdakul, M. E., Mutlu, G., Aktimur, S. & Yıldırım, T. (1995). *Erzincan dolayının jeolojisi*. Ankara: Mineral Research and Exploration Institute

Allen, C. R. (1969). Active faulting in Northern Turkey. California: Inst. Technology, Division of Geological and Planetary Sciences

Altınlı, İ. E. (1953). *Hakkâri güneyinin jeoloji incelemesi*. Ankara: TPAO

Altunsoy, M. (1993). *Karacaören (İmranli)-Diktaş (Divriği) yöresi Tersiyer çokellerinin sedimanter petroloji, petrol ana kayası ve organik fasiyes özelliklerinin incelenmesi*. Sivas: University of Cumhuriyet

Arpat, E. (1964). *Erzincan Çayırlı bölgesinin petrol olanakları.* Ankara, MTA

Arpat, E. & Şaroğlu, F. (1972). Doğu Anadolu fayı ile ilgili bazı gözlemler ve düşünceler. *MTA Dergisi*, 78, 44-50.

Ateş, Ş., Mutlu, G., Özerk, O. C., Çiçek, İ. & Gülmez, F. A. (2007). *Van ili kentleşme alanları yer bilim verileri*. Ankara: MTA

Aydınçakır, D. (2013). *Pırnakapan (Aşkale, Erzurum) civarındaki evaporitlerin mineralojik, petrografik ve jeokimyasal incelenmesi*. Trabzon: Karadeniz Teknik Üniversitesi, Fen Bilimleri Enstitüsü

Ayyıldız, T., Varol, B., Gündoğan, İ., Herece, E. & Sirel, E. (2018). *Tekman-Karayazı Havzası (GD Erzurum) Tersiyer birimlerinin sedimantolojisi ve petrol jeolojisi*. Ankara: Tübitak

Aziz, A. (1971). *Erzurum İ46b-4 v e İ46c-l paftalarının detay jeolojisi ve petrol olanakları*. Ankara: MTA

Barka, A. A. & Gülen, L. (1989). New constraints on the age and total offset of the North Anatolian fault zone: implifications for tectonics of the Eastern Mediterranean Region, METU. *J Pur App Sci*, 21, 39–63.

Batı, Z. & Sancay, R. H. (2007). Palynostratigraphy of Rupelian sediments in the Mus Basin, Eastern Anatolia, Turkey. *Micropaleontology*, 53, 249–283.

Bilgiç, T. (2008). *Geological maps of Turkey in 1: 100.000 scale: Divriği J39, J40, J41 sheets*. Ankara: the General Directorate of Mineral Research and Exploration of Turkey, Spec. Publ.

Birgili, Ş. (1968). *Muş bölgesi 1:25 000 ölçekli Karaköse J48-d3-d4 ve Muş K47-b2 paftalarının detay petrol etüdü hakkında rapor.* Ankara: MTA

Cater, I. M. L., Hanna, S. S, Ries, A. C. & Tuner, P. (1991). Tertiary evolution of the Sivas Basin, Central Turkey. *Tectonophysics*, 195, 29-46.

Dağıstan, H. & Şimşek, S. (2005). Geological and hydrogeological investigation of Kozluk-Taşlıdere (Batman) geothermal field. *Proceedings World Geothermal Congress*, 24-29 April 2015, Antalya, (pp. 1–8).

Doğan, U. (2005). Holocene fluvial development of the Upper Tigris Valley (Southeastern Turkey) as documented by archaeological data. *Quaternary International,*129 (1), 75-86.

Duran, O., Şemşir, D., Sezgin, L. & Perinçek, D. (1988). Güneydoğu Anadolu'da Midyat ve Silvan Gruplarının stratigrafisi, sedimantolojisi ve petrol potansiyeli. *TPJD Bülteni*, 1 (2), 99-126.

Duran, O., Şemşir, D., Sezgin, L. & Perinçek, D. (1989). *Güneydoğu Anadolu'da Midyat ve Silvan Gruplarının stratigrafisi, sedimantolojisi ve paleocografyası, paleontolojisi, jeoloji tarihi, rezervuar ve diyajenez özellikleri ve olası petrol potansiyeli*. Ankara: TPAO Araştırma Merkezi

Erdoğan, T. (1972). *Erzurum (Karayazı) bölgesinin jeolojisi ve petrol imkanları*. Ankara: MTA

Fairbridge, R., Erol, O., Karaca, M. & Yilmaz, Y. (1997). Background to Mid-Holocene climatic change in Anatolia and adjacent regions. In H. N. Dalfes, G. Kukla, H. Weiss (Eds.), *Third millennium bc climate change and old world* (pp. 595-609). Berlin: Springer

Gedik, A. (1985). Geology of the Tekman (Erzurum) basin and petroleum possibilities. *Bull. Miner. Res. Explor*., 103 (103–104), 1–24.

Gedik, F. (2010). Benthic foraminiferal description and biostratigraphy of Oligo-Miocene shallow-water sediments of Malatya basins. Ankara: University of Ankara

Gökmen, D. & Güngör- Yeşilova, P. (2017). Karaağaç-Ermişler Köyü (KD Van) civarındaki Kurtdeliği Formasyonuna ait

jipsli birimlerin diyajenetik süreçleri ve depolanma ortamı. 7*0. Türkiye Jeoloji Kurultayı*, 10- 14 Nisan 2017, Ankara, Türkiye.

Gökten, E. (1983) Şarkışla (Sivas) güney-güneydoğusunun stratigrafisi ve jeolojik evrimi. *Geological Bulletin of Turkey*, 26, 167-176

Güngör-Yeşilova, P. & Helvacı, C. (2013). Kurtalan sahası (GB Siirt) Germik Formasyonu Oligosen evaporitlerinin diyajenezi ve paleocoğrafik gelişimi, Türkiye. *Yerbilimleri Uygulama ve Araştırma Merkezi Dergisi*, 34, 1-22.

Güngör-Yeşilova P., Gökmen D & Yeşilova Ç. (2017). Orta-Geç Miyosen Koluz Üyesi jipsli birimlerinin paleocoğrafik evrimi ile birlikte sedimantolojik parametreler, Doğu Anadolu Bölgesi (KD Van): Neotetis Okyanusunun Kapanması ile İlgili Bir İç Havza. *Sedimantoloji Çalışma Grubu*, 14- 17 Eylül 2017, Rize, Türkiye, (pp.30-31).

Güngör-Yeşilova, P. & Helvacı, C. (2017). Petrographic study and geochemical investigation of the evaporites associated with the Germik Formation (Siirt Basin, Turkey). *Carbonates and Evaporites*, 32 (2), 177-194.

Güngör-Yeşilova, P. (2019). Bulanık (KD Muş) çevresindeki karasal evaporitlerin depolanma koşulları ve diyajenetik gelişimi ile ilgili parametreler (Doğu Anadolu, Türkiye). *IMCOFE*, 24- 26 Nisan 2019, Antalya, Türkiye, (pp.1-2).

Güngör-Yeşilova, P. & Gökmen, D. (2020). The paleodepositional environment, diagenetic and depositional conditions of the Middle-Late Miocene Koluz gypsum member (NE Van, Eastern Turkey). *Carbonates and Evaporites*, 35, 3.

Güngör-Yeşilova, P., Yeşilova, Ç., Açlan, M. & Gündoğan, I. (2020). Geochemical characteristics of gypsum lithofacies in northeastern of Muş (Eastern Anatolia-Turkey): an indication of the Neotethys closure. *Carbonates and Evaporites*, 35, 4.

Güngör-Yeşilova, P. (2020). Bulanık (Muş) Paleojen evaporitlerinin petrografik- mineralojik incelemesi ve diyajenetik tarihçesi. *Maden Tetkik ve Arama Dergisi*, 162, 83-92.

Güngör-Yeşilova, P. & Yeşilova, Ç. (2021). Depositional basin, diagenetic conditions and source of miocene evaporites in the Tuzluca Basin in Northeastern Anatolia, Turkey: Geochemical Evidence. *Geochemistry International*, 59 (13), 1293-1310.

Güngör-Yeşilova, P. (2021). Kaledibi-Çiftlikköy köyleri arasındaki jipsli istifin litofasiyes özellikleri ve çökelme ortamları (Erzincan Havzası-Doğu Anadolu). *Sedimantoloji Çalışma Grubu*, 2- 05 Eylül 2021, Balıkesir, Türkiye.

Güngör-Yeşilova, P. & Yavuz, Ş. (2021). Sedimentological and mineralogical-petrographic characteristics of Miocene evaporitic deposits (SW Erzincan). *Manas Journal of Engineering*, 9 (1), 1-16.

Güngör-Yeşilova, P. & Baran, O. (2023). origin and paleoenvironmental conditions of the Köprüağzı evaporites (Eastern Anatolia, Turkey): sedimentological, mineralogical and geochemical constraints. *Minerals*, 13 (2), 1-21.

Güngör-Yeşilova, P. (2024). Post-halite gypsum pseudomorphs with evidence of challenging climatic conditions and diagenetic replacement: a study from the southwest of Kağızman

Basin (Eastern Anatolia, Türkiye). *Bulletın of the Mineral Research and Exploration*, 174, 111-124.

Güngör-Yeşilova, P. (2024). Genesis of sulfate lithofacies between Erzincan-Divriği Basin with sedimentologic and geochemical evidences: an example from the Paleogene basins of Eastern Turkey. *Carbonates and Evaporites*, 39 (4), 103.

Gürer, Ö. F. (1994). Hekimhan-Hasançelebi yöresinin Üst Kretase stratigrafisi ve havza evrimi. *Türkiye Jeoloji Bülteni*, 37 (2), 135-148.

Gürer, Ö. F. & Gürer, A. (1999). Development of evaporites and the counterclockwise rotation of Anatolia, Turkey. *Int Geol Rev*., 41, 607–622.

Havur, E. (1972). *Erzurum I-47 C1, C2, D2, D3 paftalarının jeolojisi ve petrol imkanları*. Ankara: MTA

Hempton, M.R. & Dunne, L.A. (1984). Sedimentation in pullapart basins: Active example in eastern Turkey. *The Journal of Geology*, 92, 513–530

Hoşgörmez H., Yalçın M. N., Soylu, C. & Bahtiyar İ. (2014). Origin of the hydrocarbon gases carbon dioxide and hydrogen sulfide in Dodan Field (SE-Turkey). *Marine and Petroleum Geology*, 57, 433-444.

Hüsing, S. K., Zachariasse, W. J., Van Hinsbergen, D. J., Krijgsman, W., İnceöz, M., Harzhauser, M., Mandic, O. & Kroh, A. (2009). Oligocene Miocene basin evolution in SE Anatolia, Turkey: constraints on the closure of the eastern Tethys gateway. *Geo Soc Lon Spec Pub*, 311, 107–132.

İlker, S. (1966). *Erzurum bölgesinde Erzurum i47c1, c4, d2, d3 paftalarının detay petrol etüdü hakkında rapor.* Ankara: MTA

Karadenizli, L., Saraç, G., Şen, S., Seyitoğlu, G., Gedik, F., Kangal, Ö., Kayakıran, I., Kazancı, N., Gül, A. & Erten, H. (2009). *Batı ve Orta Anadolu Oligosen paleocoğrafyası*. Ankara: The General Directorate of Mineral Research and Exploration

Karadenizli, L., Varol, B. E., Saraç, G. & Gedik, F. (2016). Late Eocene-Early Miocene palaeogeographic evolution of Central Eastern Anatolian Basins, the closure of the Neo-Tethys Ocean and continental collision. *J. Geol. Soc. Ind.*, 88, 773–798.

Karaman, T., Poyraz, N., Bakırhan, B., Alan, I., Kadınkız, G.,Yılmaz, H. & Kılınç, F. (1993). *Malatya-Doğanşehir-Çelikhan dolayının jeolojisi*. Ankara: The General Directorate of Mineral Research and Exploration

Kavak, K. S. (1998). S*avcun ve Karacaören (Sivas GD'su) yöresinde Sivas Tersiyer Havzasinin tektonostratigrafisi, tektonik deformasyon biçimi ve sayısal görüntü işlem yöntemiyle incelenmesi*. Sivas: University of Cumhuriyet

Koçyiğit, A. (1991). Changing stress orientation in progressive intercontinental deformation as indicated by the Neotectonics of the Ankara Region (NW Central Anatolia), *Bull. Turk. Assoc. Petrol. Geol*., 31 (1), 48-55.

Kurtman, F. (1971) Sivas-Divriği arasındaki sahanın jeolojisi ve jipsli seri hakkında müşahadeler. *MTA Derg*isi, 56, 14-25.

Kurtman, F. (1973). Sivas-Hafik-Zara ve İmranlı bölgesinin jeolojik ve tektonik yapısı. *Bull. General Directorate of Mineral Research and Exploration of Turkey*, 80, 1-32.

Luttig, G. & Steffens, P. (1976). Explanatory notes for the paleogeographic atlas of Turkey from the Oligocene to Pliocene. *Bundesanstalt für Geowissenchaften und Rohstoff*, 1, 121.

Nazik, A., Gürbüz K & Erdoğan, D. (2006). Biostratigraphy and paleoenvironmental interpretation of Middle Eocene sequences from Darende-Balaban Basin (Eastern Anatolia, Turkey). *Geologica Carpathica*, 57 (2), 91-101.

Okay, A. I., Zatin, M. & Cavazza, W. (2010). Apatite fission-track data for the Miocene Arabia-Eurasia collision. *Geology* 38, 35-43.

Özdoğan, T., Kaya, O., Açıkbaş, I., Bahtiyar, I., & Siyako, M. (2011). The Miocene Lice basin of southeastern Turkey: an example of a shallow to non-marine foreland basin. Achaean to Anthropocene. *Geological Society of America Annual Meeting and Expos*, 146–148.

Özgül, N. C., Turşucu, A., Özyardımcı, N., Şenol, M., Bingöl, İ. & Uysal, Ş. (1981). *Munzur dağlarının jeolojisi*. Ankara: MTA

Özkaya, İ. (1974). Güneydoğu Anadolu Sason ve Baykan yöresinin stratigrafisi. *TMMOB JMO Yayınları*, 17, 51-72.

Palmer, M. R., Helvacı, C. & Fallick, A. E. (2004). Sulphur, sulphate oxygen and strontium, isotope composition of Cenozoic Turkish evaporates. *Chem. Geol*., 209, 341–356.

Perinçek, D. (1978). V-VI-IX. *Bölge (Güneydoğu Anadolu otokton-allokton birimler) jeoloji sembolleri*. Ankara: TPAO

Perinçek, D. (1990). Hakkâri ili ve dolayının startigrafisi, GDA Türkiye. *TPJD Bülteni*, 2, 21-68.

Platzman, E. S., Platt, J. P., Tapırdamaz, C., Sanver, M. & Rundle, C. C. (1994). Why are there no clockwise rotations along the North Anatolian Fault Zone? *J. geophys. Res*., 99, 21705-21715.

Poisson, J. C., Guezou, A., Özturk, S., İnan, H., Temiz, H., Gürsöy, K.S., Kavak, S. & Özden, S. (1996). Tectonic setting and evolution of the Sivas Basin, Central Anatolia, Turkey. *Int. Geol. Rev*., 38, 838–853.

Robertson, A. H. F., Ustaömer, T., Parlak, O., Ünlügenç, U. C., Taşlı, K. & İnan, N. (2006). The Berit transect of the Tauride thrust belt, S Turkey: Late Cretaceous–Early Cenozoic accretionary/collisional processes related to closure of the Southern Neotethys. *J. Asian Earth Sci*., 27, 108–145.

Robertson, A. H. F., Parlak, O., Rızaoğlu, T., Ünlügenç, U., İnan, N., Taşlı, K. & Ustaömer, T. (2007). Tectonic evolution of the south Tethyan ocean: evidence from the Eastern Taurus Mountains (Elâzığ region, SE Turkey). In A. C. Ries, R. W. H Butler, & R. H Graham (Eds.), *Deformation of the continental crust: the legacy of mike coward* (pp. 231–270). London: Geological Society, Special Publications

Sancay, R. H. (2005). *Palynostratigraphic and palynofacies investigation of the Oligocene-Miocene units in the Kars-Erzurum-Muş subbasins (Eastern Anatolia)*. Ankara: Middle East Technical University.

Saygılı, R. (2020). Doğu Anadolu Bölgesinin haritası. (10/11/2024 tarihinde http://cografyaharita.com adresinden ulaşılmıştır).

Sirel, E. & Gedik, F. (2011). Postmiogypsinella, a new Miogypsinidae (Foraminifera) from the Late Oligocene in Malatya Basin, Turkey. *Revue de Paleobiologie*, 30(2), 591-603.

Soytürk, N. (1973). *Murat baseni jeolojisi ve hidrokarbon olanakları*. Ankara: TPAO Arama Grubu

Steininger, F. F., Senes, J., Kleemann, K. & Rögl, F. (1985). *Neogene of the Meditteranean Tethys and Paratethys*. Vienna: International Geology Correlation Programme

Stocklin, J. (1968) Structural History and Tectonic of Iran: A Review. American Association of Petroleum Geologists Bulletin, USA, 52, 1229-1258.

Sungurlu, O. (1971). *İ45a, İ45b, İ46a, İ46b, İ47a, İ47b, paftalarına ait 1/50000'lik jeoloji haritaları*. Ankara: TPAO

Sümengen, M., Terlemez, İ., Bilgiç, T., Gürbüz, M., Ünay, E., Ozaner, S. & Tüfekçi, K. (1987). *Şarkışla-Gemerek dolayı Tersiyer Havzasının stratigrafisi, sedimantolojisi ve jeomorfolojisi*. Ankara: The General Directorate of Mineral Research and Exploration

Şahintürk, Ö. & Kasar, S. (1979). *Tekman-Pasinler-Kağızman-Tuzluca Basenlerinin stratigrafik ve tektonik analizleri ile hidrokarbon olanakları*. Ankara: TPAO

Şahintürk, Ö. (1992). *Tercan- Çayırlı Basenlerinin jeolojisi ve hidrokarbon olanakları*. Ankara: TPAO Arama Grubu

Şahintürk, Ö., Şaroğlu, F. & Çaptuğ, A. (1988b). *Doğu Anadolu (Erzurum Kars-Doğubeyazıt-Ağrı) jeoloji gezisi el kitabı*. Ankara: TPAO Arama Grubu

Şaroğlu, F. & Yılmaz, Y. (1984). Doğu Anadolu'nun neotektoniği ve ilgili magmatizması. *İhsan Ketin Sempozyumu*, 20-21 Şubat 1984, Ankara, (pp. 149-162).

Şaroğlu, F. &Yılmaz, Y. (1986). Geological evolution and basin models during neotectonic episode in the Eastern Anatolia. *Bulletin of the Mineral Research and Exploration*, 107, 70-93.

Şen, S, Antoine, P. O., Varol, B., Ayyıldız, T. & Sözeri, K. (2011). Giant rhinoceros Paraceratherium and other vertebrates from Oligocene and Middle Miocene deposits of the Kağızman-Tuzluca Basin Eastern Turkey. *Naturwissenschaften*, 98, 407-423.

Şenalp, M. (1966). *Erzurum-Muş bölgesi l :25 000 ölçekli Erzurum J47-32, J47-b1 ve Karaköse J48-c1, c2, c3, c4, J48-b3 paftalarının detay petrol etüdü*. Ankara: MTA

Şenalp, M. (1969) *Tuzluca (Kars) havzasının 1:25 000 ölçekli detay petrol etüdü raporu*. Ankara: MTA

Şengör, A. M. C. (1979). The North Anatolian Transform Fault: Its age, offset and tectonic significance. *Jour. Geol. Soc*., 136, 269-282.

Şengör, A. M. C. & Yılmaz, Y. (1981). Tethyan evolution of Turkey: a plate tectonic approach. *Tectonophysics,* 75, 181-241.

Şengör, A. M. C. & Canıtez, N. (1982). The North Anatolian Fault. In H. Berekhemer, K. Hsü (Eds.), *Alpine-Mediterranean*

geodynamics (7th ed., pp. 205–216). Washington: Am. Geophys. Union

Şengör, A. M. C. & Yılmaz Y. (1983). Türkiye'de Tetis'in evrimi; levha tektoniği açısından bir yaklaşım. T*ürkiye Jeoloji Kurumu Yerbilimleri Özel Dizisi*, 1, 3-73.

Tanrıverdi, K. (1971). *Erzurum (Söylemez) yöresinin jeolojisi ve petrol olanakları*. Ankara: MTA

Tatar, Y. (1978). Kuzey Anadolu Fay zonunun Erzincan-Refahiye arasındaki bölümü üzerinde tektonik incelemeleri. *Yerbilimleri Dergisi*, 4, 201-236.

Temiz, H., Guezou, J. C., Tatar, O., Ünlügenç, U. C. & Poisson, A. (2002). Tectonostratigraphy of the Tercan-Cayırlı Basin: Implications for the Neogene-Quaternary tectonic deformation of the Northeast Anatolian Block, Turkey. *Internatıonal Geology Revıew*, 44 (3), 243-253.

Tetiker, S., Baran H. A. & Dinç, S. (2015). Alt Miyosen yaşlı Kapıkaya Formasyonu'nun (Siirt-Kapıkaya) mineralojik özellikleri. *Batman Üniversitesi Yaşam Bilimleri Dergisi*, 5 (2), 129-146.

Turan, M. & Türkmen, İ. (1996). Stratigraphy and sedimentological features of Kuşcular Formation (Lower Paleocene). *Turkish Journal of Earth Sciences,* 5, 109-121.

Türkmen, İ. (1991). Stratigraphy and sedimentological features of Çaybağı Formation (Upper Miocene-Pliocene) in the eastern Elâzığ. *Bulletin of Turkish Geological Society*, 34 (1), 45-53.

Türkmen, İ. (2004). Facies and evaporite genesis of the Kuşçular Formation (Lower Paleocene) saline playa complex, eastern Turkey. *J. Asian Earth Sciences*, 24 (1), 91-104.

Varol, B., Şen, S., Ayyıldız, T., Sözeri, K., Karakaş, Z. & Métais, G. (2015). Sedimentology and stratigraphy of Cenozoic deposits in the Kağızman-Tuzluca Basin, Northeastern Turkey. *International Journal of Earth Sciences*, 105, 107-137.

Yalçın, H. & Bozkaya, Ö. (1996). A new discovery of the Cretaceous/Tertiary boundary from the tethyan belt, Hekimhan basin, Turkey: Mineralogical and geochemical evidence. *International Geology Review*, 38 (8), 759-767.

Yazgan, E. (1987). Geology of the northeastern Malatya and geodynamical evolution of Eastern Taurides. *Miner. Res. Explor. Inst. Turkey Report,* 2268, 1-178.

Yeşilova, Ç., Güngör-Yeşilova P. & Helvacı, C. (2011). Baykan-Kurtalan-Şirvan (Siirt) Bölgesinin jeolojisi ve bölgedeki tuzlu birimlerin incelenmesi. *64. Türkiye Jeoloji Kurultayı*, 25-29 Nisan 2011, Ankara, Türkiye, (pp.301-302).

Yeşilova, Ç & Helvacı, C. (2012). Stratigraphy, sedimentology and paleogeographical evolution of the Lice Formation, (Siirt, SE Turkey). *International Earth Sciences Congress on Aegean Regions* (IESCA 2012), 1- 05 Ekim 2012, İzmir, Türkiye, (pp. 83).

Yeşilova, Ç. & Helvacı, C. (2012). Lice Formasyonu evaporitleri ve killerinin ekonomik önemi: Baykan Kurtalan Şirvan Bölgesi (Siirt). *Yüzüncü Yıl Üniversitesi Fen Bilimleri Enstitüsü Dergisi*, 12 (2), 72-78.

Yeşilova, Ç. & Helvacı, C. (2013). Batman-Siirt kuzeyi stratigrafisi ve sedimantolojisi. *Türkiye Petrol Jeologları Derneği Bülteni*, 23 (2), 7-43.

Yeşilova P. G., Yeşilova Ç & Açlan, M. (2015). Sıradere-Doğanbey Köyü Civarı (KD Muş Havzası) evaporitli çökellerinin depolanma ortamına ön yaklaşım. *68. Türkiye Jeoloji Kurultayı*, 6-10 Nisan 2015, Ankara, Türkiye, (pp.580-581).

Yeşilova, Ç., Helvacı, C. & Carrillo, E. (2018). Evaporitic sedimentation in the Southeastern Anatolian Foreland Basin: New insights on the Neotethys closure. *Sedimentary Geology*, 369, 13-27.

Yılmaz, A., Terlemez, İ., Uysal, S. (1988). Some stratigraphic and tectonic characteristics of the area around Hınıs (southeast of Erzurum). *Bull. Miner. Res. Explor. Inst. Turk*., 108 (108), 1–21.

Yılmaz, Y. (1993). New evidence and model on the evolution of the southeast Anatolian orogen. *Geol. Soc. Am. Bull*., 105, 251–271.

Yılmaz, S., Boztuğ, D. & Öztürk, A. (1993). Geological setting, petrographic and geochemical characteristics of the Cretaceous and Tertiary igneous rocks in the Hekimhan–Hasançelebi area, northwest Malatya, Turkey. *Geol. J*., 28, 383–398.

Yılmaz, A. & Yılmaz, H. (2013). Ophiolites and ophiolitic melanges of Turkey: a review. *Turk. Jeol. Bul*., 56 (2), 61-114.

Yılmaz, A. & Yılmaz, H. (2019). Structural evolution of the Eastern Anatolian Basins: An example from collisional to postcollisional tectonic processes, Turkey. *Turkish Journal of Earth Sciences*, 28, 329-3

CHAPTER IV

Natural Monument and Geological Key; Adilcevaz (Eastern Anatolia) Tufas

Çetin YEŞİLOVA[1]
Esin ÜNAL[2]

Inroduction

The Lake Van Basin is located on the Eastern Anatolian Plateau. The plateau is a product of the compression regime that was effective after the continent-continent collision between the Eurasian and Arabian plates. Considering its geological and geomorphological features, the basin is a unique data bank in the region.

In Adilcevaz District, these tufas, which are trapped within residential areas, serve as the neighborhood's garbage area and are constantly damaged under the plowed fields. The rapidly developing

[1] Doç. Dr., Yüzüncü Yıl University Department of Geological Engineering, 65080, VAN, TURKEY ORCID ID: 0000-0002-8884-0842, cetinyesilova@yyu.edu.tr
[2] Dr. Öğr. Üyesi., Yüzüncü Yıl University Department of Geological Engineering, 65080, VAN, TURKEY ORCID ID: 0000-0002-8337-4651, esinunal@yyu.edu.tr

culture of protection today is promising in the protection of such natural structures. It should not be forgotten that not only cultural heritage but also such geological elements should be protected and all these beauties should be transferred to future generations without any problems.

Geological events and structures are the largest and most important source in understanding the evolution of the world. They help us understand many important data such as sea level fluctuations, the state of glaciers, volcanic activities, earthquakes, mass destructions and climate change throughout the world's history. According to ProGEO 2011, some of these geological and geomorphological elements are unique in the world and are rarely observed. All these elements should be evaluated as geological heritage. The Van Lake basin, which is a product of the compression regime effective after the continent-continent collision between the Eurasian and Arabian plates (Görür et al., 2015), and some of the geological-geomorphological elements in this basin can be included in the scope of geological heritage according to the above definition. The Van Lake Basin is a natural laboratory with both the lacustrine sediments and the structures it contains, and the travertines and tufas that surface in the region. At the same time, the region is a school of volcanism when considering the volcanoes of Nemrut, Ağrı, Süphan, Tendürek, Meydan, Etruscan and many others.

Lake Van, the world's largest soda lake with a history of 600,000 years (Cukur et al. 2014b; Stockhecke et al., 2014), has great importance with its formation, development, geological and geomorphological elements, and hosting many civilizations over the centuries. The sediments and rocks deposited on the shores of Lake Van, as well as the sediments accumulated on the bottom of Lake

Van, contain very valuable information in terms of lake records. In this context, the tufa formations deposited on the shores of Lake Van are geological heritage that should be protected and transferred to future generations, considering the data they contain and the beauty they offer.

The oldest units in the study area are the Lower Miocene Adilcevaz limestones. Quaternary Süphan Volcanics unconformably overlie the Adilcevaz limestones (Yeşilova and Yakupoğlu, 2008). Quaternary lacustrine sediments, travertine, tufa and old alluviums unconformably overlie all these units (Fig. 1). Apart from these, many evaporite, travertine and tufa formations attract attention in the Lake Van and surroundings (Güngör-Yeşilova and Gökmen, 2020; Güngör-Yeşilova et al., 2020; Güngör-Yeşilova and Baran, 2023; Yeşilova, 2019; Yeşilova et al., 2015a, b; 2017, 2019, 2021, 2024).

In this study, the formation conditions, importance and preservation of the Adilcevaz Tufas, which were observed in the Adilcevaz District of Bitlis Province (the area between Lake Van and Süphan Volcano) and attract attention with their similarities to the Mono Lake Tufas, will be discussed. The Adilcevaz Tufas are sediments that were deposited between 112.7 and 19.3 ka, 1701 - 1725 masl, and exhibit visually magnificent features (Yesilova et al., 2019). These natural monuments, which were determined to have deposited on the shores of Paleo Lake Van, play a key role in the region in terms of both the level changes of Lake Van and the climate. With these features, tufas, which have a unique geological importance, also offer a unique visual feast.

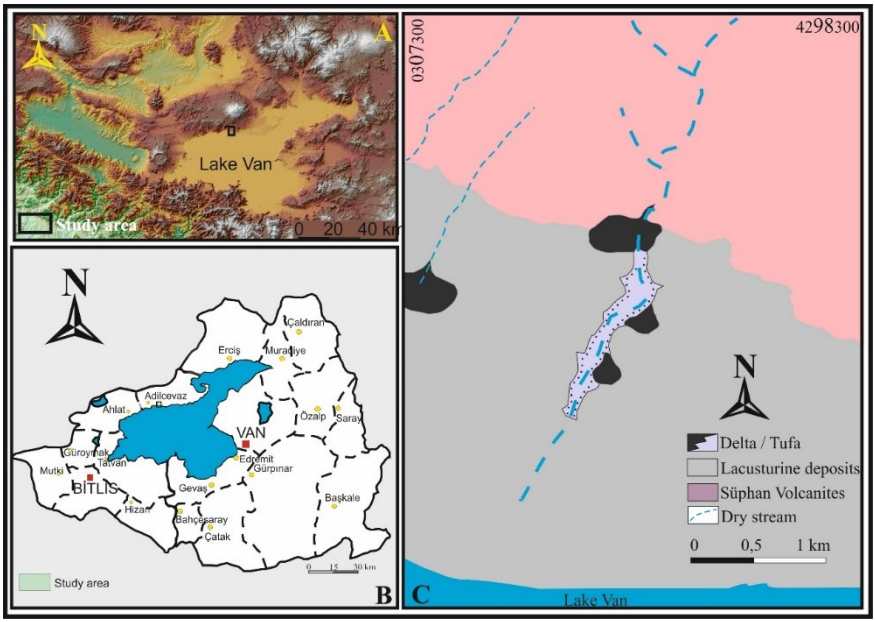

Figure 1. Location (A) and geological map (B) of the study area.

Adilcevaz Tufaları

Tufa is the general name for rocks with dense calcium carbonate and organic content deposited by cold waters with high alkalinity (Whiticar and Seuss, 1998; Perissinotto et al., 2014). Due to both their formation characteristics and composition, they are important in determining the conditions of the depositional environment (Ford and Pedley, 1996, Pentecost, 2005), climate and water level changes (Wright, 1914; Council and Bennett, 1993; Pentecost, 2005; Szabo et al. 1996). The development of tufas occurs best in humid and temperate climates (Schuster 1926; Goudie et al. 1981; Almendinger and Leete 1998; Dramis et al. 1999; Zak et al. 2002; Auque et al. 2013; Grube and Usinger 2016).

The tufas in the study area are formed within the thick sand stacks on the lake shore (Yeşilova et al., 2019, 2024 Nar, 2023). The

surrounding streams and fractures and cracks under the lake help to transport calcium-rich waters into these thick sand stacks (Yeşilova et al., 2019, 2024 Nar, 2023). Thus, the thick sand stacks serve as reservoir rocks for calcium-rich fresh waters. When the salty and denser lake waters encounter these sand stacks, the less dense fresh waters will move upwards and precipitate the calcium in their content (Kremer et al., 2019). Thus, unlike microbialites, tufa formation will occur within the thick sand stacks on the lake shore (Yeşilova et al., 2019, 2024 Nar, 2023). This tufala, which is formed due to lake level changes, can be found in the lake (rise in water level) or above the lake level (decrease in water level). Adilcevaz Tufas were also formed when Lake Van was at an average level of 1700 - 1720 meters (Yeşilova et al., 2019, 2024 Nar, 2023). They came to light with erosion when the lake level dropped to today's level.

As the lake water level rises, the tufa level also rises (Collins and Leber 2005). Tufas, which offer similar visuals in terms of formation and development with the tufas formed in Mono Lake, are formed in the area where the paleo Tosbağa stream empties into Lake Van. With the increase in lake level, upward growth occurs in tufas, thus forming tufa towers and layers (Fig. 2A, B, C) (Yeşilova et al. 2019). Tufa formations represent the current Lake Van coast of that period, and deltas that are laterally transitional with tufas prove this situation (Fig. 2D) (Yeşilova et al. 2019).

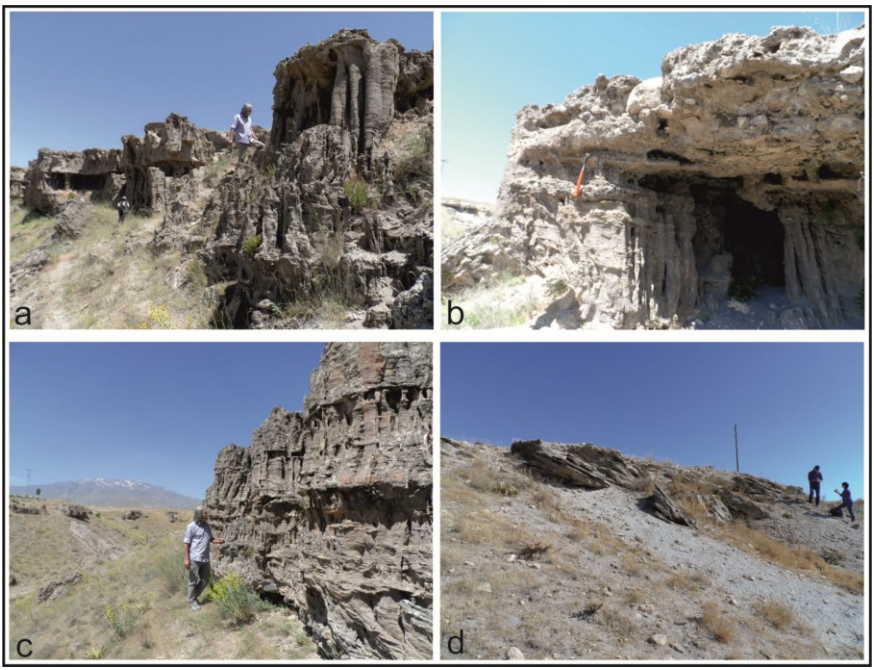

Figure 2. A. Tufa towers resulting from upward growth. B. Fluvial deposits on tufa layers (these deposits indicate the pause in tufa formation and fluvial activity in the region). C. General view of tufa layers deposited on top of each other. D. Delta deposits that are laterally transitional with tufas.

Yeşilova et al. 2019, in their study, stated that the first transgression occurred between 112.7 ka (1701 masl) and 72.5 ka (1704 masl) and a second transgression occurred between 30.1 ka (1646 masl) and 19.3 ka (1725 masl). All these lake level fluctuations related to the formation of tufas are directly related to global climate changes (Yeşilova et al. 2019). According to the values given in the relevant study, the generalized block diagram regarding the formation and development of tufas is given in Figure 3.

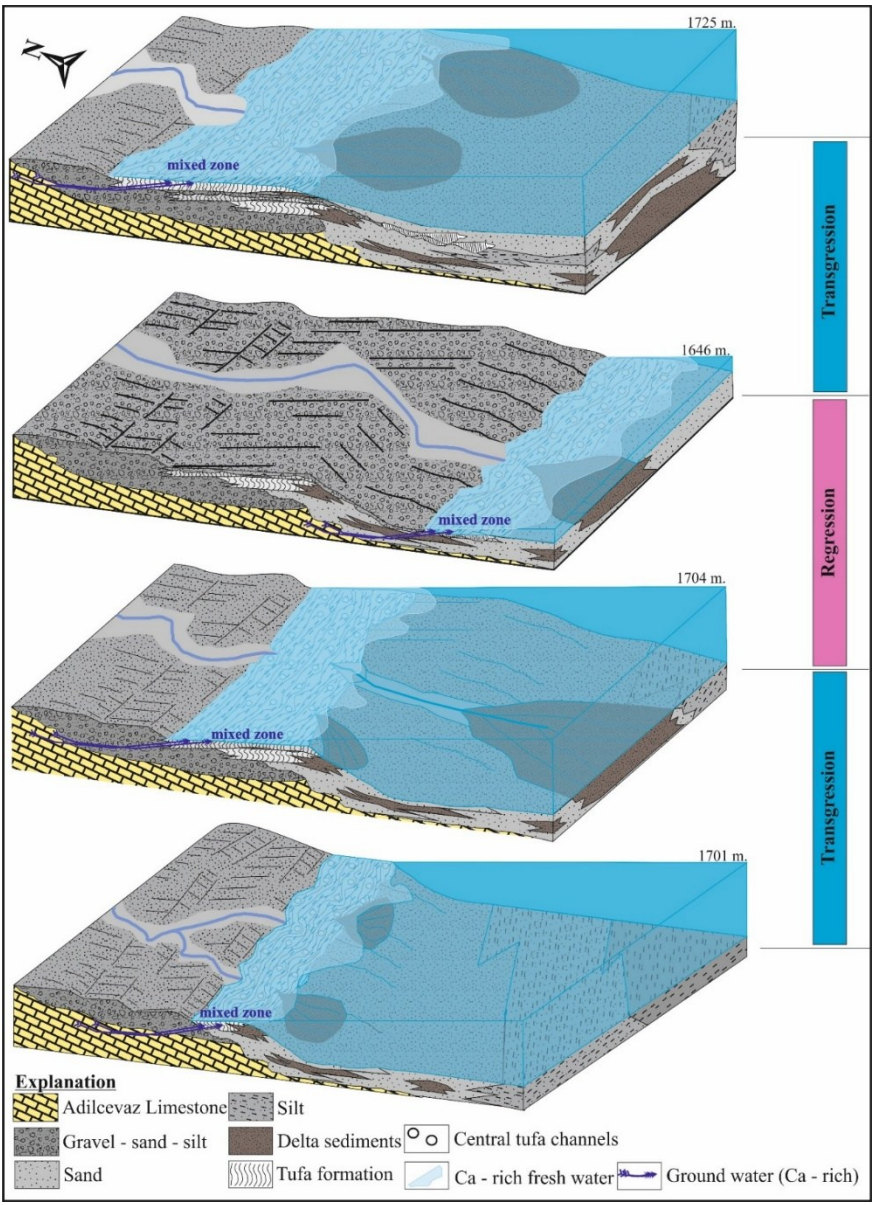

Figure 3. Block diagram showing the development of tufas (drawn according to data from Yeşilova et al., 2019).

Protection and Identification of Tufas

The tufas are located in a developing region of Turkey. With the recent investments made in the region, the region has become a center of attraction, especially for Iranian tourists. However, the approach of the local people to such geological formations has not yet reached the required levels. Unfortunately, the area where the tufas are located is currently used as a garbage dump by the surrounding small-scale businesses and local settlements (Fig. 4).

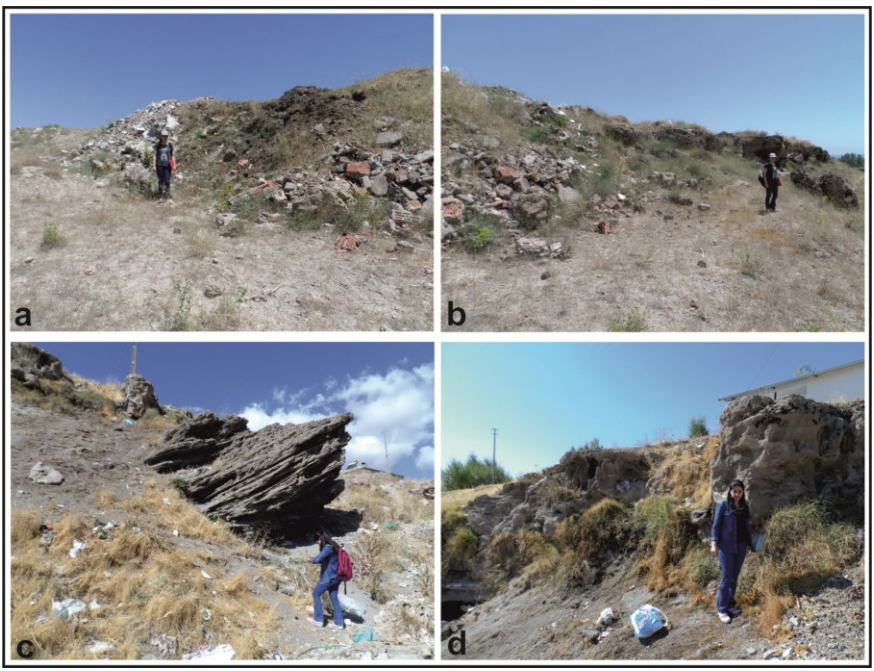

Figure 4. A-B. Construction waste in the area where the tufas are located. C-D. Domestic waste.

The tufas in the region are a bank that holds the exact climate and altitude records of Lake Van between 112.7 and 19.3 ka. At the same time, it stands out as the only tufa formation recorded on the shores of Lake Van to date. Considering the visual beauty of the tufas, it is obvious that they are rare formations that need to be

protected. For this reason, the Adilcevaz Tufas should be accepted as a part of the geological heritage. It is a fact that these formations can only be protected by raising awareness by the scientific world. Accepting these tufas as a part of the geological heritage means protecting a very important resource not only visually but also scientifically. The most important issue that should not be forgotten is the protection of such structures in the geography (Burek 2012). In the protection of such geological or geomorphological elements, school-age children and young people should be provided with collective visits to these areas, as in the examples of Italy and Greece, and the importance of these areas should be explained (Femeli et al., 2015).

In terms of promotion, first of all, the geological processes that form tufas should be explained scientifically and their paleogeographic evolution should be illuminated. Thus, scientific promotion will be realized. In terms of tourism, three stages need to be carried out in a general framework in order for the tufa field to become a national brand and increase its recognition. The first of these is the stage of naming the place (MacCannell, 1976; Alaeddinoğlu and Aliağaoğlu, 2007). After naming, the stage of revealing the boundaries of the tufa field comes. The next stage is the mechanical reproduction stage (MacCannell, 1976; Alaeddinoğlu and Aliağaoğlu, 2007). At this stage, touristic attraction gains importance and now turns into a destination or an area of experience (MacCannell, 1976; Alaeddinoğlu and Aliağaoğlu, 2007). Therefore, the tufa field is promoted with all components of the press, primarily visual, written and electronic, in the mechanical reproduction stage (MacCannell, 1976; Alaeddinoğlu and Aliağaoğlu, 2007).

Çiltepe and Uzun, (2024) stated in their study that the tufa and microbialites in the region should be evaluated together with the historical remains under the waters of Lake Van. The authors emphasize that all these values in Adilcevaz are very important and state that they are natural and cultural landscapes that show the interaction between humans and the environment (Çiltepe and Uzun, 2024).

Discussion

ProGEO, 2011., stated that some of the geological structures that contain information about the past are rare in the world, unique and at the same time geological heritage. In this context, the Adilcevaz Tufas, which offer unique beauties (Fig. 5) and also keep records of the climate of their time with the fluctuations in the lake level, fit this definition and exhibit geological heritage characteristics both in terms of formation and visuality.

The Adilcevaz Tufas do not have sufficient tourism potential on their own due to the socio-economic structure of the region and the fact that they are not yet an attraction center. There are countless natural and historical beauties in the region other than these tufas. The most striking of these are the Van Lake Microbialites, Aygır Lake (maar lake), Adilcevaz Kef Castle, Ahlat Seljuk Monumental Tombs, Ahlat Stone Houses and Nemrut Caldera (Fig. 6).

Protecting the Adilcevaz Tufas should not be limited to declaring them a geological heritage area. The most important task here falls on the local people. The contribution of these and similar areas to the economy and their direct or indirect gains should be explained to the local people. The awareness of the local people should be raised and the use of such areas as dumps should be stopped as soon as possible. The most important thing to remember

is that the greatest protectors and destroyers of such cultural and natural heritage areas are the people themselves.

Figure 5. Visual beauties of Adilcevaz Tufas.

Figure 6. A. The Microbialites of Lake Van . B. Aygır Lake (maar lake). C. Adilcevaz Kef Castle. D. Ahlat Selçuk Monumental Cemetery. E. Ahlat Old Stone Houses (cave houses). F. Nemrut Caldera.

Despite the existence of numerous geological heritage sites in the region, there are only a few publications on the subject. The most important of these are (i) Üner et al. (2017)'s study on the evaluation of Lake Van seismites as geological heritage and (ii) Çiltepe and Uzun, (2024)'s study on the Investigation of Tufa Microbialites in the Adilcevaz (Bitlis) Terrestrial Ecosystem According to the Conservation Approach. Such studies should be

sufficiently multiplied and their controlled gains should be provided to both the scientific world and the tourism world.

There is a lot of misinformation about the Adilcevaz Tufas made by people who are not experts in the subject. This information is available in newspapers, television and the internet. Most of the explanations made contain either incorrect or incomplete information. Such incorrect or incomplete information leads to information pollution and misinforms the masses. Non-experts should avoid making explanations about such structures.

Conclusion

Adilcevaz tufas should be taken under protection by being included in the geological heritage list as soon as possible, necessary markings and promotions should be made in the region, and tufas should be made one of the dynamics that will contribute to the regional economy.

The culture of protecting such structures should be instilled in people by raising awareness, giving trips and even lessons starting from primary school.

Acknowledgements. This study was supported by Yüzüncü Yıl University Scientific Research Project Council (YYÜ, BAP, Project No: FHD-2018-7652).

REFERENCES

Alaeddinoğlu, F., Aliağaoğlu, A., (2007). Savaş Alanları Turizmine Tipik Bir Örnek: Büyük Taarruz ve Başkomutan Tarihi Milli Parkı. Anatolia: Turizm Araştırmaları Dergisi,18(2); 215-225

Almendinger J.E., Leete J.H., (1998). Peat characteristics and groundwater geochemistry of calcareous fens in the Minnesota River basin , USA. — Biogeochemistr y 43: 17-41.

Auque, L.F., Arenas, C., Osacar, M.C., Pardo, G., Sancho, C., Vazquez-Urbez, M., (2013). Tufa sedimentation in changing hydrological conditions: the River Mesa (Spain). Geologica Acta 11(1):85-102

Burek, C., (2012). The role of LGAPs (Local Geodiversity Action Plans) and Welsh RIGS as local drivers for geoconservation within geotourism in Wales. Geoheritage 4(1–2):45–63

Council, T.C., Bennett, P.C., (1993).Geochemistry of ikaite formation at Mono Lake, California: Implications for the origin of tufa mounds Geology., 21; 971-974

Collins, R., Leber, K., (2005). Life at the Limits: Earth, Mars and Beyond. Lunar and Planetary Institute. Web. 4 June 2015.

Çiltepe, F., Uzun, A., (2024). An Investigation of Tufa Microbialites in the Terrestrial Ecosystem of Adilcevaz (Bitlis) According to the Conservation Approach. Geoheritage, 16;23

Çukur, D., Krastel, S., Schmincke, H.U., Sumita, M., Tomonaga, Y., Çağatay, M.N., (2014). Water level changes in Lake Van, Turkey, during the past ca. 600 ka: climatic, volcanic and tectonic controls. Journal of Paleolimnology, 52: 201–214.

Dramis F., Materazzi M., Cilla G., (1999). Influence of climate changes on freshwater travertine deposition; a new hypothesis. — Phys. Chem. Eart h (A) 24: 893-987

Fermeli, G., Hevia, G.M., Koutsouveli, A., Dermitzakis, M., Calonge, A., Steininger, F., D'Arpa, C., Di Patti, C., (2015). Geoscience teaching and student interest in secondary schools-preliminary results from an interest research in Greece, Spain and Italy. Geoheritage 7:13–24

Ford, T. D., Pedley, H. M. (1996). A review of tufa and travertine deposits of the world. Earth-Science Reviews, 41(3-4), 117-175.

Görür, N., Çağatay, MN., Zabcı, C., Sakınç, M., Akkök, R., Şile, H., Örçen, S., (2015). The Late Quaternary Tectono-Stratigraphic Evolution of The Lake Van, Turkey, Bull. Min. Res. Exp. (2015) 151: 1-46

Güngör Yeşilova, P., Gökmen, D., (2020). The paleodepositional environment, diagenetic and depositional conditions of the Middle-Late Miocene Koluz gypsum member (NE Van, Eastern Turkey). Carbonates and Evaporites, 35: 2–21.

Güngör Yeşilova, P., Yeşilova, Ç., Açlan, M., Gundogan, İ., (2020). Geochemical characteristics of gypsum lithofacies in northeastern of Mus (Eastern Anatolia-Turkey): an indication of the Neotethys closure. Carbonates and Evaporıtes, 35: 1-18.

Güngör Yeşilova, P., Baran, O., (2023). Origin and Paleoenvironmental Conditions of the Köprüağzı Evaporites (Eastern Anatolia, Turkey): Sedimentological, Mineralogical and Geochemical Constraints Minerals 2023, 13(2), 282.

Grube, A., Usinger, H., (2016): Zur Bildung von Quellmoor-Kuppen mit Quellkalk-Bildungen bei Habernis und Curau (nördliches und mittleres Schleswig-Holstein). – E&G Quaternary Science Journal, 65 (2): 156–173.

Kremer, B., Kaźmierczak, J., Kempe, S. (2019). Authigenic replacement of cyanobacterially precipitated calcium carbonate by aluminium-silicates in giant microbialites of Lake Van (Turkey). Sedimentology, 66(1), 285-304.

MacCannell, D., (1976). The tourist: a new theory of the leisure class. London: MacMillan

Nar, B., (2023). Van Gölü Mikrobiyalit Ve Tufalarının Tanımlanması ve Karşılaştırılması. Van Yüzüncü Yıl Üniversitesi, Fen Bilimleri Enstitüsü, Van. Yüksek Lisans Tezi (basılmamış) (in Turkish).

Pentecost, A., (2005). Travertine. Springer, Berlin, 446 pp.

Perissinotto, R., Bornman, T.G., Steyn, P.-P., Miranda, N.A.F., Dorrington, R.A., Matcher, G.F., et al. (2014. Tufa stromatolite ecosystems on the South African south coast. S Afr J Sci. 110(9/10), Art. 8 pages.

ProGEO, (2011). Conserving our shared geoheritage—a protocol on geoconservation principles, sustainable site use, management, fieldwork, fossil and mineral collecting. http://www.progeo.se/progeo-protocol-definitions-20110915.pdf (13 October 2015)

Schuster, O. (1926): Postglaziale Quellkalke Schleswig-Holsteins und ihre Molluskenfauna in Beziehung zu den Veränderungen des Klimas und der Gewässer. – Archiv für Hydrobiologie, 16: 1–73.

Stockhecke M., Sturm M., Brunner İ, Schmincke H.U., Sumita M., Kipper R., Çukur D., Kwiecien O., Anselmetti F.S., (2014). Sedimentary Evolution and Environmental History of Lake Van (Turkey) Over the Past 600.000 Years. Sedimentology, 61: 1830-1861.

Uner, S., Aliriz, M. G., Ozsayin, E., Selcuk, A. S. ve Karabiyikoglu, M. (2017). Earthquake Induced Sedimentary Structures (Seismites): Geoconservation and Promotion as Geological Heritage (Lake Van-Turkey). Geoheritage, 9(2), 133–139. doi:10.1007/s12371-016-0186-z

Whiticar, M., Suess, E., (1998). The cold carbonate connection between Mono Lake, California and the Bransfield Strait, Antarctica. Aquatic Geochemistry. 4, 429–454.

Wright, W.B., (1914. The Quaternary Ice Age. Macmillan and Co.: London, Web.

Yeşilova, Ç., Yakupoğlu T., (2008). Adilcevaz Kireçtaşının (Van Gölü Kuzeyi) Mikrofasiyes Özellikleri. Türkiye Jeoloji Bülteni, 50 (1): 27-38.

Yeşilova, Ç., Güngör Yeşilova, P., Açlan, M., (2015a). Edremit (Van) Travertenlerinin Fasiyes Analizi (in Turkish). 68. Türkiye Jeoloji Kurultayı, 578-579, Ankara, Türkiye

Yeşilova, Ç., Üner, S., Güngör Yeşilova, P., Açlan, M., Alırız, M.G. (2015b). Kuvaterner Yaşlı Edremit Travertenleri'nin Fasiyes Özellikleri ve Oluşum Ortamları (Van Gölü Havzası-Doğu Anadolu) (in Turkish). Traverten - Tufa Çalıştayı, Pamukkale Üniversitesi Mühendislik Fakültesi, Denizli. 54-55.

Yeşilova, Ç.,, Açlan, M., Güngör Yeşilova, P., (2017). Dereiçi Travertenlerinin Sedimantolojik Özellikleri ve Jeomiras

Öğelerinin Değerlendirilmesi. Sedimantoloji Çalışma Grubu_2017 (pp.28-29). Rize Türkiye

Yeşilova, Ç., (2019). Preliminary approach to paleogeographic properties of Edremit (Van) Travertines, eastern Turkey. IESCA, 60p. 7-11 October 2019, İzmir.

Yeşilova, Ç., Gülyüz, E., Huang, C.R., Shen., C.C., (2019). Giant Tufas of Lake Van Record Lake-Level Fluctuations and Climatic Changes in Eastern Anatolia, Turkey. Palaeogeography, Palaeoclimatology, Palaeoecology, 533 DOI: 10.1016/j.palaeo.2019.05.048.

Yeşilova, Ç., Güngör-Yeşilova, P., Açlan, M., Tsai-Luen, Y., Chuan-Chou, S., (2021). U-Th ages and Facies Properties of Edremit Travertine/Tufas, Van, Eastern Anatolia: Implications of Neo-tectonic for the region. Geological Quarterly 65(2): 1 – 20.

Yeşilova, Ç., Nar, B., Landman, G., (2024). Van Gölü Tufaları; Jeolojik Özellikleri ve Van Gölü Mikrobiyalitleriyle Karşılaştırılması. Sedimantoloji Çalışma Grubu 2024 (pp.35-36). Tunceli Türkiye

Zak K., Lozek V., Kadlec J., Hladikova J., Cilek V., (2002). Climate-induced changes in Holocene calcareous tufa formations, Bohemian Karst, Czech Republic. Quaternary International 91:137–152.

CHAPTER V

Relationship Between Physical and Abrasion Properties and Cutting Performance of Igneous Rocks

İsmail İNCE[1]
Hayri ARABACI[2]
Mustafa FENER[3]

1. Introduction

Rocks have been widely used as building blocks for centuries. Recently, the use of rocks as building materials has increased significantly. This increase has brought to the forefront the importance of cutting performance, which is the most important operating cost in the conversion of rocks into building materials. This has led many researchers to investigate the cutting performance

[1] Assoc. Prof., Konya Technical University, Faculty of Engineering and Natural Sciences, Department of Geological Engineering, Konya/Turkey, Orcid: 0000-0002-6692-7584, iince@ktun.edu.tr
[2] Professor, Selcuk University, Faculty of Technology, Department of Electrical and Electronics Engineering, Konya/Turkey, Orcid: 0000-0002-9212-0784, hayriarabaci@selcuk.edu.tr
[3] Professor, Ankara University, Faculty of Engineering, Department of Civil Engineering, Ankara/Turkey, Orcid: 0000-0003-0491-3205, mfener@ankara.edu.tr

of rocks (Ataei et al., 2012; Ghaysari et al., 2012; Sadegheslam et al., 2013; Almasi et al., 2017; Yilmazkaya et al., 2018; Kahraman et al., 2004; Yurdakul and Akdaş, 2012; Huang et al., 2018). Kahraman et al. (2004) investigated the relationship between slab production and rock properties and developed prediction models. Ataei et al. (2012) investigated the relationship between sawability and energy consumption. Sadegheslam et al. (2013) investigated the relationship between cutting speed and rock properties of carbonate rocks. Yilmazkaya et al. (2018) developed artificial neural network and regression models using physical, strength and cutting properties for cutting natural stone samples. Yurdakul and Akdaş (2012) estimated the cutting energy values of large-diameter circular diamond saw block cutters for carbonate rocks through physical, strength, saw blade diameter and depth of cut. Bayram (2020) statistically evaluated the relationships between unit energy and cutting parameters and environmental parameters and developed a model. This model predicted unit energy values with high correlation value. In this study, the relationships between energy consumed in the cutting process and rock physical and wear properties were investigated using a saw with automatic cutting feature..

2. Material and Method

In order to investigate the relationship between the cutting performance of the samples and their physical and abrasion properties, 16 rock samples were collected from magmatic rock (plutonic, volcanic and pyroclastic) quarries operated in Anatolia (Turkey). Firstly, samples (core and aggregate) were prepared from the collected rocks in accordance with the relevant standards and

recommended test methods (ISRM, 2007; BS 812 1990). The prepared core samples were divided into two groups to determine their physical properties and energy consumed during cutting. While the methods recommended in ISRM (2007) were taken into consideration in determining the dry density and porosity values of the samples, the method recommended in ASTM E494 (2010) was used in determining the P-wave velocity values of the rocks.

In determining the Böhme abrasion (BA) and aggregate impact value (AIV) values of rocks, EN 14157 (2004) and BS 812 (1990) standards were used, respectively. Böhme abrasion test is defined as the abrasion value BA value as a result of the rotation of the sample on the rotating drum for 352 revolutions (after 16 cycles consisting of 22 revolutions) when the sample on the abrasion disk scattered with standard abrasive powder is exposed to a pressure of 0.06 N/mm^2. AIV test is defined as the resistance of the aggregate to sudden shock or impact when a standard weighted pestle (14 kg) is dropped 15 times from a height of 38 cm on a 750 g aggregate sample with a certain sieve gap (14 mm, 10 mm).

The energy consumed during the cutting of magmatic rocks was calculated by measuring the currents and voltages drawn by the motor during the cutting process of 54.7 mm diameter core samples in the BRILLANT 250 brand automatic cutting device. The BRILLANT 250 used in cutting the samples is an automatic wet cutting machine for materialography, mineralogy, and composite materials.

The motor's energy consumed (P) was calculated using the current, voltage (V), and sample cut-off times (t) obtained when the core samples were cut.

$$\boldsymbol{P(t_i) = V(t_i)I(t_i)} \quad (1)$$

The total energy (E_t) consumed by the motor during the cutting process was obtained from the integral of the instantaneous power (P) drawn between the start (t_0) and end (t_1) of the cutting process.

$$\boldsymbol{E_t = \int_0^{t_1} P(t)dt} \quad (2)$$

The net energy consumed (E_{net}) was obtained by subtracting system and motor losses (E_{lost}) from the total energy consumed by the system to cut the sample (E_t).

$$\boldsymbol{E_{net} = E_t - E_{lost}} \quad (3)$$

3. Results and Discussion

3.1 Some mineralogical and petrographic characteristics

In this study, 16 samples of different types of igneous rocks (plutonic, volcanic, pyroclastic) collected from quarries operated in Anatolia were used. The related rock classifications were made using the mineralogical composition of the samples obtained from thin sections. The main mineralogical components of the pyroclastic samples are volcanic glass, plagioclase and rock fragments. Pyroclastic samples were named as Lithic Tuff and Vitric tuff according to Schmid (1981) classification. Plutonic and volcanic rocks were defined according to Streickeisen (1979). According to

this classification, plutonic samples are named as granite while volcanic samples are named as dacite and andesite.

3.2 Physical and abrasion properties

Statistical analyses of physical (dry density, porosity, P-wave velocity) and abrasion properties (Böhme abrasion and aggregate impact strength test) obtained from rocks used in the study are presented in Table 1.

Dry density values of igneous rocks used in the study are between 1.22-2.68 g/cm^3. Granites have the highest dry density and these samples are in the 'medium' rock class according to the dry density classification of NBG (1985). Other samples are in the 'very low' rock class according to the dry density classification of NBG (1985). Porosity values of rocks vary between 0.65% and 36.83% and these rocks show 'low – very high' porous rock properties according to the porosity classification of NBG (1985). P-wave velocity values of rocks vary between 2.02 and 4.42 km/s. BA values of rocks vary in a wide range and are between 5.21-46.74 cm^3/50cm^2. The aggregate impact strength of rocks varies between 53.65% and 87.39%.

Table 1: Descriptive statistics of data used in the analysis

Variables	Data	Minimum	Maximum	Mean	Std. deviation	Variance
ρ_d- g/cm^3	16	1.22	2.68	1.81	0.45	0.20
n -%	16	0.65	36.83	21.92	11.69	136.59
Vp -km/s	16	2.02	4.42	2.84	0.75	0.56
BA-cm^3/50cm^2	16	5.21	46.74	24.70	9.91	98.30
AIV-%	16	53.65	87.39	69.62	11.11	123.38

ρ_d: dry density, n: porosity, Vp: P-wave velocity, BA: Böhme abrasion, AI: aggregate impact value

3.3 Net energy expended while cutting the sample estimate of igneous rocks

The relationship between Enet values and the physical and abrasion values of the rocks was analysed using simple regression (linear, power, exponential, logarithmic and polynomial) analysis. The correlations between Enet values and the physical properties of rock samples are presented in Figure 2. The highest correlation coefficient between Enet and Vp was determined in the exponential relationship with 0.8871. The highest correlation relationship between Enet and n and dry density was determined in logarithmic (R^2: 0.7689) and exponential (R^2: 0.7422) relationships, respectively (Figure 1).

The correlation relationships between the Enet values Enet and the abrasion properties (BA and AIV) of the igneous rock samples are shown in Figure 2. The correlation coefficient for the simple regression relationship between Enet and BA and AIV is 0.9706 and 0.5437 respectively. The highest correlation coefficient between Enet and physical and abrasion properties was determined

in BA. This can be explained by the fact that the minerals that resist cutting and the minerals that resist abrasion are the same.

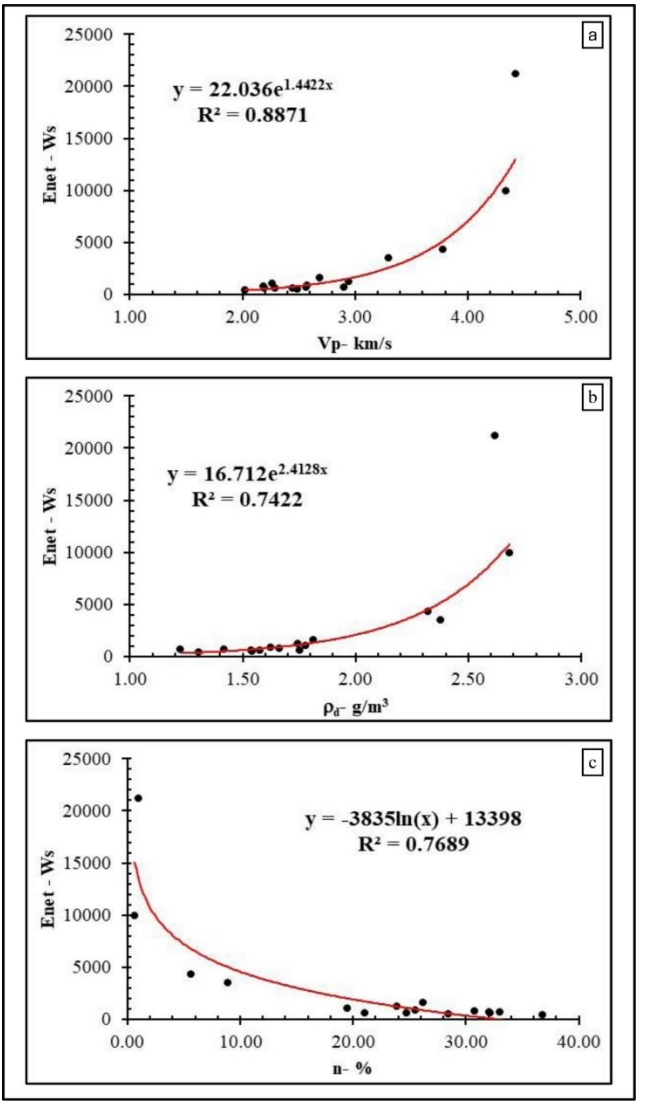

Figure 1: Relationship between net energy consumed and physical properties a) P-wave velocity, b) dry density, c) porosity

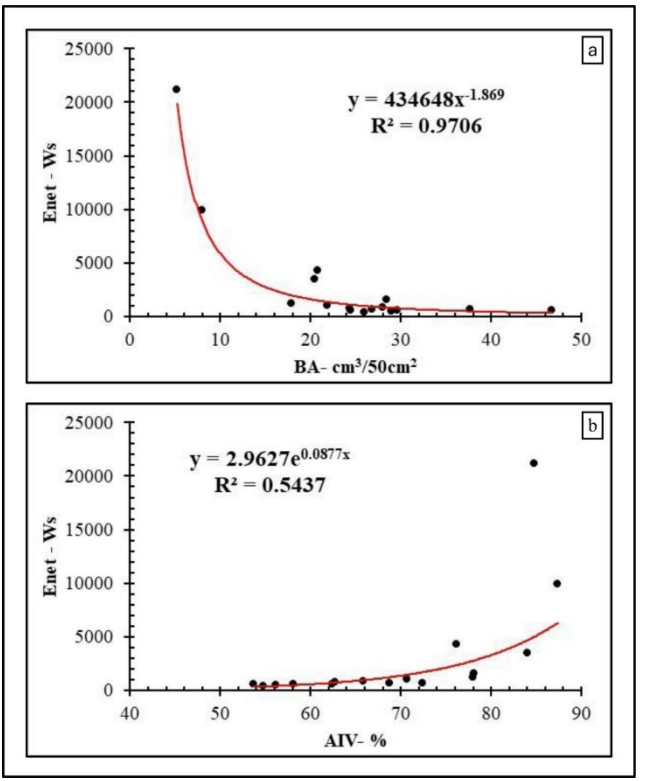

Figure 2: Relationship between net energy consumed and abrasion properties a) Böhme abrasion, b) aggregate impact value

5. Conclusion

In this study, simple regression analysis was used to predict the Enet values of 16 igneous rocks using physical and abrasion rates. The main results obtained from the simple regression analysis are as follows:

In the simple regression analysis used in the study, the best relationship between physical properties and Enet is between Enet and Vp. The correlation coefficient in this relationship is 0.8871.

The best relationship between the abrasion properties of igneous rocks and Enet was found between Enet and BA, with a correlation coefficient of 0.9706.

This high correlation relationship is the direct relationship between the main parameters affecting wear and cutting energy. The Böhme abrasion value can be used to practically estimate the Enet value.

References

Almasi, S. N., Bagherpour, R., Mikaeil, R., Ozcelik, Y., & Kalhori, H. (2017). Predicting the building stone cutting rate based on rock properties and device pullback amperage in quarries using M5P model tree. Geotechnical and Geological Engineering, 35(4), 1311-1326.

Ataei, M., Mikaeil, R., Hoseinie, S. H., & Hosseini, S. M. (2012). Fuzzy analytical hierarchy process approach for ranking the sawability of carbonate rock. International Journal of Rock Mechanics and Mining Sciences, 50, 83-93.

ASTM E494 (2010). Standard Practice for Measuring Ultrasonic Velocity in Materials. ASTM International, West Conshohocken.

Bayram, F. (2020). Doğal taşların dairesel testereli kesiminde birim enerjinin kesim ve ortam parametrelerinden kestirimi. Afyon Kocatepe Üniversitesi Fen ve Mühendislik Bilimleri Dergisi, 20(2): 340-347 (in Turkish).

BS 812 (1990). Methods for Determination of Aggregate Impact Value (AIV). London, 12 p.

EN 14157 (2004). Natural Stone Determination of the Abrasion Resistance. CEN, 13 p.

Ghaysari, N., Ataei, M., Sereshki, F., & Mikaiel, R. (2012). Prediction of performance of diamond wire saw with respect to texture characteristics of rock. Archives of Mining Sciences, 57(4).

Huang, G., Zhang, M., Huang, H., Guo, H., & Xu, X. (2018). Estimation of power consumption in the circular sawing of stone

based on tangential force distribution. Rock Mechanics and Rock Engineering, 51(4), 1249-1261.

ISRM (2007). The complete ISRM suggested methods for rock charac-terization, testing and monitoring: 1974–2006. In: Ulusay R, Hud- son J (eds) Suggested methods prepared by the commis¬sion on testing methods. ISRM Turkish National Group, Ankara, Turkey.

Kahraman, S., Fener, M., & Gunaydin, O. (2004). Predicting the sawability of carbonate rocks using multiple curvilinear regression analysis. International Journal of Rock Mechanics and Mining Sciences, 41(7), 1123-1131.

NBG 1985. Engineering Geology and Rock Engineering: Norwegian Group of Rock Mechanics. Fornebu, Norway.

Sadegheslam, G., Mikaeil, R., Rooki, R., Ghadernejad, S., & Ataei, M. (2013). Predicting the production rate of diamond wire saws using multiple nonlinear regression analysis. Geosystem Engineering, 16(4), 275-285.

Schmid R (1981). Descriptive nomenclature and classifcation of pyroclastic deposits and fragments: recommendations of the international union of geological sciences subcommission on the systematics of igneous rocks. Geologische Rundschau, 70, 794–799.

Streickeisen A (1979) Classifcation and nomenclature of volcanic rock lomprophyres, corbanatites and millitic rocks. Geol 7:331–335 28.

Yilmazkaya, E., Dagdelenler, G., Ozcelik, Y., & Sonmez, H. (2018). Prediction of mono-wire cutting machine performance parameters using artificial neural network and regression models. Engineering Geology, 239, 96-108.

Yurdakul, M., & Akdas, H. (2012). Prediction of specific cutting energy for large diameter circular saws during natural stone cutting. International Journal of Rock Mechanics and Mining Sciences, 53, 38-44.

CHAPTER VI

Estimation of Uniaxial Compressive Strength (UCS) Values of Igneous Rocks Using Gene Expression Programming (GEP)

Mehmet Can BALCI[1]
İsmail İNCE[2]

1. Introduction

Geotechnical parameters constitute the input parameters for engineering projects to be constructed in soil or rock. Among these parameters, uniaxial compressive strength (UCS) is the most important input parameter. There are different standards for the determination of UCS, such as ISRM, ASTM, EN, etc. The most time consuming and expensive part of these standards is sampling. There are also some rock types for which it is not possible to take samples with the dimensions and properties specified in the standards. This has led to the development of indirect methods (point

[1] Asst. Prof., Batman University, Faculty of Engineering and Architecture, Department of Civil Engineering, Batman/Turkey, Orcid: 0000-0003-3737-2556, mehmetcan.balci@batman.edu.tr

[2] Assoc. Prof., Konya Technical University, Faculty of Engineering and Natural Sciences, Department of Geological Engineering, Konya/Turkey, Orcid: 0000-0002-6692-7584, iince@ktun.edu.tr

load test, Schimdt hammer rebound, Leeb hardness, etc.) to determine the UCS value of rocks. In addition, researchers have increased studies on the prediction of UCS value using physical and mechanical properties of rocks. Initially, simple and multiple regression analyses were used to determine UCS (Tugrul and Zarif 1999; Yasar and Kahraman 2001, 2014; Yasar and Erdoğan 2004; Kahraman et al 2005). In the twenty-first century, researchers have developed new methods and methodologies (soft computing models) to predict UCS. In these soft computing models, UCS values were estimated using different rock properties (Heidari et al 2018; Tariq et al 2019; Jin et al 2022; Özdemir 2022; Qiu et al 2022; Wei et al 2023, Wang et al 2023). Recently, Genetic Expression Programming (GEP) approaches have also been widely used to predict UCS (Ince et al 2019; Xue 2022; Khatti and Grover 2024). The aim of this study is to determine UCS using practical and inexpensive non-destructive testing techniques that can be used both in the field and in the laboratory. For this purpose, UCS values of igneous rocks were estimated by GEP using Leeb hardness (HL) and P-wave velocity as input parameters, which determine surface hardness through low application energy.

2. Material and Method

2.1 Sampling and laboratory tests

Fifty rock samples were collected from quarries opened in igneous rocks (igneous, volcanic and pyroclastic) operating in different regions of Anatolia. NX diameter (54 mm) core samples were prepared from 30x30x30 cm homogeneous rock blocks taken

from the quarries in accordance with the recommendations of ISRM (2007) for use in experimental studies.

The Vp, HL and UCS values of the rocks were determined using the prepared core samples in accordance with the relevant standards (ASTM E494 2010; ASTM D7012 2014). The standards specified in ASTM E494 (2010) were used for P-wave velocity determination of the samples. For each rock, P-wave velocity (Vp) measurement was repeated three times and the arithmetic mean of these measurements was taken as P-wave velocity. The UCS value was determined according to the methods recommended in ASTM D7012 (2014). For each rock unit, 3 samples were measured and these values were averaged.

Although the Leeb surface hardness test has a universal standard for metals, there is no existing standard for this test in rocks. However, some researchers have emphasized that the length to diameter (L/D) ratio should be ≥1.5 for HL test measurements in core samples (Ghorbani et al., 2023; Çelik et al., 2023). In this study, the L/D ratio recommended by the researchers for HL measurements was followed. Insize ISH-PHB brand D-probe was used to determine the HL value. The test was performed at 20 different points perpendicular to the bottom and top surfaces of the samples, evenly distributed over the surface of the samples. The arithmetic mean of the measurements made in each sample was defined as the HL value of the sample.

2.2 Genetic expression programming (GEP) approach

GEP is a new evolutionary algorithm developed by Ferreira in 2001 using genetic algorithm (GA) and genetic programming (GP). According to Ferreira (2001), in GEP, individuals encode the linear sequences of a genome with fixed dimensions used in GAs and in a tree structure of different sizes and shapes used in GP. This tree structure is called expression trees (ETs). The GEP model consists of function set, terminal set, fitness function, control parameters and stopping condition.

The ETs for the GEP model developed to predict the UCS values of igneous rocks are given in Figure 1. During training and testing of the GEP model, Vp (do) and HL (d1) values were defined as input variables, while UCS value was defined as output variable (Table 1). Fifty igneous rock samples were used in this study. Thirty-eight randomly selected samples were used as the training set for the GEP approaches, while the remaining samples were used as the test set for the GEP approaches. Gene X pro Tools 4.0 software was used to predict the UCS values of the rocks with the GEP method.

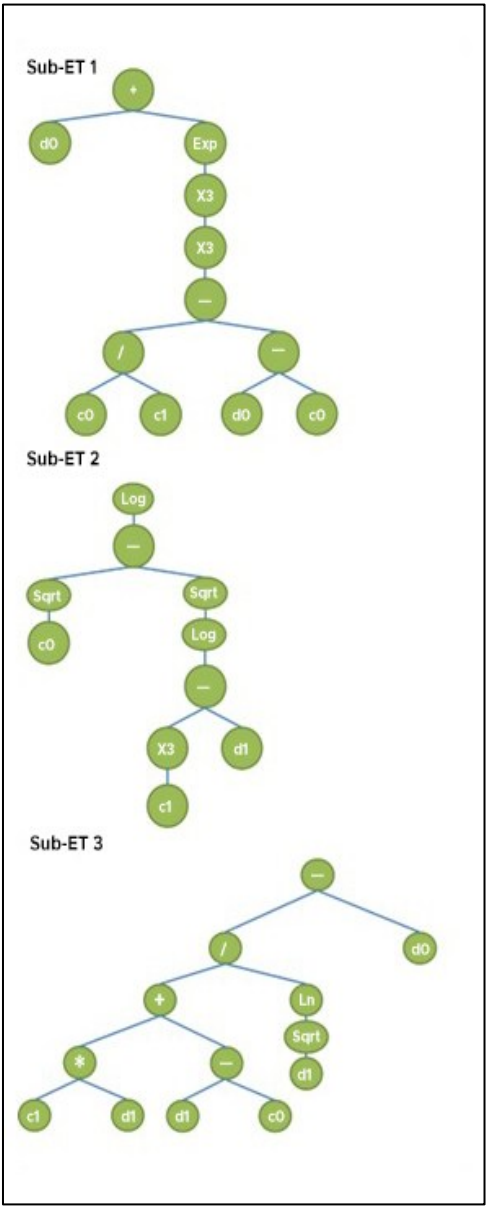

Figure 1: Expression tree of GEP model

The parameters used in the GEP model to predict the UCS value of the rocks are given in Table 1. The equations used in the equation of the developed GEP model are presented in Table 2.

Table 1: Parameters of GEP approach model

Parameter definition	GEP-I
Function set	+, -, *, /, Sqrt, x^3, log, ln, exp
Chromosomes	30
Head size	8
Number of genes	3
Linking function	Multiplication
Mutation rate	0.044
Inversion rate	0.1
One point recombination rate	0.3
Two point recombination rate	0.3
Gene recombination rate	0.1
Gene transposition rate	0.1

Table 2: Coefficients used in the GEP model

Coefficients	Values
G1C0	-0.536102
G1C1	-0.167785
G2C0	7.657654
G2C1	9.986512
G3C0	-9.994416
G3C1	-0.053192

3. Results and Discussion

3.1 Some physical properties of rocks

The input and output parameters of the GEP model developed to estimate the UCS value of the rocks used in the study are given in Table 3. The P-wave velocity value of the rocks varied between 1.56 and 5.38 km/s, while the HL value was determined

between 220.00 and 896.70. The UCS values of the rocks vary in a wide range (7.57-167.40 MPa).

Table 3: The input and output quantities used in GEP approach model

	Data used in the models		
Input variables	Minimum	Maximum	St. deviation
Vp	1.56	5.38	1.05
HL	220.00	896.70	193.83
Output variable			
UCS MPa	7.57	167.40	41.24

Vp: P-wave velocity, HL: Leeb hardness, UCS: Uniaxial compressive strength

3.2 Prediction of uniaxial compressive strength values of ıgneous rocks

The relationship between UCS values and P-wave velocity and HL values of the rocks was investigated using simple regression (linear, power, exponential, logarithmic and polynomial) analysis. The correlations between UCS values and physical properties of rock samples are presented in Figure 2. The highest correlation coefficient between UCS and Vp was determined in exponential relationship with 0.7076, while the highest correlation (R^2; 0.878) between UCS and HL was determined in exponential relationship (Figure 2). In these two approaches, it was observed that the deviations from the experimental UCS value increased in the prediction of high UCS values.

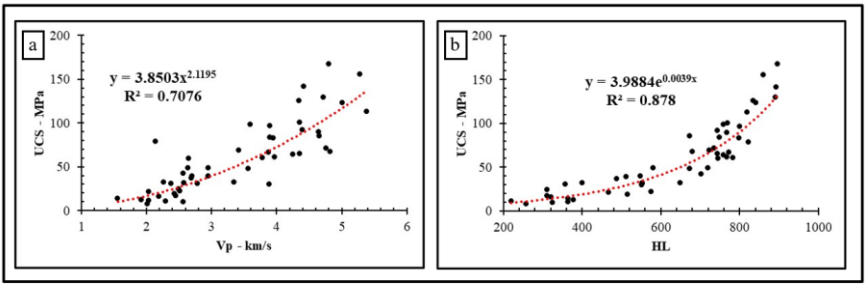

Figure 2: Relationships between the UCS and physical properties of the samples, a) P-wave velocity, b) HL

The validity of this model was checked through mean absolute error (MAE), root mean squared error (RMSE) and correlation coefficient (R^2) (Equations 1-3). The statistical parameters of the developed model are given in Table 2.

$$MAE = \frac{1}{n}[\sum_{i=1}^{n}|t_i - o_i|] \qquad (1)$$

$$RMSE = \sqrt{\frac{1}{n}\sum_{i=1}^{n}(t_i - o_i)^2} \qquad (2)$$

$$R^2 = \frac{(n\sum t_i o_i - \sum t_i \sum o_i)^2}{(n\sum t_i^2 - (\sum t_i)^2)(n\sum o_i^2 - (\sum o_i)^2)} \qquad (3)$$

Where t is the value obtained from the experiment, o is the calculated value and n is the total number of data.

The MAE and RMSE values for the training set and testing set of the GEP approach model developed for the prediction of UCS value are 9.95 and 12.68 and 10.07 and 11.05, respectively. The correlation coefficient value of this model is 0.9218 in the training set and 0.9099 in the testing set (Table 4, Figure 3).

Table 4: The UCS statistical values of GEP approach model

Statistical parameters	GEP-I	
	Training set	Testing set
MAE	9.95	10.07
RMSE	12.68	11.05
R^2	0.9218	0.9099

The comparison between the prediction values obtained from this GEP approach model and the experimental results shows the high generalization capacity of the proposed model. The statistical values (MAPE, RMSE and R^2) given in Table 4 show that the proposed models predict the UCS values quite successfully and the predicted values are very close to the experimental results.

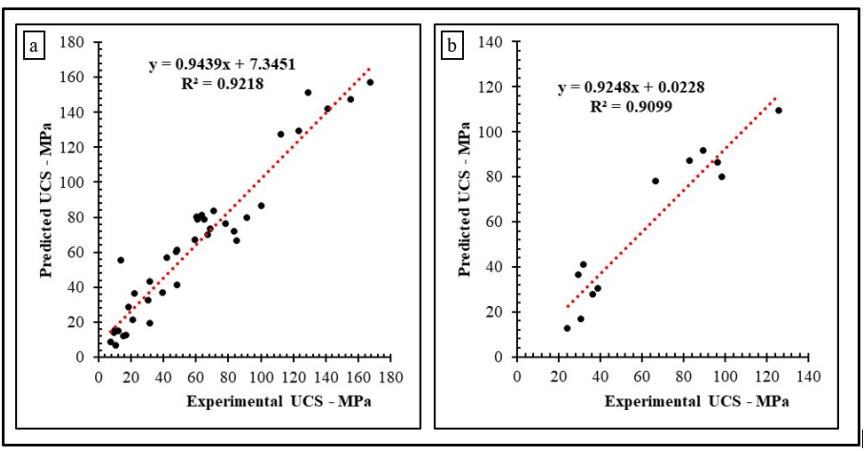

Figure 3: Relationship between measured and predicted UCS: a) Training set, b) Testing set

5. Conclusion

In this study, simple regression analysis and genetic programming approaches were used to predict the UCS values of 50

igneous rocks using HL and P-wave velocity. According to the analysis, obtained main conclusions are the following:

The best relationship obtained in the simple regression analysis used in the study is between HL and UCS with a correlation coefficient of 0.789.

In the developed GEP approach, the number of genes was chosen as 3 and multiplication was used as the link function. The results obtained from the GEP approaches and experiments are quite consistent with each other. The R2 values of the training and test sets of the developed GEP model are greater than 0.90. Moreover, the validity of this model is confirmed by MAE and RMSE values.

References

ASTM E494 (2010). Standard Practice for Measuring Ultrasonic Velocity in Materials. ASTM International, West Conshohocken

ASTM D7012 (2014). Standard Test Methods for Compressive Strength and Elastic Moduli of Intact Rock Core Specimens under Varying States of Stress and Temperatures, American Society for Testing and Materials, West Conshohocken

Çelik, S. B., Çobanoğlu, İ., Koralay, T., & Gireson, K. (2023). Investigation of the Leeb hardness test in rapid characterisation of rock cores with particular emphasis on the effect of length to diameter ratio. International Journal of Mining, Reclamation and Environment, 1-20.

Ghorbani, S., Hoseinie, S. H., Ghasemi, E., & Sherizadeh, T. (2023). Adoption of ASTM A956-06 Leeb hardness testing standard to rock engineering applications. Construction and Building Materials, 364, 129886.

Heidari, M., Mohseni, H., & Jalali, S. H. (2018). Prediction of uniaxial compressive strength of some sedimentary rocks by fuzzy and regression models. Geotechnical and Geological Engineering, 36, 401-412.

İnce, İ., Bozdağ, A., Fener, M., & Kahraman, S. (2019). Estimation of uniaxial compressive strength of pyroclastic rocks (Cappadocia, Turkey) by gene expression programming. Arabian Journal of Geosciences, 12, 1-13.

Jin, X., Zhao, R., Ma, Y. (2022). Application of a hybrid machine learning model for the prediction of compressive strength and elastic modulus of rocks. Minerals, 12(12), 1506. https://doi.org/10.3390/min12121506

Kahraman, S. (2001). Evaluation of simple methods for assessing the uniaxial compressive strength of rock. International Journal of Rock Mechanics and Mining Sciences, 38(7), 981-994.

Kahraman, S., Gunaydin, O., & Fener, M. (2005). The effect of porosity on the relation between uniaxial compressive strength and point load index. International Journal of Rock Mechanics and Mining Sciences, 42(4), 584-589.

Kahraman, S. (2014). The determination of uniaxial compressive strength from point load strength for pyroclastic rocks. Engineering Geology, 170, 33-42.

Khatti, J., Grover, K. S. (2024). Estimation of intact rock uniaxial compressive strength using advanced machine learning. Transportation Infrastructure Geotechnology, 11(4), 1989-2022.

Özdemir, E. (2022). A new predictive model for uniaxial compressive strength of rock using machine learning method: artificial intelligence-based age-layered population structure genetic programming (ALPS GP). Arabian Journal for Science and Engineering. 47(1), 629–639. https://doi. org/10.1007/s13369-021-05761-x

Qiu, J., Yin, X., Pan, Y., Wang, X., Zhang, M. (2022) Prediction of uniaxial compressive strength in rocks based on

extreme learning machine improved with metaheuristic algorithm. Mathematics, 10(19), 3490 . https://doi. org/10.3390/math10193490

Tariq, Z., Abdulraheem, A., Mahmoud, M., Elkatatny, S., Ali, A.Z., Al-Shehri, D., Belayneh, M.W. (2019). A new look into the prediction of static Young's modulus and unconfined compressive strength of carbonate using artifi cial intelligence tools. Petroleum Geoscience, 25(4), 389–399. https://doi.org/10.1144/petgeo2018-126

Tuğrul, A., & Zarif, I. H. (1999). Correlation of mineralogical and textural characteristics with engineering properties of selected granitic rocks from Turkey. Engineering geology, 51(4), 303-317.

Wang, M., Zhao, G., Liang, W. and Wang, N. (2023). A comparative study on the development of hybrid SSA-RF and PSO-RF models for predicting the uniaxial compressive strength of rocks. Case Studies in Construction Materials. e02191. https://doi.org/10.1016/j.cscm.2023.e02191

Wei, X., Shahani, N.M., Zheng, X. (2023). Predictive modeling of the uniaxial compressive strength of rocks using an artificial neural network approach. Mathematics 11(7), 1650. https://doi.org/10. 3390/math11071650

Xue, X. (2022). A novel model for prediction of uniaxial compressive strength of rocks. Comptes Rendus Mécanique, 350(G1), 159–170 . https://doi.org/10.5802/crmeca.109

Yasar, E., & Erdogan, Y. (2004). Correlating sound velocity with the density, compressive strength and Young's modulus of

carbonate rocks. International Journal of Rock Mechanics and Mining Sciences, 41(5), 871-875.

BÖLÜM VII

Dünit Bloklarının Önemi, Oluşumları Ve Özellikleri: Guleman Ofiyoliti Örneği

Ayşe Didem KILIÇ[1]

Giriş

Geçmişten günümüze ofiyolit kavramı farklı araştırmacılar (Coleman, 1971; Dewey ve Bird, 1971…vb. gibi) tarafından peridotit, gabro, diyabaz, spilit ve bunlarla ilişkili diğer kayaçlar için kullanılan ve magmatik provensle oluşan topluluk olarak ifade edilmiştir. Okyanus litosferinin parçalarının kıta kenarına bindirmesi esnasında levha kenarlarının yenildiğini ifade eden araştırmacılar, okyanus kabuğunda belirlenen peridotit gabro-diabaz yastık lav serilerinin orojenik kuşaklarda da bulunduğunu ifade etmişlerdir. Magmatik provens sonucunda oluşan ve peridotitlerin kütleler halinde katılaştığını ve bunun gabrolar tarafından takip edildiğini, piroksenitlerinde bu arada oluştuğu şeklinde basit bir tanımlama

[1] Doç. Dr., Fırat Üniversitesi, Mühendislik Fakültesi, Jeoloji Bölümü, Elazığ/Türkiye, Orcid: 0000-0002-6804-6764 (Orcid lütfen link değil 16 haneli rakamları yazınız.), adkilic@firat.edu.tr

yapmışlardır. Okyanus kabuğunun kta üzerine yerleşmesi ile oluşan ofiyolit, tektonitler, kümülatlar, izotrop gabro, levha-dayk karmaşığı ile bunları kesen diyabaz ve plajiyogranit daykları tarafından kesilmektedir.

Alp-Himalaya kuşağı içerisinde okyanus sırtı, orojenik dağ zincirleri ve yitim zonu içerisinde oluşan ofiyolitler, Afrika ve Avrasya kıtaları arasında önemli bir konumda yeralan Türkiye'de oldukça yaygındır. Neotetis okyanusunun Kretase zamanından itibaren kapanmasıyla oluşan Türkiye ofiyolitleri, kapanma sırasında bölgede etkili olan sıkışmalı rejim ürünleridir (Rızaoğlu ve diğ., 2004; Önen, 2003; Kılıç, 2009).

Guleman ofiyoliti, Güneydoğu Anadolu bölgesindeki önemli ofiyolit yerleşimlerinden biridir. Peridotit, tektonitler, ultramafik ve mafik kümülatlardan oluşan birim; Tektonitler, kümülatlar, plajiyogranit, diyabaz daykları ve bazik volkanik kayaçlardan oluşur. Tektonitler, dünit ve podiform kromit içeren harzburjitlerden oluşurken, kümülatlar; dünit-verlit-klinopiroksenit ardalanması ve bantlı gabrolardan oluşur. Guleman ofiyoliti bazik volkanik karmaşık içermemektedir. Ancak, volkaniklerle kökensel ilişkili olduğu düşünülen Caferi volkanitleri yayılım sunmaktadır (Özkan ve Öztunalı, 1984). Kalınlığı 4 km'yi aşan tektonitler tüm ofiyolit kütlesinin % 60'ı kadardır. Ultramafik kümülatlar, dünitler içerisinde saçılımlı bantlı kromitlerden, verlit ve klinopiroksenite geçer. Kümülat seviye bantlı gabro, izotropgabro, troktolit ve olivin gabro ile temsil edilmektedir. (Özkan ve Öztunalı, 1984). Gabroların en tipik özelliği, hızlı kristalleşme oranına işaret eden adkümülat ve heteradkümülat doku izlenmesidir (Özkan ve Öztunalı, 1984; Parlak ve diğ. 2004).

Alpin tip peridotitler ve ofiyolitlerin ultramafik bölümlerinin bir temsili olan (Irvine, 1974; Coleman 1977; Moores 1969; Harkins et al. 1980) dünitik bloklar, genellikle harzburjit ve/veya lerzolit içerisinde birkaç metre büyüklüktedir. Dünitik blokların oluşumuyla ilgili iki görüş bulunmaktadır. Bunlardan biri magmatik işlevler, bir diğeri ise H_2O'lu metasomatizmadır. Magmatik kökenli oluşumu savunan araştırmacılar, dünitik blokların mantodaki kısmi ergime sırasındaki yüksek sıcaklıkta oluştuğunu ve bunun en önemli kanıtının dirençli refrakter kalıntıları olarak gösterir (Dick 1977a, 1977b; Dick ve Sinton 1979). Diğer bir grup araştırmacı, Üst mantoya geçen bazaltik magmaların geride kalan kristal kümülatları olarak dünitik blokları ifade eder (Moores, 1969; Dick 1977a). Gregory (Hopson ve diğ., 1981) and Dick (1977a, b) ise dünitik blokların, dünitlerle harzburjitik duvarın reaksiyonu sonucu oluşabileceğini belirtir. Metasomatik kökeni savunan araştırmacılar ise, dünitik blokların sulu akışkanlarla subsolidüs reaksiyonlar sırasında peridotit içerisindeki piroksen ile olivinin yer değiştirmesi sonucu oluşabileceğini belirtirler (Dungan and Lallement 1977). Bu teoriler, üst mantodaki sıcaklık ve uçucu bileşenlerden önemli farklılık gösterir. Kısmi ergimeyle dünitlerin oluşması ancak yüksek sıcaklık veya alt peridotit solidüs sıcaklığında mümkündür. Her iki model, ergime sırasında yalnızca olivinin stabil olduğunu ileri sürmektedir. Şayet, dünitleri metasomatik kökenli olarak kabul edersek, üst manto ve/veya kabuk boyunca büyük bir H_20 akışı olması gerekir ki; Okyanus litosferinde hidrotermal sirkülasyonlar oldukça derinde gerçekleşir (Kılıç, 2009).

Dünitik bloklara dünyanın bazı yerlerinde (Trinity ofiyoliti, Bushveld kompleksi) rastlanmıştır (Hopson ve diğ., 1981). Peridotitler tarafından çevrelenen bağımsız bu kütleler, Guleman

ofiyoliti içerisinde de mevcuttur. Bu çalışma, Guleman ofiyoliti'ndeki birkaç metre boyutuna varan dünitik kütlelerin petrografisi, jeokimyası ve kökenini belirlemek amacını taşımaktadır.

2. Guleman Ofiyolitinin Petrografisi

Guleman ofiyoliti, tabandan tavana doğru tektonitler, ultramafik-mafik kümülatlar, izotrop gabrolar ile unları kesen diyabaz daykları ve plajiyogranitdn oluşur (Kılıç, 2006). Manto tektonitleri dünit ve harzburzjitlerle, ultramafik kümülatlar dünit, verlit ve serpantinitler ile mafik kümülatlar olivinli gabro, normal gabro ve izotrop gabrodan oluşmaktadır. Bazik volkanik seviye olmadığından Guleman ofiyoliti eksik dizi karakterlidir.

Dünitik bloklar ise harzburjit ve mafik kümülat geçişinde birbirinden bağımsız bloklar şeklindedir (Şekil). Bu kütlelerin yapısı, dünitik bir çekirdeği çevreleyen harzburjit, gabro veya piroksenittir. Harzburjit/gabro/piroksenit, matrikstir. Dünitik blokların farkedilebilir özelliği serpantinleşme, talk ve klorit alterasyonunun nadiren izlenmesidir. Guleman ofiyoliti dünitik kütleleri, küçük boyutlu bir magma odası üzerindeki blok faylanmalar sonucu veya yüksek sıcaklıktaki dünitik eriyikle harzburjitik yanduvar arasındaki reaksiyon sonucu oluşabilir.

Harzburjit, verlit ve klinopiroksenitler genellikle granüler, nadiren elek veya poiklitik doku özelliği gösterirler (Şekil). Kümülat gabrolar, kümülat doku özelliğine sahiptir (Şekil). Dünitik bloklar içerisindeki dünitler benzer şekilde granüler dokulu olup, %90'nın üzerinde olivin içerirler.

Guleman ofiyoliti kümülat seviyeye ait kayaçlarda, magmatik tabakalanma, minerallerin çökelimiyle eş yaşlı faylanma(magma odasında) ve benzeri gibi kristal segregasyonuna işaret eden yapılar ve dokular izlenir (Özkan ve Öztunalı, 1984).

Kümülatlarda krom, olivin, klinopiroksen, plajiyoklas, hornblend ve kuvars şeklinde izlenen fraksiyonel kristalleşme, gabro kayaçlarında izotrop gabrolarda bantlanmalar şeklinde izlenmektedir (Şekil). Kümülat seviyenin üst bölümlerini oluşturan izotrop gabrolar, klinopiroksen (%35), olivin (%25) ve plajiyoklaz (%40) minerallerinden oluşurken, normal gabroar, klinopiroksen (%40) ve plajiyoklaz (%60)'tan oluşur. İzotrop gabrolarla tabakalı gabrolar arasındaki önemli fark, doku ve plajiyoklazların anortit oranıdır (Beccaluva ve diğerleri, 1994). Bu oran incelenen izotrop gabrolarda %10 kadardır. Normal gabrolarla izotrop gabroların geçişinde izlenen plajiyogranitler, açık renkleri ve ince taneli granüler doku göstermeleri ile kolayca kümülat seviyede fark edilen kayaç türüdür. Plajiyogranitler, >%60-65 plajiyoklaz ($An_{>20}$), %20 kuvars, %15 biyotit, manyetit ve diğer mineralleri içerirler. Plajiyogranitlerin bir diğer özelliği yarı öz şekilli plajiyoklazlarda zonlanma görülmesidir (Şekil). Diyabaz daykları, ofiyolitik seriyi farklı seviyelerde kesen yaklaşı 0.5cm.den 1m.ye kadar değişen genişliğe sahip bu kayaçlar, intersertal dokuya sahiptirler. Mineralojik bileşimler, plajiyoklaz (%60-65), klinopiroksen (%35-40) ve ikincil mineraller (%5)dir. Plajiyoklazlar, prizmatik tane şekline sahiptir. Yerleşme sonrası gelişen erozyon, Guleman Ofiyoliti'nin levha-dayk karmaşığı seviyesini etkilemiştir. Bazı araştırmacılar (Özkan ve Öztunalı, 1984; Kılıç, 2009), Caferi volkanitlerini, Guleman Ofiyoliti'nin bazik volkanik seviyesi olduğu ve tektonik hareketlerle (DAF'a bağlı) ofiyolitten koparak, kuzeyde Maden Karmaşığı üzerine yerleştiğini ifade ederler.

3. Guleman Ofiyoliti Dünit Blokların Oluşumu

Dünit blokları, harzburjitik bir hamur içerisinde dünit çekirdekleri içerir. Farklı büyüklükte bloklar olarak bulunan bu kütleler (100 cm. den 1.5 metreye kadar), harzburjitlerle kümülatların geçişinde dağınık konumlanan bu bloklar (Şekil) Guleman ofiyoliti içerisinde dağılım göstermektedir. Dünit

kütlelerinin başlangıçtaki yönelimi oluşumu tahmin etmek zordur. Ancak, peridotit'in yükselmesi sırasında faylanmayla gabro ve diyorit plütonlarının sokulumu dünit kütlelerini yerleşim sırasında deforme etmiş ve döndürmüş olabilir. Daha sonraki faylar nedeniyle dünit blokları harzburjit ve kümülat dünit birimi içerisinde dağınıktır.

Dünit bloklarının oluşumları ile ilgili olarak; Hidrotermal, kristal kümülat ve kısmi ergime kökeni ifade edilir. Bazı araştırmacılar ( ), piroksen içeren protolitin içindeki akışkanlarıdan olivinin çökeldiğini ve dünitlerin subsolidüs koşulları altında oluştuğunu belirtir. Bu teori, Bushveld (Bunchanan ve diğ., 1999; Cameron, 1978), Stillwater (McCallum, 1996), Duke adası karmaşığı (Irvine 1974), Burro peridotitleri (Burch 1969) ve Canyon ofiyoliti (Dungan and Lallemant, 1977) dünitlerinde görülmektedir. Stratiform intrüzyonu kadar veya daha küçük olan bu karmaşık ve ofiyolitler, geç evrede peridotitlerde plastik deformasyon gösterirler. Plastik deformasyon kabuk ortamında H_2O'lu akışkanların bulunduğu subsolidüs koşullarında gelişir. Canyon peridotinde dünit-harzburjit sınırında bol miktarda amfibollerin varlığı, bu özelliği doğrulamaktadır (Dungan and Lallemant, 1977).

Dünitik blokların kilometrelerce boyutlarda ve düzlemsel bir yapı sunduğu Vourinos ofiyoliti (Moores 1969) ve Samail ofiyolitini (Hopson et al. 1981; Boudier and Coleman 1981) örnek göstererek kristal kümülat teoriyi savunmaktadır. Düzlemsel (tabular) şekilleri, magmatik dayklara işaret etmektedir (Hopson ve diğerlerine, 1981). Coleman ve Boudier (1981), Harkins ve diğerleri. (1980) ve Moores (1969), bu dünit kütlelerinin okyanus ortası sırtları altında yükselen pikritik eriyiklerden ayrılan olivin ile doldurulmuş kanalları veya besleyici daykları (feeder dikes) işaret eder. Boudier ve Coleman (1981), birçoğunun başlangıçta böyle bir modelin öngördüğü gibi dikey yönde oluştuğunu belirtmiştir. Semail ofiyolitine ait dünit bloklarında yapılan çalışmada araştırmacılar, subsolidüs koşulları

altında hidrotermal işlevlerle oluşur. Okyanus ortası sırtı ofiyolitlerinden biri olan, Semail ofiyolitindeki dünitik blokların 1550 km derinlikte ve yitimden hemen önce oluşan yapısal seviyede gelişmiştir (Boudier and Coleman 1981). Okyanusal litosferin bu bölgesi, okyanus ortası sırtı bazaltlarının düşük su içeriğine bağlı olarak anhidrozdur (Bedard, 1991). Bu bloklar peridotit hala sıcak iken oluşur. Sıcaklığın, sulu peridotit solidüsünün üzerinde olduğunu gösteren en önemli kanıtın plastik deformasyon olduğudur (Boudier and Coleman, 1981). Eğer H/O mevcut olsaydı peridotit erimiş olacaktı (Green 1973). Dünitik bloklar, mantodaki kısmi ergimeyle üretilen refrakter kalıntı olarak ifade eden (Dick,1984; Dick and Sinton 1979), Trinity peridotitindeki dünitik bloklarınsa, ya kısmi ergimenin büyük oranda tamamlanıp eriyiğin uzaklaştığı bir durumda veya ergime-uzaklaşma anında olauştuğunu mümkün görmektedirler. Ancak, akışkanların yaygın olduğu metasomatizmada bu işlevlere eşlik edebilir. Bloklardan farklı olarak levhamsı kütleler, bazaltik eriyikten olivinin çökelimi veya eriyikle peridotit duvar kayacının kısmi asimilasyonuyla oluşabilir.

Dünit blokların magmatik kökenli olduğu; dünit oluşumu sırasında sulu subsolidüs reaksiyonları için bir kanıtın olmaması, plajiyoklaz lerzolitlerde iz miktarda amfibolün varlığı (Canyon Mountain) (Dungan and Lallemant, 1977) ve dünit-peridotit geçişindeki küçük kıvrımlar, dünit blokları oluştuktan sonra oldukça sıcak ve plastik deformasyona uğrayan peridotit kayaçlarında yüksek sıcaklıkta korunmuş minerallerin varlığı ile anlaşılır. Bazı dünit bloklarında, oikokristal klinopiroksenler, intersitial plajiyoklas ve kromit ceplerinin varlığı magmatik kökenin işaretidir (Taylor and Epstein 1962a, b). Yukarıda ifade edilen teorilerle karşılaştırıldığında, Guleman ofiyoliti dünit blokları magmatik kökenli olup, peridotitin ergimesi sırasında magma odası yan duvarlarında gerçekleşen blok faylanmalarla oluşabileceği düşünülmektedir.

4. Dünit Blokların Jeokimyası

Dünit bloklarının çekirdek ve hamur kesimlerinden alınan örneklere ana oksit XRF analiz sonuçları Tablo 1'de verilmiştir.

Tablo 1: Guleman ofiyolit dünit bloklarının çekirdek ve kenarından alınan örneklerin XRF sonuçları

Ana oksit(%)	Dt-1	Dt-2	Hz-1	Hz-2	Gb-1	Gb-2
SiO_2	36.35	39.57	43.66	42.05	49.44	52.13
Al_2O_3	0.48	0.55	1.55	1.07	16.72	8.2
Fe_2O_3	11.03	9.13	7.22	6.93	9.11	15.04
MgO	36.75	34.46	41.35	42.71	7.2	11.52
CaO	0.83	2.4	2.01	1.01	8.29	9.77
Na_2O	0.08	0.1	0.1	0.2	3.44	0.54
K_2O	0.01	0.02	0.02	0.02	1.07	0.03
TiO_2	0.03	0.04	0.02	0.02	1.52	0.47
P_2O_5	0.05	0.06	0.09	0.07	0.33	0.08
MnO	0.10	0.10	0.11	0.08	0.12	0.19
A.K.	11.23	10. 03	3.55	4.34	2.46	2.01
Toplam	96.94	93.46	99.68	99.50	97.73	99.96
CaO/Al_2O_3	1.85	4.36	1.28	0.48	0.49	1.19
Mg#	0.76	0.79	0.85	0.86	0.44	0.43

Buna göre çekirdekte bulunan dünitin MgO değeri %34.46-36.75, Fe_2O_3 değeri %9.13-11.03 ve ultrabaziklerin özelliğini ifade eden SiO_2 içeriği ise % 36.35–36.57 arasındadır. Bu oran, harzburjitlerde % 42.05-43.66 ve gabrolarda %49.44-52.13^tür. Serpantinleşme arttıkça Ateşte Kayıp (AK) değeri (%11.23 gibi) de artmaktadır. Tablo 1'de dünitlerin Al_2O_3 miktarı %0.48-0.55 arasında değişmektedir. Coleman (1977) tarafından ifade edilen, Alpin tip peridotitlerdeki dünitlerin Al_2O_3 değerinin (% 0.35) biraz üzerindedir. Yüksek Al_2O_3'ün sebebi, ultrabazik kayaçlarda alterasyona bağlı olarak artan kil mineralleri ve Al_2O_3 içeren minerallerin (piroksen ve spinel) varlığına bağlamıştır. TiO_2 miktarları % 0,03 – 0,04 arasındadır. Bu alkali oksitlerin miktarı, üst mantoda bu elementlerin tüketilme seviyelerini belirlemektedir

(Örgün, 1992). Dünitlerin Mg# değerleri 0.9 – 0.94 arasında değişmektedir. Örneklerin Mg# değerlerinin yüksek olması, yitim zonu dünitlerin yüksek forsterit içeriğine sahip olduklarının işaretidir.

Al_2O_3-MgO diyagramında dünit örnekleri düşük Al_2O_3 (0,48 – 0.55) içerikleri nedeniyle, az tüketilmiş pirolit alanında yeralır (Şekil). Dünitlerin bu özelliği, manto ergimesinin kalıntıları olmasından kaynaklanır. Örneklerin yüksek CaO içeriği, alterasyona işaret etmektedir.

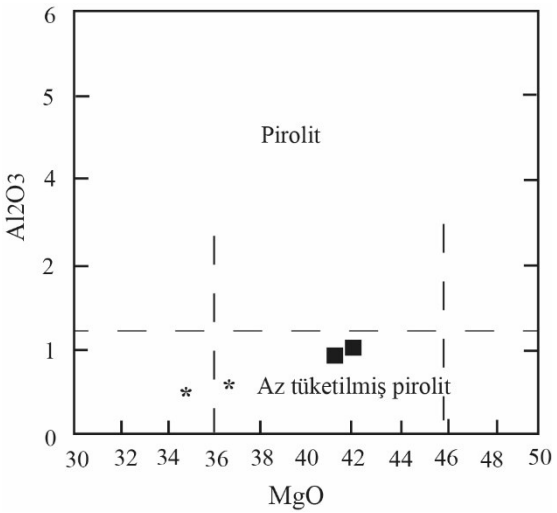

Şekil 1:İncelenen harzburjit ve dünitlere ait MgO-Al_2O_3 diyagramındaki dağılımları (Ringwood, 1975)

5. Tartışma ve Sonuçlar

Guleman ofiyoliti, Üst Triyas'tan itibaren Anadolu levhası ile Arap levhası arasındaki açılmaya başlayan Neotetis Okyanusu'nun güney kolunun, Üst Kretase' den itibaren kuzeye doğru dalmaya başlaması ile bu okyanus kabuğu üzerindeki açılmaya bağlı oarak gelişen Supra-subduction zonu

ofiyolitlerdendir. Harzburjit tip bu ofiyolit içerisindeki dünit blokları, benzerlerine Trinity, Bushveld ve Vourinos ofiyolitinde de görülen eşdeğerleri ile kıyaslayarak oluşumlarını belirlemeye çalışmaktır.

Bazaltik magmanın pikritik eriyikleri hakkında önemli bir işaret olan dünit blokları, başlangıçta olive doygun olmayan eriyiklerle yan duvar reaksiyonuyla veya olivinin fraksiyonel kristalizasyonuyla oluşur. Oluşumları ile ilgili olarak, magmatik, hidrotermal-metasomatik ve kristal kümülat işlevlerle oluşum şeklinde farklı görüşler vardır. Dünitlerde Al, Ca, K, Na, Ti ve Si oksitlerin normal değerlere göre yüksek olması, duvar kayaçlarından koparılan parçaların minimum ergimeyle asimilasyonu sonucudur. Dünit bloklarının petrografisi, ofiyolit istifini oluşturan kayaç türlerinin bileşimiyle benzerlik göstermektedir. Diğer eşdeğerleri ile karşılaştırıldığında, Guleman ofiyoliti dünit blokları dünitik çekirdek ve onu çevreleyen harzburjit ve/veya gabrodan oluşmaktadır. Dünitteki diğer fazlara göre olivinin fazla miktarda bulunması, pikritik eriyiklerle yan duvar arasındaki reaksiyonların işaretidir. Dünit bloklarının farklı büyüklüğe sahip olması, magma odası blok faylanmalara bağlanmıştır ( ).

Kaynaklar

Bedard, J.H. 1991. Cumulate recycling and crustal evolution in the Bay of Islands ophiolite. Journal of Geology 99, 225–249.

Buchanan, P. C., Koeberl, C. and Reimold, W.U., (1999). Petrogenesis of the Dullstroom Formation, Bushveld magmatic province, South Africa. Contributions to Mineralogy and Petrology 137, 133-146.

Cameron, E. N., (1978). The Lower Zone of the Eastern Bushveld Complex in the Olifants River Trough. Journal of Petrology, 19,437-462.

Coleman, R.G. (1977). Ophiolites, PJ Wyllie (ed) Springer-Verlag, New York, 229.

Davis, G.A., Holdaway, M.J., Lipman, P.W., Romey, W.D. (1965). Struture, metamorphism, and plutonism in the south-central Klamath Mountains, California. Geol Soc Am Bull, 76 ,933-966.

Dewey, J. F., Bırd, J. M., (1971). Origin and emplacement of ophiolite suite:Appalachian ophiolites in Newfoundland. Journal of Geophysical Research,76, 3179-3206.

Dick, H. J. B., Sinton, .J.M. (1979). Compositional layering in apline peridotites: evidence tbr pressure solution creep in the mantle. Journal of Geology, 87,403-416.

Dıck, H.J.B., Bullen, T. (1984). Chromian spinel as a petrogenetic indicator in abyssal and alpine-type peridotites and spatially associated lavas. Contributions to Mineralogy and Petrology 86, 54–76.

Dungan, M.A., Lallemant, H.G. (1977). Formation of small dunite bodies by metasomatic transformation of harzburgite in the Canyon Mountain ophiolite, northeast Oregon. In: Magma Genesis, 1977. Ore Dept Geol Min Ind Bull 96, 128.

Green, D.H., (1973). Experimental melting studies on model upper mantle compositions at high pressure under both water-saturated and water-undersaturated conditions. Earth Planet Sci Lett 19,37-53.

Harkins, M.E., Green, M.W., Moores, E.H. (1980). Multiple intrusive events documented from the Vourinous ophiolite complex, northern Greece. Am J Sci 280-A, 284-495.

Irvine, T.N. (1974). Petrology of the Duke Island ultramafic complex, southeastern Alaska. GeoI Soc Am., 138, 240.

Kılıç, A. D., (2005). Hazar Gölü (Sivrice-Elazığ) güneyinin petrografik ve petrolojik özellikleri. Fırat Üniversitesi Fen BilimleriEnstitüsü, Elazığ, Doktora Tezi, 103.

Kılıç, A. D. (2009). Petrographical and geochemical properties of plagiogranites and gabbros in Guleman ophiolite. Bulletin of the Mineral Research and Exploration, 139(139), 33-49.

Kılıç, A.D., (20129. Petrogesis of subduction zone and dunite bodies. Journal of Earth Science and Engineering, 2, 377-386.

McCallum, D.S., (1996). The Stillwater Complex. Developments in Petrology, 15, 441-483.

Moores, E. (1969). Petrology and structure of the Vourinous ophiolite complex of northern Greece. Geol Soc Am Spec Pap, 118, 74.

Mysen, B.O., Boettche,r A.L. (1975). Melting of a hydrous mantle: II. Geochemistry of crystals and liquids formed by anatexis of mantle peridotite at high pressures and temperatures as a function of controlled activities of water, hydrogen and carbon dioxide. J Petrol, 16, 549-593.

Önen, P., (2003). Neotethyan ophiolitic rocks of the Anatolides of NW Turkey and comparison with Tauride ophiolites. J. Geol. Soc., London, 160, 947-962.

Örgün, Y. (1992). Topuk – Göynükbelen (Orhaneli – Bursa) yöresi nikel oluşumlarının kökensel incelenmesi, Doktara Tezi, İ.T.Ü Fen Bilimleri Enstitüsü, İstanbul.

Özkan, Y. Z., (1982). Guleman (Elazığ) ofiyolitinin jeolojisi ve petrolojisi. Yerbilimleri Dergisi, 3-4/6, 33-39.

Özkan, Y.Z., Öztunalı, Ö., (1984) Petrology of the Magmatic Rocks of Guleman Ophiolite in the Geology of the Taurus Belt. International Symposium Proceedings, Maden Tetkik ve Arama Enstitüsü, Ankara, Turkey, 285-293.

Ringwood, A. E., (1975). Composition and petrology of the Earth's mantle. McGraw Hill Inc., New York, 618.

Rızaoğlu, T., Parlak, O., Höck, V. And İşler, F. (2006). Nature and significance of Late Cretaceous ophiolitic rocks and its relation to the Baskil granitoid in Elazığ region, SE Turkey. Geol. Soc. London Spec Publication, 260, 327-350.

Robertson, A.H.F., Dıxon, J.E., (1984). Introduction: aspects of the geological evolution of the eastern Mediterranean. In: Robertson, A.H.F. and Dixon, J.E. (eds.), The geological evolution of the eastern Mediterranean. Geological Society of London Special Publication, 17, 1-74.

Shervais, J. W. (1979). Thermal emplacement model for the alpine lherzolite massif at Balmuccia, Italy. J Petrol 20, 4, 795-820.

Stolper, E. (1980). A phase diagram for mid-ocean ridge basalt: preliminary results and implications for petrogenesis. Contrib Mineral Petrol ,74,13- 27.

Taylor, H.P., Epstein, S. (1962a). Relationship between 180/160 ratios in coexisting minerals in igneous and metamorphic rocks. Part I: Principles and experimental results. Geol Soc Am Bull 73:461-480

Taylor, H.D., Epstein, S. (1962b). Relationship between lsO/160 ratios in coexisting minerals of igneous and metamorphic rocks. Part II: Applications to petrologic problems. Geol Soc Am Bull, 73, 675- 694.